Regulation of Mammalian Membranous Adenylyl Cyclases by Diterpenes and MANT-Nucleotides

Dissertation

zur Erlangung des Doktorgrades der Naturwissenschaften (Dr. rer. nat.) der Naturwissenschaftlichen Fakultät IV – Chemie und Pharmazie – der Universität Regensburg

vorgelegt von

Miriam Erdorf

aus Burghausen

2010

Diese Arbeit entstand in der Zeit von Juli 2007 bis Juli 2010 unter der Leitung von Herrn Prof. Dr. R. Seifert am Institut für Pharmakologie und Toxikologie der Naturwissenschaftlichen Fakultät IV – Chemie und Pharmazie – der Universität Regensburg.

Das Promotionsgesuch wurde eingereicht im Juli 2010.

Tag der mündlichen Prüfung: 27.08.2010

Prüfungsausschuss:

Prof. em. Dr. Dr. h.c. J. Barthel	(Vorsitzender)
Prof. Dr. R. Seifert	(Erstgutachter)
PD. Dr. K. Höcherl	(Zweitgutachter)
Prof. Dr. J. Heilmann	(Drittprüfer)

Für Florian

In memoriam avi mei.

Danksagungen

Es ist an der Zeit, mich ganz herzlich bei all den Menschen zu bedanken, die zum Gelingen dieser Arbeit beigetragen haben:

Zuallererst möchte ich mich bei meinem Doktorvater Herrn Prof. Dr. Roland Seifert bedanken für die interessanten Themengebiete, die ich bearbeiten durfte, für die sachkundige und erfahrene Unterstützung sowie die hilfreichen Ratschläge und wegweisenden Ideen. Vielen Dank für die mir entgegengebrachte Geduld bei allen Diskussionen und den Beistand bei Problemlösungen.

Danke auch an Herrn PD. Dr. Klaus Höcherl für die anfängliche Hilfe bei Internet-Recherchen, die Unterstützung bei der Auswahl der AC-Primer und der Erstellung des Zweitgutachtens.

Auch Herrn Prof. Dr. Jörg Heilmann möchte ich Dank sagen für die Übernahme des Amtes als Drittprüfer sowie Herrn Prof. em. Dr. Dr. h.c. Josef Barthel für den Vorsitz in der Prüfungskommission.

Ich möchte mich ebenfalls bei Herrn Prof. Dr. Frieder Kees für alle wissenschaftlichen Ratschläge und die zeitweise Betreuung im letzten Drittel meiner Doktorarbeit bedanken. Seine gute Laune und die zahlreichen Witze haben mich nicht selten zum Lächeln gebracht.

Für die wissenschaftliche Zusammenarbeit im Bereich Molecular Modeling bedanke ich mich bei Prof. Dr. Tung-Chung Mou und Prof. Dr. Stefan Dove.

Herrn Prof. Dr. Günther Bernhardt und Dr. Johannes Mosandl danke ich für die Einführung in die Arbeit am Tecan Plattenleser und die hilfreichen Tipps und konstruktiven Gespräche über Fluoreszenzmessung mit adhärenten Zellen.

Ich danke Herrn Prof. Dr. Robert Schupfner für die Einweisung in radioaktives Arbeiten sowie Herrn Prof. Dr. Thilo Spruß und Herrn Engelbert Meier für die reibungslose Bereitstellung der Kaninchennieren.

Vielen Dank an Herrn Prof. Dr. Jens Schlossmann für die Möglichkeit auch nach Prof. Seiferts Wechsel nach Hannover den Arbeitsplatz in Regensburg zu behalten.

Dr. Martin Göttle möchte ich Dank sagen für die kritische Betrachtung meiner Arbeit, das stets offene Ohr für Fragen und die jahrelange Geduld. Danke auch für die spannende Gestaltung unserer Pausen und für die Rotwein-gestützten Diskussionen nach Feierabend.

Ich möchte mich auch bei Dr. Erich Schneider bedanken, der jederzeit für so manche wissenschaftliche und nicht-wissenschaftliche Diskussion zu haben war und mit seinem trockenen Humor den Labor-Alltag etwas aufgelockert hat.

Ein herzliches Dankeschön möchte ich ebenfalls an meine Bürokollegin Heidrun Appl richten für ihr Verständnis, ihren Überblick in jeder Situation, die zahlreichen Tipps, die mir die Arbeit am Computer erheblich erleichtert haben, jeden wertvollen, unterstützenden Beistand, ihre Kekse und dafür, dass sie mir zu einer Freundin geworden ist.

Frau Susanne Brüggemann und Frau Astrid Seefeld danke ich für ihre fachkundige Unterstützung bei den AC-Assays und ihre Hilfe v.a. auch in den Anfangstagen meiner Labortätigkeit. Auch der restlichen Truppe sowie allen ehemaligen Mitarbeitern am Lehrstuhl für Pharmakologie und Toxikologie möchte ich für das äußerst angenehme Arbeitsklima und die lockere Atmosphäre danken. Es hat Spaß gemacht, mit ihnen zu arbeiten!

Danke auch den Austauschstudenten Petra Kos (Erasmus) und Taehun Kim (DAAD) sowie meiner Wahlpflichtpraktikantin Claudia Scharl, die mit Ihrer Mitarbeit bei der Entstehung dieser Arbeit geholfen haben.

Ein besonderer Dank geht an meinem LK-Bio Lehrer Reinhard Meindl, dessen Rat, ich solle meine Ziele nicht zu hoch stecken, mir stets Ansporn auch in schwierigen Tagen war.

Bei meiner Freundin Sandra Sittenthaler bedanke ich mich herzlich für ihren unermüdlichen Zuspruch aus der Ferne, jede willkommene Ablenkung und die guten Ratschläge bei Problemstellungen aller Art.

Auch meinen Eltern bin ich sehr dankbar, dass sie mir die ganze Zeit hindurch unterstützend und liebevoll zur Seite standen. Sie haben während meiner Studien- und Promotionszeit oft mit mir gebangt, gehofft und haben mir den nötigen Rückhalt gegeben. Danke!
Einen herzlichen Dank auch an meine Oma, die nie den Glauben an mich verloren hat und auch oder gerade in schwierigen Situationen mit ihrer Liebe und Hilfsbereitschaft zu mir stand. Sie hat mir stets ein Stück ihrer Lebenserfahrung mit auf den Weg gegeben.

Schließlich danke ich von Herzen meinem Freund Florian, der mir mit seiner tiefen und unerschütterlichen Liebe die ganze Zeit hindurch Kraft und Halt gegeben hat. Danke für alles, was ich mit Dir erleben durfte. Ich liebe Dich unglaublich!

Es ist besser, harten Fakten zu vertrauen,

als weiche Modelle immer wieder zu verbiegen.

Erich Schneider

Contents

List of Figures

List of Tables

Abbreviations

1d-FS	1-deoxy-forskolin
5-HT	serotonin
6A7DA-FS	6-acetyl-7-deacetyl-forskolin
7DA-FS	7-deacetyl-forskolin
9d-FS	9-deoxy-forskolin
AC	adenylyl cyclase
ADP	adenosine 5'-diphosphate
ATP	adenosine 5'-triphosphate
AVP	[8-arginine]vasopressin
BODIPY-FS	boron-dipyrromethene-forskolin
Bp	base pair(s)
BSA	bovine serum albumin
$[Ca^{2+}]_i$	intracellular concentrations of free calcium
CaM	calmodulin
cAMP	cyclic adenosine 3',5'-monophosphate
cDNA	copy desoxyribonucleic acid
CNS	central nervous system
DMB-FS	7-deacetyl-7-(*N*-methyl)piperazino-γ-butyryloxy)-forskolin
DMSO	dimethylsulfoxid
EC_{50}	agonist concentration which induces 50% of the maximum effect
EDTA	ethylenediaminetetraacetic acid (chelator)
EGTA	ethylene glycol tetraacetic acid (chelator)
E_{max}	efficacy (maximal enzyme response)
ER	endoplasmatic reticulum
FS	forskolin
GDP	guanosine 5'-diphosphate
GPCR	G protein-coupled receptor
GTP	guanosine 5'-triphosphate
GTPγS	guanosine 5'-[γ-thio]triphosphate
IBMX	3-isobutyl-1-methylxanthine
IP_3	inositol 1, 4, 5-trisphosphate
kDA	kilo Dalton

K_m	Michaelis-Menten constant
LTP	long term potentiation
mAC	mammalian AC
MANT-NTP	2'(3')-*O*-(*N*-methylanthraniloyl)-nucleoside 5'-triphosphate
MANT-NTPγS	2'(3')-*O*-(*N*-methylanthraniloyl)-nucleoside 5'-[γ-thio]triphosphate
mRNA	messenger ribonucleic acid
PDE	phosphodiesterase
P_i	inorganic phosphate
PKA	protein kinase A
PKC	protein kinase C
PKD	polycystic kidney disease
PLC	phospholipase C
PP_i	inorganic pyrophosphate
r^2	correlation coefficient
RMSD	root mean square deviations
RT-PCR	reverse transcription-polymerase chain reaction
SD	standard deviation
Sf9	insect cell line of *Spodoptera frugiperda*
Tris	tris(hydroxymethyl)aminomethan
V_{max}	maximum velocity of an enzymatic reaction

Chapter 1

Structural, Regulatory and Pharmacological Fundamentals of Mammalian Membranous Adenylyl Cyclases

A.1 Mammalian Membranous Adenylyl Cyclases

A.1.1 The cAMP Signaling Pathway

Over 50 years ago Sutherland and Rall (Berthet *et al*., 1957a; Berthet *et al*., 1957b) discovered the role of cyclic adenosine 3',5'-monophosphate (cAMP) in biological effects (Sutherland, 1972). cAMP is one of the various small molecules referred to as "second messenger" that relay signals form receptors on the cell surface to target molecules inside the cell. The concept of second messenger signaling is now well established. The second messenger pathways concerning G proteins as transducers arose to one of the best studied of the cell surface signal transduction pathways. The effects of cAMP as second messenger are broad and often very complex. One of the key roles is its influence during cell development, e.g. by modulation of the progression within the cell cycle (Hanoune and Defer, 2001), the regulation of gene transcription (Rodbell, 1980) and its growth-stimulatory effect (Dumont *et al*., 1989). The second messenger molecule is also involved in blood coagulation (Steer and Salzman, 1980), neuronal function (Kebabian, 1977) and the control of immune (Parker *et al*., 1974) and visual responses (Bitensky *et al*., 1971). This diversity of regulatory features is closely related to the variety of potential regulators of cAMP synthesis and degradation (Hanoune and Defer, 2001).

Adenylyl cyclases (ACs) are integral membrane proteins which catalyze the conversion from ATP to cAMP (Ishikawa and Homcy, 1997; Hurley, 1998) (Fig. **A.1**). Activation of these effector proteins transfers signals from the extracellular to the cytosolic side (Cooper *et al*., 1995; Defer *et al*., 2000) and contributes to cross-talks in different cell systems and signaling structures (Iyengar, 1993; Sunahara *et al*., 1996).

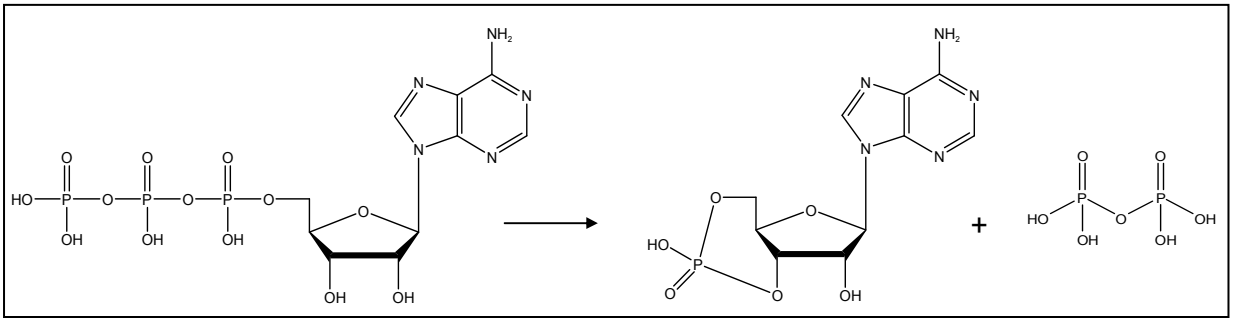

Fig. A.1. Adenylyl cyclase reaction. AC catalyzes the conversion of ATP into cAMP and pyrophosphate. The resulting amount of cAMP is measured as an indicator of enzyme activity.

Neurotransmitters, hormones, odorants and autacoids act as first messenger molecules *via* activation of G protein-coupled receptors (GPCRs). GPCRs are cell membrane proteins consisting of seven hydrophobic transmembrane segments, an extracellular amino terminus and an intracellular carboxyl terminus (Kolakowski, 1994; Palczewski *et al*., 2000). Having identified over 800 members of GPCRs, they are the largest family in the human genome (Kobilka, 2007). These receptors communicate with heterotrimeric, membrane-associated G proteins, which in turn activate ACs. G proteins can be divided into a G_{α} subunit, associated with guanosine 5'-diphosphate (GDP) in the inactive state and a $G_{\beta\gamma}$ heterodimer. Receptor activation leads to the release of GDP and its replacement by GTP. Subsequently, a conformational change induces the dissociation of GTP-bound G_{α} subunit from the $G_{\beta\gamma}$ dimer. ACs can be modulated by the free G_{α} subunit, either in a stimulatory ($G_{S\alpha}$ family) or in an inhibitory ($G_{i\alpha}$ family) way (Gilman, 1987; Iyengar, 1993; Kristiansen, 2004). The active state of G_{α} is terminated by its GTPase activity, which means the cleavage of GTP into GDP and inorganic phosphate (P_i), and its reassociation with $G_{\beta\gamma}$.

Furthermore, cAMP activates cyclic nucleotide-gated ion channels or directly interacts with protein kinase A (PKA) promoting further phosphorylation steps (Defer *et al*., 2000). In turn, PKA activation is involved in cell growth, metabolism, differentiation and transcriptional regulation (Wing and Robinson, 1968; Rodbell, 1980; Dumont *et al*., 1989). Without any phosphorylation, cAMP can also prompt protein-protein interactions, e.g. in signaling of Rap1 proteins (Kawasaki *et al*., 1998).

Second messenger signaling is terminated by the degradation of cAMP. Cyclic nucleotide phosphodiesterases (PDEs) break the phosphodiester bond of cAMP and therefore regulate the localization, duration, and amplitude of cyclic nucleotide signaling within subcellular domains.

A.1.2 Structure and Catalytic Mechanism of Mammalian ACs

Using analysis of amino acid sequences and molecular cloning techniques, nine mammalian membrane-bound AC isoforms have been identified so far. These ACs are integral glycoproteins with a calculated molecular weight of 119 to 175 kDa. They share a considerable degree of sequence homology in their primary and tertiary structure (Tang and Gilman, 1992; Yan *et al*., 1996; Tang and Hurley, 1998). Fig. **A.2** shows the proposed structure of membrane-bound ACs. The short variable amino-terminus (*N*) is located in the cytoplasma, followed by 12 stretches of hydrophobic residues arranged in two sets of six successional transmembrane spanning α-helices (M_1 and M_2). The sequence of M_1 and M_2 is separated by a large hydrophilic loop of 360 to 390 amino acids (C_1) and terminated by a cytoplasmic domain containing 255 to 330 amino acids (C_2) and the carboxyl-terminus (*C*) (Iyengar, 1993; Sunahara *et al*., 1996). C_1 and C_2 form the catalytic core (Tang *et al*., 1995) and can both be further divided into “a” and “b” subdomains (Zhang *et al*., 1997a; 1997b). The intracellular regions C_{1a} and C_{2a} are highly conserved and share 50 to 90% of sequence homology among the different AC isoforms (Sunahara *et al*., 1996).

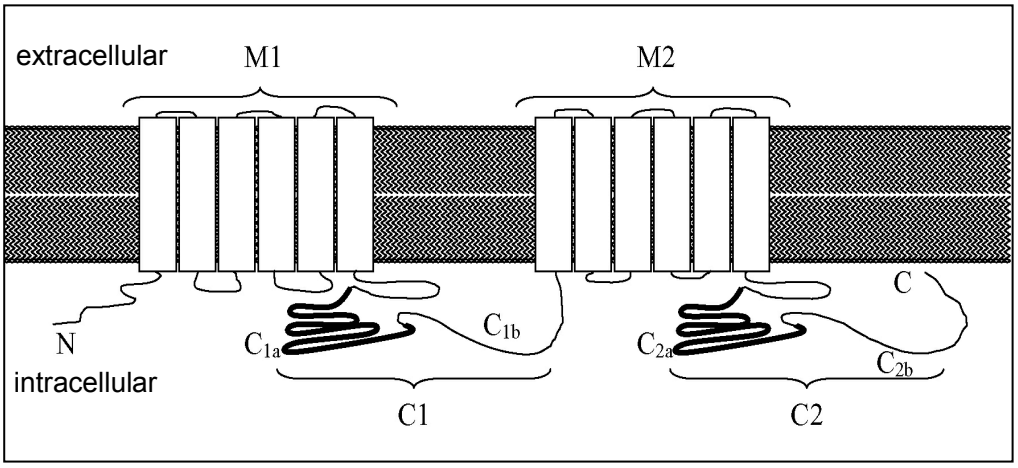

Fig. A.2. Schematic illustration of a mammalian membrane-bound AC (Tang and Gilman, 1992; Sunahara *et al*., 1996). The proposed structure is characterized by the intracellular *N*- and *C*-termini, the two membrane-spanning domains M_1 and M_2 and the cytosolic regions C_1 and C_2. The formation of the catalytic core by the two subdomains C_{1a} and C_{2a} is responsible for the conversion of ATP into cAMP.

Crystallographic and mutational studies revealed the essential role of these two domains, forming the critical cleft in AC reaction (Mou *et al*., 2005). In the presence of activators like forskolin or $G_{S\alpha}$, a conformational change enhances the affinity of C_{1a} to C_{2a} (Whisnant *et al*., 1996; Yan *et al*., 1996). During catalysis, an interface between the two domains is formed by the interaction of polar and charged regions (Tang and Gilman, 1992; Zhang *et al*., 1997a; 1997b). C_{1b} and C_{2b} are less conserved, and their role is as yet poorly understood. C_{1b} is assumed to be responsible for isoform-specific regulation (Yan *et al*., 2001; Beeler *et al*., 2004). The predicted functions of the two transmembrane domains are on the one hand a stable anchoring at the plasma membrane and on the other hand the coordination of C_1/C_2 interaction (Hanoune *et al*., 1997; Hurley, 1998).

Binding of ATP induces another conformational change (proof reading), which enables the enzyme to bind the substrate (Yoo *et al*., 2004). Hydrogen bonds between the nitrogen (^{1}N)-atom of the adenine base and Lys938 and in addition, between the (^{6}N)-atom and Asp1018 (numbering according to AC2) ensure specifity for adenine (Liu *et al*., 1997; Tesmer *et al*., 1997). For example, due to the high similarity of ACs to guanylyl cyclases (GCs), GTP is bound to AC with 10-fold lower affinity, but no turnover to cGMP takes place (Sunahara *et al*., 1998; Tang and Hurley, 1998; Beuve, 1999).

The conversion of ATP into cyclic AMP is initiated by the binding of the adenine base into a hydrophobic pocket at the catalytic site (Tang and Hurley, 1998). The negatively charged phosphate tail of the nucleotide with its α-, β- and γ-phosphate interacts with the positive side chains from both sides of the cleft, e.g. Arg484, Arg1029 and Lys1065 (numbering from AC2) as well as Arg398 and Arg1011 (numbering from AC1) (Tang and Hurley, 1998). The catalysis is induced by the inversion of the configuration at the α-phosphate. Subsequently, the pyrophosphate is displaced by an intramolecular nucleophilic attack of the 3'-OH group of the ATP ribose on the 3'-oxygen atom of the α-phosphate (Eckstein *et al*., 1981; Dessauer *et al*., 1996; Liu *et al*., 1997; Tang and Hurley, 1998).

Mutagenesis and kinetic analysis uncovered an essential role for Asn1025 and Arg1029 of C_2 in catalysis (Yan *et al*., 1997; Zhang *et al*., 1997a; 1997b). Both amino acids form a water-mediated interaction with the adenine (Yan *et al*., 1997). Arg1029 interacts with the α-phosphorus atom (Liu *et al*., 1997, Tesmer *et al*., 1997), while Asn1025 is close to the 3'-O atom of the current ATP complex and assists Arg1029

in stabilizing the transition state or the leaving group. Asp354 in AC1 is identified to be the crucial catalytic base (Liu *et al*., 1997; Tesmer *et al*., 1997), because mutations of this amino acid have disruptive effects on the binding of ATP and lead to complete inactivation of AC (Tang *et al*., 1995).

For adequate AC activity, Mg^{2+} or Mn^{2+} is required in molar excess of ATP (Garbers and Johnson, 1975; Somkuti *et al*., 1982). A single Mg^{2+} ion binds to a pair of aspartates on C_1 (Tesmer *et al*., 1997), a second metal ion binding site is contained within the C_2 domain (Mitterauer *et al*., 1998). These divalent cations are supposed to participate in catalysis by activating the 3'-OH group and/or stabilizing the transition state of the α-phosphate (Mitterauer *et al*., 1998). Nevertheless, the precise molecular mechanism of this catalytic reaction is still unknown, due to the lack of crystallographic structures of holo-ACs with substrate or substrate analogs.

A.1.3 AC Isoform-Specific Regulatory Mechanisms

Adenylyl cyclases do not only exist as multiple isoforms with specific molecular diversity, they are also characterized by regulatory complexity with distinct signal integration (Defer *et al*., 2000; Kristiansen, 2004).

A.1.3.1 $G_{S\alpha}$

The common GPCR signal transduction pathway leads from receptor activation *via* a conformational change in the G protein to the interaction of the $G_{S\alpha}$ subunit with AC. This progression characterizes the major mechanism to activate AC and subsequently produce cAMP (Tang *et al*., 1992). Activation through $G_{S\alpha}$ represents, with few qualitative and quantitative differences, the only natural feature, shared by all AC isoforms (Iyengar, 1993; Sunahara *et al*., 1996). The dissociation from the $G_{\beta\gamma}$ complex allows the α-subunit to directly interact and activate AC at a picomolar concentration (Tang and Hurley, 1998). Mutagenic mapping discovered a functional association of $G_{S\alpha}$ with both cytoplasmic domains C_1 and C_2 (Sunahara *et al*., 1997; Tesmer *et al*., 1997). The $G_{S\alpha}$ binding site at adenylyl cyclase has been localized to a small hydrophobic region of C_{1a} and, additionally, to a much larger negatively charged and also hydrophobic gap on C_{2a} (Tesmer *et al*., 1997; Yan *et al*., 1997a). Binding of $G_{S\alpha}$ enhances the connection of the two cytoplasmic loops and imposes a conformational change on the catalytic core. While the key residues converge to the 3'-OH group of ATP, the active site wraps around ATP and catalysis proceeds faster (Harry *et al*., 1997; Sunahara *et al*., 1997; Tesmer *et al*., 1997).

A.1.3.2 $G_{i\alpha}/G_{o\alpha}$

Agonist occupation of GPCRs can also generate inhibition of ACs mediated through a subunit of $G_{i\alpha}$ or $G_{o\alpha}$ (Tang and Gilman, 1991; Kozasa and Gilman, 1995; Taussig and Gilman, 1995). By direct interaction with the C_1 domain, $G_{i\alpha}$ stabilizes a more open and inactive conformation of the catalytic cleft. In contrast to $G_{S\alpha}$, which uniformly activates all AC isoforms, the subsequent actions of $G_{i\alpha}$ are isoenzyme-specific (Chen and Iyengar, 1993; Taussig *et al*., 1993a; Rodbell, 1995). For certain AC subtypes, such as types 5 and 6, which are predominantly expressed in kidney, and type 1 in the brain, $G_{i\alpha}$ acts as a non-competitive inhibitor of $G_{S\alpha}$ stimulation

(Taussig *et al*., 1993a; Dessauer *et al*., 1998; Defer *et al*., 2000). This repressive effect on ACs can be blocked by pertussis toxin. Pertussis toxin catalyzes the ADP-ribosylation of $G_{i\alpha}/G_{o\alpha}$ subunits and thus, uncouples them from their membrane-bound receptors (Defer *et al*., 2000; Watts and Neve, 2005). In the opposite, enzyme activity of the AC isoforms 2 and 8 are not altered by $G_{i\alpha}/G_{o\alpha}$ (Chen and Iyengar, 1993; Lustig *et al*., 1993; Taussig *et al*., 1993a). Characterizing the response of ACs to modulation by $G_{i\alpha}/G_{o\alpha}$-coupled receptors can even lead to the activation, rather than inhibition, of adenylyl cyclases depending on the duration of receptor stimulation (Gao and Gilman, 1991; Tang *et al*., 1992). On the one hand, acute and short activation of $G_{i\alpha}/G_{o\alpha}$-coupled receptors inhibits AC and attenuates cyclic AMP accumulation, but on the other hand, prolonged stimulation of $G_{i\alpha}/G_{o\alpha}$-coupled receptors typically sensitizes AC to subsequent activation by FS or $G_{S\alpha}$-coupled receptors (Watts and Neve, 2005).

A.1.3.3 $G_{\beta\gamma}$

In addition to G_{α} modulation, the $G_{\beta\gamma}$ complex is a reasonably potent and direct effector on ACs, too (Tang and Gilman, 1991; Taussig *et al*., 1993b; Kristiansen, 2004). Only low concentrations of $\beta\gamma$ can be achieved by activation of $G_{S\alpha}$ whereas the stimulation of $G_{i\alpha}/G_{o\alpha}$ yields substantially higher concentrations, reflecting a variety of cross-talks between different receptors (Federman *et al*., 1992; Bygrave and Roberts, 1995; Bayewitch *et al*., 1998a). For instance, stimulation of G_q-coupled receptors can mediate mobilization of intracellular calcium *via* $G_{q\alpha}$ and additionally increase cAMP accumulation *via* modulation of AC by $\beta\gamma$ (Gilman, 1987). Depending on the affected AC isoform, the $G_{\beta\gamma}$ complex displays different effects: direct stimulation in presence of $G_{S\alpha}$ was observed in ACs 2, 4 and 7 (Gao and Gilman, 1991; Tang and Gilman, 1991), direct inhibition was determined at ACs 1, 5, 6 and 8 (Robishaw *et al*., 1986; Smigel, 1986; Bayewitch *et al*., 1998b) and finally no direct effect was seen with ACs 3 and 9 (Fig. **A.3**) (Iyengar, 1993).

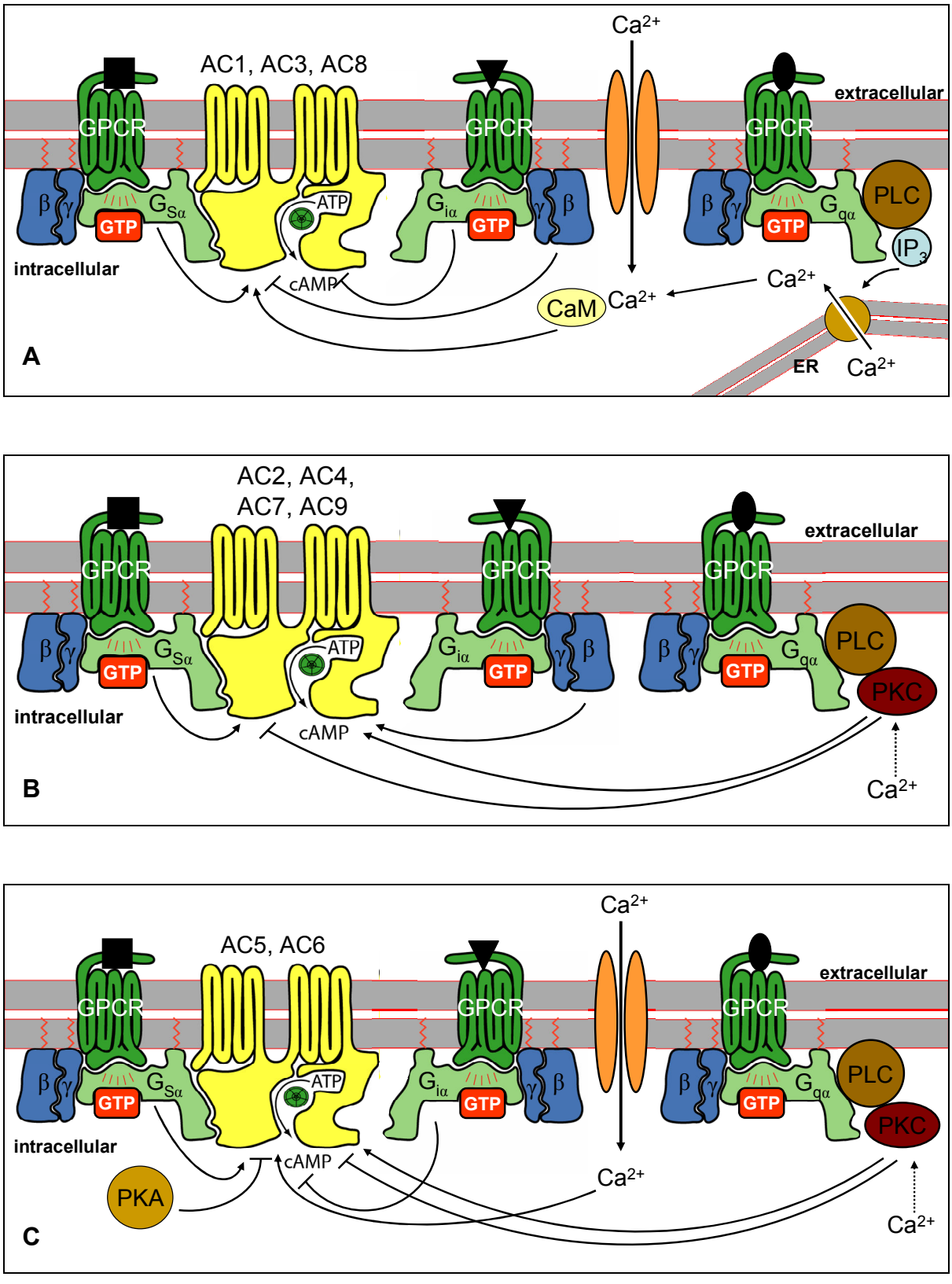

Fig. A.3. Patterns of regulation of AC activity (Sunahara *et al.*, 1996). Due to their relationship to distinct modulators, the AC isoforms can be divided into three categories: Ca^{2+}/CaM-stimulated enzymes 1, 3 and 8 (**A**), Ca^{2+}-insensitive isoforms 2, 4, 7 and 9 (**B**) and finally Ca^{2+}-inhibitable ACs 5 and 6 (**C**). After GPCR activation (■ / ▼ / ⬮), the modulation of the AC isoforms can be in a stimulatory (↑) or inhibitory (⊤) manner according to the distinct regulator. PKA / PKC, protein kinase A / C; PLC, phospholipase C; IP_3, insitol 1,4,5-trisphosphate; ER, endoplasmatic reticulum.

A.1.3.4 Ca^{2+}/CaM

Calmodulin is an endogenous calcium-sensor protein, which modulates the activity of ACs 1, 3 and 8 (Fig. **A.3A**) (Tang *et al*., 1991; Choi *et al*., 1992b; Cali *et al*., 1994). ACs 1 and 8 are activated by direct binding of the Ca^{2+}/CaM complex to a putative binding site located in the C_{1b} helical region of AC1 (Vorherr *et al*., 1993) or in the C_2 region of AC8 (Levin and Reed, 1995). However, the precise mechanism of Ca^{2+}/CaM activation is still unknown. All responses of ACs to Ca^{2+}/CaM are highly synergistic with $G_{S\alpha}$ or FS (Choi *et al*., 1992a; Sunahara *et al*., 1996). Although AC8 needs a 5 to 10 times higher concentration of Ca^{2+}/CaM than AC1, the required concentration of Ca^{2+} is still in the physiological range (0.1 to 1 μM). In contrast, the effects on AC3 depend on supra-normal Ca^{2+}-concentrations (> 1 μM) (Choi *et al*., 1992b). *In vivo* AC3 and AC9 can be inhibited *via* Ca^{2+}-dependent calmodulin kinase II and calcineurin, respectively (Cali *et al*., 1994; Antoni *et al*., 1995; Wei *et al*., 1996).

A.1.3.5 $[Ca^{2+}]_i$

Besides the Ca^{2+}/CaM-dependent AC family, the two subtypes AC5 and AC6, are strikingly inhibited by submicromolar concentrations of free Ca^{2+} ($[Ca^{2+}]_i$) (Fig. **A.3C**) (Krupinski *et al*., 1992; Cooper *et al*., 1998; Guillou *et al*., 1999). The inhibition of AC5 by $[Ca^{2+}]_i$ involves the catalytic domains (Hu *et al*., 2002) and is additive to the effect of $G_{i\alpha}$ activation (Defer *et al*., 2000). It has been shown that both AC isoforms are affected by physiologically relevant concentrations of $[Ca^{2+}]_i$. Their inhibition is more intensely mediated by the extracellular entry of Ca^{2+} through L-type Ca^{2+}-channels rather than the release from intracellular stores (Yoshimura and Cooper, 1992; Cooper *et al*., 1994; Cooper *et al*., 1995). The relation to physiological relevance and the higher order of AC regulation by $[Ca^{2+}]_i$ are still matter of investigation.

In addition, all AC isoforms are inhibited by submillimolar concentrations of $[Ca^{2+}]_i$. This non-physiological effect is possibly competitive with Mg^{2+}, the essential cation for AC reaction (Sunahara *et al*., 1996; Cooper, 2003).

A.1.3.6 PKA and PKC

In addition to their regulation by G protein subunits and $[Ca^{2+}]_i$, mammalian adenylyl cyclases are also subjected to complex regulation by phosphorylation *via*

protein kinase A (PKA) or protein kinase C (PKC). AC5 and AC6 are sensitive for phosphorylation by PKA, which disrupts binding of $G_{S\alpha}$ to AC and causes inactivation (Iwami *et al*., 1995). Certain agonists can activate G_q-coupled receptors, leading to PKC activation, which in turn modulates ACs in an isoform-specific manner (Levin and Reed, 1995). PKC activates several AC isoforms like ACs 1, 2, 3, 5 and 7 by the interaction of their *C*-terminus with specific phosphorylation sites (Fig. **A.3**). This, in turn, increases the cyclase activity (Bol *et al*., 1997). In contrast, $G_{S\alpha}$-stimulated AC4 and AC6 activity is decreased in presence of PKC mediated by the *N*-terminal region (Fig. **A.3B**,**C**) (Kawabe *et al*., 1994; Zimmermann and Taussig, 1996; Lai *et al*., 1999).

A.1.3.7 FS

The diterpene forskolin (FS) is a very lipophilic compound extracted from the roots of the Indian plant *Coleus forskohlii* (Seamon and Daly, 1986; Yan *et al*., 1998a). FS has been utilized as a pharmacologic agent in studies relating to the biochemistry and regulation of AC and cAMP in diverse systems (Seamon *et al*., 1981). FS potently activates all cloned mammalian adenylyl cyclases except type 9 by interaction with the two homologous cytoplasmic domains (C_1 and C_2) that form the catalytic core (Metzger and Lindner, 1981; Iyengar, 1993; Premont *et al*., 1996). Sequence analysis revealed that one amino acid (Leu912, AC2 labeling) is absolutely conserved in the C_2 domain among FS-sensitive type 1 to 8, but differs in FS-insensitive type 9 enzyme (Yan *et al*., 1997a). A single change of Tyr1082 to leucine of mammalian type 9 enzyme can confer both binding and activation by forskolin (Zhang *et al*., 1997b; Yan *et al*., 1998).

Based on chrystallographic studies, Leu912 is located at the interface of the C_1/C_2 complex, where FS directly binds and interacts with AC (Fig. **A.4**) (Tang and Gilman, 1995; Whisnant *et al*., 1996; Dessauer *et al*., 1997; Scholich *et al*., 1997). The FS-binding site in the catalytic core is very close to the $G_{S\alpha}$-binding site. Although there is a greater distance to the ATP binding site, forskolin still affects ATP binding (Yan *et al*., 1998). FS enhances the adhesiveness of the two cytoplasmic domains and stabilizes the dimer by closing a hydrophobic gap (Zhang *et al*., 1997b).

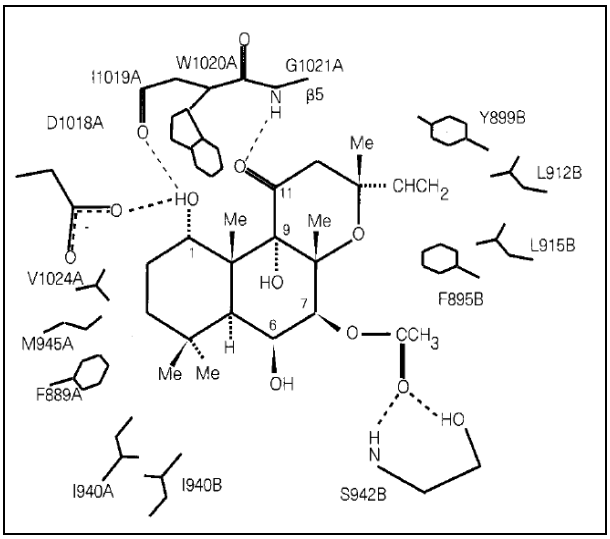

Fig. A.4. Proposed interactions of forskolin and the catalytic core of AC (Zhang *et al*., 1997b). The dotted lines indicate the hydrogen bonds between the hydroxyl-groups of FS and the critical amino acids of the catalytic core. Amino acid labelling with "A" refers to the C_1 domain, "B" stands for the C_2 subunit.

Interactions between forskolin and adenylyl cyclase are predominantly hydrophobic. However, specificity is enhanced by hydrogen bonds between the 1-OH and 9-OH groups of FS and C_1 and between the 7-acetyl-group and Ser942 (AC2 labeling) at C_2 (Fig. **A.4**) (Sutkowski *et al*., 1994; Robbins *et al*., 1996; Yan *et al*., 1998). Based on these interactions, special modifications of the FS structure generate a variety of FS analogs, e.g. 1-deoxy-FS, 9-deoxy-FS or 7-deacetyl-FS. These FS derivatives can be used to uncover isoform-specific binding modes between the diterpenes and ACs and thus, characterize the interplay between activators and ACs (Pinto *et al*., 2008; 2009). Although FS probably does not participate in physiological cAMP signaling, its exceptional efficacy makes it essential to understand its mode of actions. The striking effect in a natural regulatory system suggests that the FS binding pocket might bind an as yet unidentified physiological hydrophobic activator (Zhang *et al*., 1997b).

A.1.3.8 P-Site Inhibitors

ACs are subject to inhibition by a class of non-competitive adenosine analogs known as P-site inhibitors (Desaubry *et al*., 1996a; 1996b). These inhibitors are ribose-modified (deoxy- and 3'-phosphorylated) adenosine analogs which suppress catalysis by acting directly on ACs (Dessauer and Gilman, 1997). They potently

interfere with the catalytic site of AC when elevated concentrations of the reaction product pyrophosphate (PP_i) additionally enhance their binding (Dessauer and Gilman, 1997; Dessauer *et al*., 1999).

A.1.3.9 MANT-Nucleotides

Nucleoside triphosphates substituted with an *N*-methylanthraniloyl (MANT)-group at the 2'- or 3'-oxygen of the ribose were serendipitously identified to act as potent AC inhibitors (Gille and Seifert, 2003a; 2003b). MANT-inhibitors occupy the same position in the catalytic site as P-site inhibitors and substrate analogs. The MANT-fluorophore is integrated into a hydrophobic pocket at the interface of C_1 and C_2 and interacts with lipophilic residues like Phe400, Trp1020 and Val1006 (Mou *et al*., 2005). It acts like a barrier, which prevents the catalytic core of AC to change from the open to the closed conformation (Mou *et al*., 2005). Thus, no cAMP synthesis can be catalyzed. Fig. **A.5** shows the general structure of different MANT-nucleotides and the hydrolysis stable nucleoside-γS-triphosphates.

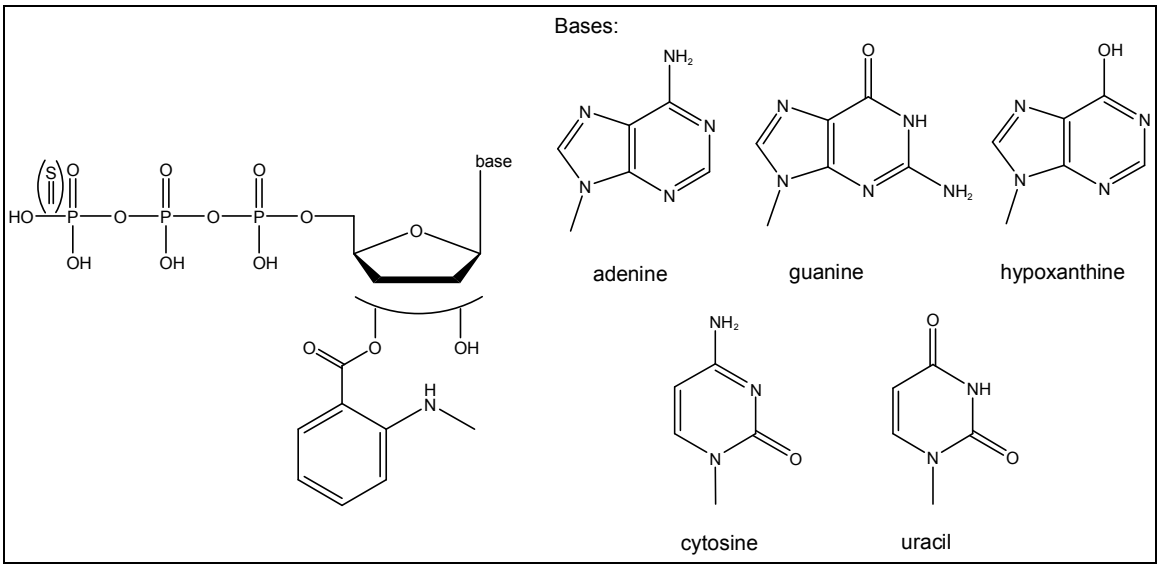

Fig. A.5. Structure of 2'(3')-*O*-(*N*-methylanthraniloyl)- (MANT)-substituted nucleotides. Different purine and pyrimidine bases attached to the ribose serve as substrate to the AC binding site. Substitution of the oxygen in the phosphate tail stabilizes the nucleotide for degradation. The MANT-group spontaneously isomerizes between the 2'- and 3'-OH of the ribose.

Substantial differences in interactions between the base and/or different substitution patterns at the phosphate tail of the inhibitors and the binding site of ACs are reported (Mou *et al*., 2006). The catalytic core of ACs was found to be spacious and flexible, binding both purine and pyrimidine nucleotides but with varying affinities.

Moreover, the specific order of inhibitory potency determined for special ACs, can be used to characterize and discriminate between the different AC isoforms. The isoform-specific inhibition patterns can also serve as basis for the development of isoform-selective AC inhibitors. Their application as novel therapeutic drugs could lead to new therapies of various diseases associated with AC activation.

A.1.4 Tissue Distribution and (Patho)Physiological Relevance of AC Isoforms

In all mammalian tissues, at least one AC isoform can be found, which integrates different regulatory pathways through cross-talk with other signal transduction systems (Sunahara *et al*., 1996; Hanoune and Defer, 2001). The determination of the precise expression and attribution to special tissues is crucial to classify the activation patterns and to clarify the physiological relevance of the different members of the AC family. Over the years, biochemical analysis, recombinant technologies, the generation of knock-out mice and transgenic animals delivered insights into the physiological roles of AC in defined tissues (Tab. **A.1**) (Hanoune and Defer, 2001).

A.1.4.1 Localization, Functions and Pathophysiological Relevance of ACs

- AC isoform 1 is expressed in neurons (Xia *et al*., 1993) and abundant in certain areas of the brain, such as in hippocampus, neocortex and the granular cells of cerebellum (Mons *et al*., 1993). AC1 knock-out studies discovered the critical role of this isoform in synaptic plasticity and long-term potentiation (LTP) (Wu *et al*., 1995; Storm *et al*., 1998). LTP is the ability of two neurons to communicate with each other and provide a long-lasting enhancement in signal transmission (Villacres *et al*., 1998). Moreover, $AC1^{-/-}$ mice showed altered transmission of neuropathic pain (Vadakkan *et al*., 2005) and subsequently a changed behaviour. AC1 overexpression in mouse forebrain enhanced recognition and neuromodulation (Wang *et al*., 2004), which confirmed its crucial role in learning and memory (Choi *et al*., 1992a; Villacres *et al*., 1993; Xia and Storm, 1997).

In 1994, Schnecko *et al.* discovered the relationship between neural AC isoforms and Alzheimer's disease (Schnecko *et al*., 1994). Ca^{2+}/CaM sensitive ACs, in particular AC1, are significantly reduced in hippocampus and cerebellum from patients suffering from Alzheimer's disease (Yamamoto *et al*., 1997). The neuropathological changes in the brain as well as excessive activation of neuronal receptors result in a damage and dying of nerve cells (Wang *et al*., 2007). Because of the connection of AC1 with learning and memory (Wang *et al*., 2004), modulation of AC1 may be a novel approach in neurodegenerative diseases and Alzheimer's disease (Sadana and Dessauer, 2009). For the development of new potential disease-modifying treatments, the development biomarkers would be the next step to

specify particular states of the disease (Rosenberg and Hillis, 2009).

Additionally, AC1 synthesis is strikingly dependent from the circadian rhythm pointing to function as a key regulator of melatonin production and release (Defer *et al*., 2000).

Tab. A.1. Tissue-specific expression of AC isoforms, potential roles and possible contributions to malfunction of organs (Iyengar, 1993; Sunahara *et al*., 1996; Hanoune *et al*., 1997; Defer *et al*., 2000; Ludwig and Seuwen, 2002).

AC isoform	Tissue distribution	Predicted functions and association with pathophysiological states
AC1	Brain, neural tissue	Learning, memory, Alzheimer's disease, melatonin release
AC2	Brain, lung, platelets, skeletal muscle	Synaptic plasticity, cell differentiation, respiration
AC3	Olfactory epithelium, genitals, colon, brain	Sense of smell, sperm function
AC4	Widespread Kidney, heart, liver, uterus	Synaptic coordination, oocyte maturation,
AC5	Kidney, heart, brain	Cardiac contraction, heart failure, polycystic kidney disease
AC6	Widespread Kidney, heart	Cardiac contraction, heart failure
AC7	Brain, cerebellar granula, platelets, heart, lung	Depression, drug dependency
AC8	Hippocampus, testis, lung	Neuroendocrine function, drug dependency
AC9	Brain, endocrine tissues	Long-term potentiation, signaling between motoneurons

- Together with AC1, Ca^{2+}-insensitive AC type 2 is predominant in a number of brain regions (Furuyama *et al*., 1993) and regulates synaptic plasticity and neuronal differentiation (Mons *et al*., 1993; Matsuoka *et al*., 1997). Expression of AC2 with its stimulation by PKC is found to modulate cell differentiation and results in inhibition of

cell cycle progression (Smit *et al*., 1998). AC2 is also known to be the prevalent isoform in lung (Feinstein *et al*., 1991), pointing to regulatory mechanisms in pulmonary artery myocytes (Furuyama *et al*., 1993; Jourdan *et al*., 2001). Furthermore, strong expression levels of AC2 have been detected in postmitotic neuronal cells and in platelets (Premont *et al*., 1992; Hanoune and Defer, 2001) as well as in skeletal muscle and testis (Ludwig and Seuwen, 2002).

- Coexpression of AC3 with $G_{S\alpha}$ and G_{olf}, an olfactory form of $G_{S\alpha}$, is exposed in olfactory neuroepithelium indicating an involvement of AC3 in sense of smell (Bakalyar and Reed, 1990). AC3 knock-out studies confirmed its crucial role in olfaction and olfaction related responses (Wong and Storm, 2002). In spite of the presence of other AC isoforms in olfactory cilia, behavioural studies with $AC3^{-/-}$ mice showed a complete anosmia (Wong *et al*., 2000). Although AC3 was originally thought to be exclusively expressed in olfactory epithelium, up to date, a broad tissue distribution is described with high levels in placenta, testis, ovary and colon (Yang *et al*., 1999; Ludwig and Seuwen, 2002). Low levels are reported in brain, heart, adrenal medulla, lung and retina (Xia *et al*., 1992; Abdel-Majid *et al*., 2002).

- AC isoform 4 is widely distributed in a variety of tissues with an appropriate multiplicity of physiological roles. The ability of AC4 in the hippocampus to detect coincident activation of $G_{S\alpha}$- and $G_{i\alpha}$-coupled receptors indicates an association in synaptic plasticity by coordinating such overlapping synaptic inputs (Baker *et al*., 1999). Another prominent pattern of AC4 is the expression in uterus (Suzuki *et al*., 1997) and the contribution to oocyte maturation arrest (Guzman *et al*., 2005) as well as the subjection of the AC4 expression level to sex steroids (Asano *et al*., 2005). Other organs with high levels of AC4 occurrence are e.g. liver, heart and kidney (Gao and Gilman, 1991). Unfortunately, the distinct physiological role of AC4 in each of these tissues is still subject of survey.

- Ca^{2+}-sensitive ACs 5 and 6 create a subgroup within the mammalian AC family (Katsushika *et al*., 1992). AC6 is a widespread subtype found in all organs, whereas AC5 is more restricted to special tissues (Hanoune and Defer, 2001). In the heart, particularly in cardiac myocytes, both ACs are the main isoforms. $[Ca^{2+}]_i$ mediates the regulation of AC5 and probably also of AC6 in cardiac tissue (Hanoune and Defer, 2001). The physiological relevance of this Ca^{2+}-inhibition is mainly induced by Ca^{2+}-influx *via* L-type Ca^{2+}-channels (Yu *et al*., 1993).

Models of heart failure discovered cardioprotective effects of AC6 and cardiac regulation of heart rate and contractility responses of both, AC5 and AC6 (Roth *et al*., 1999; Tepe *et al*., 1999). During heart failure, the expression rate of AC6 decreases, whereas the level of AC5 keeps constant (Ping *et al*., 1997). This indicates a different subcellular location of ACs 5 and 6. In fact, AC5 is found to be essentially present in myocytes, contrary to non-myocytic AC6 (Yu *et al*., 1995). AC5 knock-out models are protected against cardiomyopathy and oxidative stress (Yan *et al*., 2007). Additionally, they show an apparently increased life span. In contrast, overexpression of AC5 in heart reveals no cardioprotective effects. AC activity enhances during overexpression without impaired heart function and cardioprotective mechanisms (Hanoune and Defer, 2001). In the opposite, AC6 overexpression restores normal cardiac function. Enhanced AC6 activity improves contractility (Gao *et al*., 2002) and increases survival in cardiac hypertrophy and cardiomyopathy (Roth *et al*., 2002). Accordingly, AC regulation in heart is very complex and it seems that AC5 and AC6 play opposing roles during pathophysilogical states of heart function.

The second major tissue with an abundant expression of AC5 and AC6 are the kidneys. AC6 is present all along the nephron, in the medulla (Shen *et al*., 1997), the collecting tubule and the thick ascending limb (Chabardés *et al*., 1996). However, AC5 is more restricted to the glomerulus and the cortical part of the kidney (Ludwig and Seuwen, 2002). Ca^{2+} is known to play a crucial role in urine concencentration, thus, the capacitative Ca^{2+}-entry and the intracellular Ca^{2+}-release are important regulators of the ACs in the kidney as well (Chabardés *et al*., 1999). An increase in extracellular Ca^{2+}-concentration decreases the hormone-dependent cAMP accumulation (Chabardés *et al*., 1996). Moreover, renal urine production can be regulated by the antidiuretic hormone vasopressin *via* V_2-receptor mediated cAMP production (Takaichi *et al*., 1986). In parallel, the high responsiveness of renal ACs to activation by glucagon strongly indicates a crucial role of ACs in renal homeostasis (Ahloulay *et al*., 1995).

- Although the structure of AC7 is closely related to AC2, a quite different expression pattern is reported throughout the brain (Hellevuo *et al*., 1995). mRNA of AC7 is particularly present in cerebellar granula (Sunahara *et al*., 1996). Against the background, that reduced activity of the cAMP signaling system has been involved in the etiology of depressed individuals, AC7 could have a sex-specific implication in depression (Hines *et al*., 2006). Overexpression of AC7 in the CNS modified the

acute responsiveness toward ethanol and increased the sensitivity to morphine analgesia (Yoshimura *et al*., 2000; Patel *et al*., 2001). A quite widely distribution was observed with further occurrence of AC7 in heart (Krupinski *et al*., 1992), lung (Ludwig and Seuwen, 2002), platelets and postmitotic neuronal cells (Hanoune and Defer, 2001).

- AC8 is a brain-specific protein (Parma *et al*., 1991; Krupinski *et al*., 1992) and the only Ca^{2+}/CaM-stimulated isoform expressed in the hippocampus (Matsuoka *et al*., 1992; Cali *et al*., 1994; Mons and Cooper, 1994). This indicates the importance of AC8 in neuroendocrine function (Wong *et al*., 1999) and drug dependence (Matsuoka *et al*., 1994; Lane-Ladd *et al*., 1997). In AC8 knock-outs, neurological defects illustrate the critical role of CaM-regulated ACs in higher brain function (Sunahara and Taussig, 2002). However, neither increased anxiety nor long-term depression appear in single knock-out mice of AC8 after treatment with repeated stress tests (Schaefer *et al*., 2000). In contrast, AC1/AC8 double knock-outs fail in both long-term memory and long-term potentiation (Wong *et al*., 1999).

AC8 appearance was also reported in testis (Defer *et al*., 1994) and lung (Muglia *et al*., 1999).

- AC9 belongs to the most abundant isoforms in brain (Antoni *et al*., 1998a). It is present in postsynaptic dendrites of the neocortex and hippocampus and seems to be involved in signaling between motoneurons (Antoni *et al*., 1998b). AC9 is potently inhibited by the Ca^{2+}/CaM-activated protein phosphatase calcineurin (Antoni *et al*., 1995). Co-localization of calcineurin with AC9 (Paterson *et al*., 2000) and the coincidental presence of CaM-dependent AC1, AC8 and CaM kinase II indicate a high relevance for homeostasis of brain function and particularly LTP (Lu *et al*., 1996; Antoni *et al*., 1998b; Hanoune and Defer, 2001). Depletion of the AC9 analog in *Caenorhabditis elegans* prevents the organ from $G_{S\alpha}$-induced neurodegeneration and cell death (Berger *et al*., 1998; Korswagen *et al*., 1998). This indicates the relationship of AC9 to signaling and regulation in motoneurons (Defer *et al*., 2000). AC9 is further expressed in several peripheral endocrine tissues like ovaries and testis (Hanoune and Defer, 2001).

A.1.4.2 Connection between Polycystic Kidney Disease and Renal ACs

Polycystic kidney disease (PKD) is a renal disease, inherited in a more prevalent autosomal dominant or in a less frequently autosomal recessive manner

(Guay-Woodford and Desmond, 2003; Torres *et al*., 2007). In the autosomal dominant form, two genes are identified to be associated with the pathogenesis: PKD1 and PKD2. These genes encode for the membranous glycoproteins polycystin 1 and polycystin 2, respectively. Polycystin 1 is a receptor associated with ciliary sensory and cell adhesion. Polycystin 2 regulates the renal tubular and vascular development and in its additional function as a cation channel, it controls the flow of Ca^{2+} in the renal plasma membrane (Hughes *et al*., 1995; Mochizuki *et al*., 1996). Autosomal recessive polycystic kidney disease is linked to a single gene disruption of PKHD1, encoding for fibrocystin (Bergmann *et al*., 2004). Both forms are characterized by overlapping symptoms like numerous fluid-filled cysts in the kidneys (Fig. **A.6**), tubular dilatation and defective ciliogenesis (Grantham, 1997). Patients suffer from renal pain, hypertension and frequent urinary tract infections. Blood in the urine often indicates renal function abnormalities and renal insufficiency. In the end-stage, large cysts also affect other tissues like liver and pancreas (Torres and Harris, 2006). During the last decade, a major role of cAMP levels in the proliferation of renal cyst epithelial cells and the promotion of fluid production was discovered (Yamaguchi *et al*., 2000; Grantham, 2003). In response to AC agonists, increased levels of cAMP and cAMP analogs, the proliferation of epithelial cells in cyst walls is increased. cAMP also enhances fluid secretion and thus, leads to an enlargement of renal cysts (Sullivan and Grantham, 1996). Unfortunately, until now, no treatment was found to slow cyst formation or disease progression. Only palliative therapies ease the severity of the symptoms (Wuthrich *et al*., 2009). With AC-dependent cAMP regulation being a key factor in PKD, renal AC isoform-specific inhibition provides a target for the pharmacological treatment of this disorder.

Fig. A.6. Polycystic kidney. The picture was taken from the Institute for Molecular and Cellular Anatomy, Prof. Dr. R. Witzgall, University of Regensburg, Germany; (*http://www.biologie.uni-regensburg.de/Anatomie/index.html*).

A.2 Several Clues and Unanswered Questions

In summary, the isoform-specific structure of the catalytic core of AC isoforms allows many different regulatory mechanisms to operate solitarily or simultaneously. It is perfectly suited to their physiological roles to react to multiple signals with their distinct effects. Nevertheless, many questions remain unanswered, e.g. first of all, why do cells express multiple isoforms of AC? And how are the mechanisms regulated to distinguish the stimulatory or inhibitory outcomes? What is the exact role of the transmembrane domains? What is the endogenous ligand for the forskolin binding site? What exact roles do ACs play in mental disorders, cardiac function or regulatory properties in the kidney and what are the distinct mechanisms? Genetic knock-out models and further structure analysis will be necessary to define the specific physiological and biochemical roles of each AC family member. A further clue for investigation would be the identification of the proteins' role under disease conditions. The basis for precise development of isoform-specific and selective pharmaceuticals is the detailed characterization of AC isoforms in all tissues. The clarification of all physiological and pathophysiological roles will lead to the development of new therapeutic approaches.

A.3 Scope and Objectives of this Thesis

Polycystic kidney disease, heart failure, Alzheimer's disease and mood disorders are only a few of the numerous pathophysiological states caused by malfunction of the adenylyl cyclase family. The nine mammalian membranous AC isoforms play a crucial role in transmembrane signaling events of the G protein-coupled receptor (GPCR) cascade and catalyze the formation of the universal second messenger cAMP. Since mACs are expressed in a tissue-specific manner, isoform-selective and specific modulation by activators like forskolin and analogs or inhibitors like MANT-nucleotides may be a promising novel therapeutic strategy.

The aim of this thesis is the characterization of the regulation and modulation of AC isoforms using a sensitive and robust assay system. It is planned to clarify the effects of FS and six FS derivatives on recombinant ACs expressed in Sf9 insect cells. In a biochemical assay we will determine the characteristic AC activity of all seven diterpenes, rendering their pharmacological profile. Therefore, the structure-activity relationships for the studied diterpenes will be explored. Additionally we will

investigate the precise contribution of the divalent metal ions Mg^{2+} in comparison to Mn^{2+}, serving as cofactors for mACs. By docking ligands to the isoform-specific mAC model, we aim at explaining preferences of ligands for both metal ions. With respect to potential therapeutic applications, the clarification of AC regulation is essential. The precise mechanism of AC regulation by isoform-selective activators in combination with the influence of the divalent metal ions will provide the basis for the development of novel drugs targeting mACs.

Furthermore, this thesis intends to characterize AC activity in the two main parts of the kidney. The expression patterns of the different AC isoforms in renal cortex and medulla will be investigated using molecular biological approaches. Biochemical methods will be used to analyze differences in activation, inhibition and regulation of the AC isoforms in rabbit cortex and medulla membranes. GPCR agonist-mediated AC activity, analysis of Ca^{2+}-dependent or calmodulin-sensitive cAMP formation and the inhibitory profile of eight 2'(3')-*O*-(*N*-methylanthraniloyl) (MANT)-nucleoside 5'-([γ-thio])triphosphates will differentiate between the renal AC types and identifiy the prevalent cortical and medullary AC isoform. Since PKD is characterized by an overproduction of cAMP predominantly in the collecting duct and the distal nephrons, potent inhibitors affecting selectively renal AC isoforms could constitute a novel approach to treat PKD.

A.4 References

Abdel-Majid RM, Tremblay F and Baldridge WH (2002) Localization of adenylyl cyclase proteins in the rodent retina. *Brain Res Mol Brain Res* **101**:62-70.

Ahloulay M, Dechaux M, Laborde K and Bankir L (1995) Influence of glucagon on GFR and on urea and electrolyte excretion: direct and indirect effects. *Am J Physiol* **269**:F225-235.

Antoni FA, Barnard RJ, Shipston MJ, Smith SM, Simpson J and Paterson JM (1995) Calcineurin feedback inhibition of agonist-evoked cAMP formation. *J Biol Chem* **270**:28055-28061.

Antoni FA, Palkovits M, Simpson J, Smith SM, Leitch AL, Rosie R, Fink G and Paterson JM (1998a) Ca^{2+}/calcineurin-inhibited adenylyl cyclase, highly abundant in forebrain regions, is important for learning and memory. *J Neurosci* **18**:9650-9661.

Antoni FA, Smith SM, Simpson J, Rosie R, Fink G and Paterson JM (1998b) Calcium control of adenylyl cyclase: the calcineurin connection. *Adv Second Messenger Phosphoprotein Res* **32**:153-172.

Asano K, Okawa T, Matsuoka I, Suzuki Y and Sato A (2005) Effects of sex steroids on expression of adenylyl cyclase messenger RNA in rat uterus. *J Endocrinol Invest* **28**:357-362.

Bakalyar HA and Reed RR (1990) Identification of a specialized adenylyl cyclase that may mediate odorant detection. *Science* **250**:1403-1406.

Baker LP, Nielsen MD, Impey S, Hacker BM, Poser SW, Chan MY and Storm DR (1999) Regulation and immunohistochemical localization of $\beta\gamma$-stimulated adenylyl cyclases in mouse hippocampus. *J Neurosci* **19**:180-192.

Bayewitch ML, Avidor-Reiss T, Levy R, Pfeuffer T, Nevo I, Simonds WF and Vogel Z (1998a) Differential modulation of adenylyl cyclases 1 and 2 by various G_{β} subunits. *J Biol Chem* **273**:2273-2276.

Bayewitch ML, Avidor-Reiss T, Levy R, Pfeuffer T, Nevo I, Simonds WF and Vogel Z (1998b) Inhibition of adenylyl cyclase isoforms 5 and 6 by various $G_{\beta\gamma}$ subunits. *FASEB J* **12**:1019-1025.

Beeler JA, Yan SZ, Bykov S, Murza A, Asher S and Tang WJ (2004) A soluble C_{1b} protein and its regulation of soluble type 7 adenylyl cyclase. *Biochemistry* **43**:15463-15471.

Berger AJ, Hart AC and Kaplan JM (1998) $G_{S\alpha}$ -induced neurodegeneration in *Caenorhabditis elegans*. *J Neurosci* **18**:2871-2880.

Bergmann C, Senderek J, Küpper F, Schneider F, Dornia C, Windelen E, Eggermann T, Rudnik-Schöneborn S, Kirfel J, Furu L, Onuchic LF, Rossetti S, Harris PC, Somlo S, Guay-Woodford L, Germino GG, Moser M, Buttner R and Zerres K

(2004) PKHD1 mutations in autosomal recessive polycystic kidney disease (ARPKD). *Hum Mutat* **23**:453-463.

Berthet J, Rall TW and Sutherland EW (1957a) The relationship of epinephrine and glucagon to liver phosphorylase. IV. Effect of epinephrine and glucagon on the reactivation of phosphorylase in liver homogenates. *J Biol Chem* **224**:463-475.

Berthet J, Sutherland EW and Rall TW (1957b) The assay of glucagon and epinephrine with use of liver homogenates. *J Biol Chem* **229**:351-361.

Beuve A (1999) Conversion of a guanylyl cyclase to an adenylyl cyclase. *Methods* **19**:545-550.

Bitensky MW, Gorman RE and Miller WH (1971) Adenylyl cyclase as a link between photon capture and changes in membrane permeability of frog photoreceptors. *Proc Natl Acad Sci USA* **68**:561-562.

Bol GF, Hulster A and Pfeuffer T (1997) Adenylyl cyclase type 2 is stimulated by PKC *via C*-terminal phosphorylation. *Biochim Biophys Acta* **1358**:307-313.

Bygrave FL and Roberts HR (1995) Regulation of cellular calcium through signaling cross-talk involves an intricate interplay between the actions of receptors, G proteins, and second messengers. *FASEB J* **9**:1297-1303.

Cali JJ, Zwaagstra JC, Mons N, Cooper DM and Krupinski J (1994) Type 8 adenylyl cyclase. A Ca^{2+}/calmodulin-stimulated enzyme expressed in discrete regions of rat brain. *J Biol Chem* **269**:12190-12195.

Chabardés D, Firsov D, Aarab L, Clabecq A, Bellanger AC, Siaume-Peréz S and Elalouf JM (1996) Localization of mRNAs encoding Ca^{2+}-inhibitable adenylyl cyclases along the renal tubule. Functional consequences for regulation of the cAMP content. *J Biol Chem* **271**:19264-19271.

Chabardés D, Imbert-Teboul M and Elalouf JM (1999) Functional properties of Ca^{2+}-inhibitable type 5 and type 6 adenylyl cyclases and role of Ca^{2+} increase in the inhibition of intracellular cAMP content. *Cell Signal* **11**:651-663.

Chen J and Iyengar R (1993) Inhibition of cloned adenylyl cyclases by mutant-activated $G_{i\alpha}$ and specific suppression of type 2 adenylyl cyclase inhibition by phorbol ester treatment. *J Biol Chem* **268**:12253-12256.

Choi EJ, Wong ST, Hinds TR and Storm DR (1992a) Calcium and muscarinic agonist stimulation of type 1 adenylyl cyclase in whole cells. *J Biol Chem* **267**:12440-12442.

Choi EJ, Xia Z and Storm DR (1992b) Stimulation of the type 3 olfactory adenylyl cyclase by calcium and calmodulin. *Biochemistry* **31**:6492-6498.

Cooper DM (2003) Regulation and organization of adenylyl cyclases and cAMP. *Biochem J* **375**:517-529.

Cooper DM, Karpen JW, Fagan KA and Mons NE (1998) Ca^{2+}-sensitive adenylyl cyclases. *Adv Second Messenger Phosphoprotein Res* **32**:23-51.

Cooper DM, Mons N and Karpen JW (1995) Adenylyl cyclases and the interaction between calcium and cAMP signalling. *Nature* **374**:421-424.

Cooper DM, Yoshimura M, Zhang Y, Chiono M and Mahey R (1994) Capacitative Ca^{2+} entry regulates Ca^{2+}-sensitive adenylyl cyclases. *Biochem J* **297** 437-440.

Defer N, Best-Belpomme M and Hanoune J (2000) Tissue specificity and physiological relevance of various isoforms of adenylyl cyclase. *Am J Physiol Renal Physiol* **279**:F400-416.

Defer N, Marinx O, Stengel D, Danisova A, Iourgenko V, Matsuoka I, Caput D and Hanoune J (1994) Molecular cloning of the human type VIII adenylyl cyclase. *FEBS Lett* **351**:109-113.

Desaubry L, Shoshani I and Johnson RA (1996a) 2',5'-Dideoxyadenosine 3'-polyphosphates are potent inhibitors of adenylyl cyclases. *J Biol Chem* **271**:2380-2382.

Desaubry L, Shoshani I and Johnson RA (1996b) Inhibition of adenylyl cyclase by a family of newly synthesized adenine nucleoside 3'-polyphosphates. *J Biol Chem* **271**:14028-14034.

Dessauer CW and Gilman AG (1997) The catalytic mechanism of mammalian adenylyl cyclase. Equilibrium binding and kinetic analysis of P-site inhibition. *J Biol Chem* **272**:27787-27795.

Dessauer CW, Posner BA and Gilman AG (1996) Visualizing signal transduction: receptors, G proteins, and adenylate cyclases. *Clin Sci (Lond)* **91**:527-537.

Dessauer CW, Scully TT and Gilman AG (1997) Interactions of forskolin and ATP with the cytosolic domains of mammalian adenylyl cyclase. *J Biol Chem* **272**:22272-22277.

Dessauer CW, Tesmer JJ, Sprang SR and Gilman AG (1998) Identification of a $G_{i\alpha}$ binding site on type 5 adenylyl cyclase. *J Biol Chem* **273**:25831-25839.

Dessauer CW, Tesmer JJ, Sprang SR and Gilman AG (1999) The interactions of adenylate cyclases with P-site inhibitors. *Trends Pharmacol Sci* **20**:205-210.

Dumont JE, Jauniaux JC and Roger PP (1989) The cyclic AMP-mediated stimulation of cell proliferation. *Trends Biochem Sci* **14**:67-71.

Eckstein F, Romaniuk PJ, Heideman W and Storm DR (1981) Stereochemistry of the mammalian adenylate cyclase reaction. *J Biol Chem* **256**:9118-9120.

Federman AD, Conklin BR, Schrader KA, Reed RR and Bourne HR (1992) Hormonal stimulation of adenylyl cyclase through G_i protein $\beta\gamma$ subunits. *Nature* **356**:159-161.

Feinstein PG, Schrader KA, Bakalyar HA, Tang WJ, Krupinski J, Gilman AG and Reed RR (1991) Molecular cloning and characterization of a Ca^{2+}/calmodulin-

insensitive adenylyl cyclase from rat brain. *Proc Natl Acad Sci USA* **88**:10173-10177.

Furuyama T, Inagaki S and Takagi H (1993) Distribution of type II adenylyl cyclase mRNA in the rat brain. *Brain Res Mol Brain Res* **19**:165-170.

Gao BN and Gilman AG (1991) Cloning and expression of a widely distributed (type 4) adenylyl cyclase. *Proc Natl Acad Sci USA* **88**:10178-10182.

Gao MH, Bayat H, Roth DM, Yao Zhou J, Drumm J, Burhan J and Hammond HK (2002) Controlled expression of cardiac-directed adenylyl cyclase type 6 provides increased contractile function. *Cardiovasc Res* **56**:197-204.

Garbers DL and Johnson RA (1975) Metal and metal-ATP interactions with brain and cardiac adenylate cyclases. *J Biol Chem* **250**:8449-8456.

Gille A and Seifert R (2003a) 2'(3')-*O*-(*N*-methylanthraniloyl)-substituted GTP analogs: a novel class of potent competitive adenylyl cyclase inhibitors. *J Biol Chem* **278**:12672-12679.

Gille A and Seifert R (2003b) MANT-substituted guanine nucleotides: a novel class of potent adenylyl cyclase inhibitors. *Life Sci* **74**:271-279.

Gilman AG (1987) G proteins: transducers of receptor-generated signals. *Annu Rev Biochem* **56**:615-649.

Grantham JJ (1997) Polycystic kidney disease: huge kidneys, huge problems, huge progress. *Trans Am Clin Climatol Assoc* **108**:165-170; discussion 170-162.

Grantham JJ (2003) Lillian Jean Kaplan International Prize for advancement in the understanding of polycystic kidney disease. Understanding polycystic kidney disease: a systems biology approach. *Kidney Int* **64**:1157-1162.

Guay-Woodford LM and Desmond RA (2003) Autosomal recessive polycystic kidney disease: the clinical experience in North America. *Pediatrics* **111**:1072-1080.

Guillou JL, Nakata H and Cooper DM (1999) Inhibition by calcium of mammalian adenylyl cyclases. *J Biol Chem* **274**:35539-35545.

Guzman L, Romo X, Grandy R, Soto X, Montecino M, Hinrichs M and Olate J (2005) A $G_{\beta\gamma}$ stimulated adenylyl cyclase is involved in *Xenopus laevis* oocyte maturation. *J Cell Physiol* **202**:223-229.

Hanoune J and Defer N (2001) Regulation and role of adenylyl cyclase isoforms. *Annu Rev Pharmacol Toxicol* **41**:145-174.

Hanoune J, Pouille Y, Tzavara E, Shen T, Lipskaya L, Miyamoto N, Suzuki Y and Defer N (1997) Adenylyl cyclases: structure, regulation and function in an enzyme superfamily. *Mol Cell Endocrinol* **128**:179-194.

Harry A, Chen Y, Magnusson R, Iyengar R and Weng G (1997) Differential regulation of adenylyl cyclases by $G_{S\alpha}$. *J Biol Chem* **272**:19017-19021.

Hellevuo K, Yoshimura M, Mons N, Hoffman PL, Cooper DM and Tabakoff B (1995) The characterization of a novel human adenylyl cyclase which is present in brain and other tissues. *J Biol Chem* **270**:11581-11589.

Hines LM, Hoffman PL, Bhave S, Saba L, Kaiser A, Snell L, Goncharov I, LeGault L, Dongier M, Grant B, Pronko S, Martinez L, Yoshimura M and Tabakoff B (2006) A sex-specific role of type 7 adenylyl cyclase in depression. *J Neurosci* **26**:12609-12619.

Hu B, Nakata H, Gu C, De Beer T and Cooper DM (2002) A critical interplay between Ca^{2+} inhibition and activation by Mg^{2+} of AC5 revealed by mutants and chimeric constructs. *J Biol Chem* **277**:33139-33147.

Hughes J, Ward CJ, Peral B, Aspinwall R, Clark K, San Millan JL, Gamble V and Harris PC (1995) The polycystic kidney disease 1 (PKD1) gene encodes a novel protein with multiple cell recognition domains. *Nat Genet* **10**:151-160.

Hurley JH (1998) The adenylyl and guanylyl cyclase superfamily. *Curr Opin Struct Biol* **8**:770-777.

Ishikawa Y and Homcy CJ (1997) The adenylyl cyclases as integrators of transmembrane signal transduction. *Circ Res* **80**:297-304.

Iwami G, Kawabe J, Ebina T, Cannon PJ, Homcy CJ and Ishikawa Y (1995) Regulation of adenylyl cyclase by protein kinase A. *J Biol Chem* **270**:12481-12484.

Iyengar R (1993) Molecular and functional diversity of mammalian $G_{S\alpha}$-stimulated adenylyl cyclases. *FASEB J* **7**:768-775.

Jourdan KB, Mason NA, Long L, Philips PG, Wilkins MR and Morrell NW (2001) Characterization of adenylyl cyclase isoforms in rat peripheral pulmonary arteries. *Am J Physiol Lung Cell Mol Physiol* **280**:L1359-1369.

Katsushika S, Chen L, Kawabe J, Nilakantan R, Halnon NJ, Homcy CJ and Ishikawa Y (1992) Cloning and characterization of a sixth adenylyl cyclase isoform: types V and VI constitute a subgroup within the mammalian adenylyl cyclase family. *Proc Natl Acad Sci USA* **89**:8774-8778.

Kawabe J, Iwami G, Ebina T, Ohno S, Katada T, Ueda Y, Homcy CJ and Ishikawa Y (1994) Differential activation of adenylyl cyclase by protein kinase C isoenzymes. *J Biol Chem* **269**:16554-16558.

Kawasaki H, Springett GM, Mochizuki N, Toki S, Nakaya M, Matsuda M, Housman DE and Graybiel AM (1998) A family of cAMP-binding proteins that directly activate Rap1. *Science* **282**:2275-2279.

Kebabian JW (1977) Biochemical regulation and physiological significance of cyclic nucleotides in the nervous system. *Adv Cyclic Nucleotide Res* **8**:421-508.

Kobilka BK (2007) G protein-coupled receptor structure and activation. *Biochim Biophys Acta* **1768**:794-807.

Kolakowski LF, Jr. (1994) GCRDb: a G protein-coupled receptor database. *Receptors Channels* **2**:1-7.

Korswagen HC, van der Linden AM and Plasterk RH (1998) G protein hyperactivation of the *Caenorhabditis elegans* adenylyl cyclase SGS-1 induces neuronal degeneration. *EMBO J* **17**:5059-5065.

Kozasa T and Gilman AG (1995) Purification of recombinant G proteins from Sf9 cells by hexahistidine tagging of associated subunits. Characterization of alpha 12 and inhibition of adenylyl cyclase by α_z. *J Biol Chem* **270**:1734-1741.

Kristiansen K (2004) Molecular mechanisms of ligand binding, signaling, and regulation within the superfamily of G protein-coupled receptors: molecular modeling and mutagenesis approaches to receptor structure and function. *Pharmacol Ther* **103**:21-80.

Krupinski J, Lehman TC, Frankenfield CD, Zwaagstra JC and Watson PA (1992) Molecular diversity in the adenylylcyclase family. Evidence for eight forms of the enzyme and cloning of type 6. *J Biol Chem* **267**:24858-24862.

Lai HL, Lin TH, Kao YY, Lin WJ, Hwang MJ and Chern Y (1999) The *N* terminus domain of type 6 adenylyl cyclase mediates its inhibition by protein kinase C. *Mol Pharmacol* **56**:644-650.

Lane-Ladd SB, Pineda J, Boundy VA, Pfeuffer T, Krupinski J, Aghajanian GK and Nestler EJ (1997) CREB (cAMP response element-binding protein) in the locus coeruleus: biochemical, physiological, and behavioral evidence for a role in opiate dependence. *J Neurosci* **17**:7890-7901.

Levin LR and Reed RR (1995) Identification of functional domains of adenylyl cyclase using *in vivo* chimeras. *J Biol Chem* **270**:7573-7579.

Liu Y, Ruoho AE, Rao VD and Hurley JH (1997) Catalytic mechanism of the adenylyl and guanylyl cyclases: modeling and mutational analysis. *Proc Natl Acad Sci USA* **94**:13414-13419.

Lu YF, Tomizawa K, Moriwaki A, Hayashi Y, Tokuda M, Itano T, Hatase O and Matsui H (1996) Calcineurin inhibitors, FK506 and cyclosporin A, suppress the NMDA receptor-mediated potentials and LTP, but not depotentiation in the rat hippocampus. *Brain Res* **729**:142-146.

Ludwig MG and Seuwen K (2002) Characterization of the human adenylyl cyclase gene family: cDNA, gene structure, and tissue distribution of the nine isoforms. *J Recept Signal Transduct Res* **22**:79-110.

Lustig KD, Conklin BR, Herzmark P, Taussig R and Bourne HR (1993) Type 2 adenylyl cyclase integrates coincident signals from G_S, G_i, and G_q. *J Biol Chem* **268**:13900-13905.

Matsuoka I, Giuili G, Poyard M, Stengel D, Parma J, Guellaen G and Hanoune J (1992) Localization of adenylyl and guanylyl cyclase in rat brain by *in situ* hybridization: comparison with calmodulin mRNA distribution. *J Neurosci* **12**:3350-3360.

Matsuoka I, Maldonado R, Defer N, Noel F, Hanoune J and Roques BP (1994) Chronic morphine administration causes region-specific increase of brain type 8 adenylyl cyclase mRNA. *Eur J Pharmacol* **268**:215-221.

Matsuoka I, Suzuki Y, Defer N, Nakanishi H and Hanoune J (1997) Differential expression of type I, II, and V adenylyl cyclase gene in the postnatal developing rat brain. *J Neurochem* **68**:498-506.

Metzger H and Lindner E (1981) The positive inotropic-acting forskolin, a potent adenylate cyclase activator. *Arzneimittelforschung* **31**:1248-1250.

Mitterauer T, Hohenegger M, Tang WJ, Nanoff C and Freissmuth M (1998) The C_2 catalytic domain of adenylyl cyclase contains the second metal ion (Mn^{2+}) binding site. *Biochemistry* **37**:16183-16191.

Mochizuki T, Wu G, Hayashi T, Xenophontos SL, Veldhuisen B, Saris JJ, Reynolds DM, Cai Y, Gabow PA, Pierides A, Kimberling WJ, Breuning MH, Deltas CC, Peters DJ and Somlo S (1996) PKD2, a gene for polycystic kidney disease that encodes an integral membrane protein. *Science* **272**:1339-1342.

Mons N and Cooper DM (1994) Adenylyl cyclase mRNA expression does not reflect the predominant Ca^{2+}/calmodulin-stimulated activity in the hypothalamus. *J Neuroendocrinol* **6**:665-671.

Mons N, Yoshimura M and Cooper DM (1993) Discrete expression of Ca^{2+}/calmodulin-sensitive and Ca^{2+}-insensitive adenylyl cyclases in the rat brain. *Synapse* **14**:51-59.

Mou TC, Gille A, Fancy DA, Seifert R and Sprang SR (2005) Structural basis for the inhibition of mammalian membrane adenylyl cyclase by 2'(3')-*O*-(*N*-methylanthraniloyl)-guanosine 5 '-triphosphate. *J Biol Chem* **280**:7253-7261.

Mou TC, Gille A, Suryanarayana S, Richter M, Seifert R and Sprang SR (2006) Broad specificity of mammalian adenylyl cyclase for interaction with 2',3'-substituted purine- and pyrimidine nucleotide inhibitors. *Mol Pharmacol* **70**:878-886.

Muglia LM, Schäfer ML, Vogt SK, Gürtner G, Imamura A and Muglia LJ (1999) The 5'-flanking region of the mouse adenylyl cyclase type 8 gene imparts tissue-specific expression in transgenic mice. *J Neurosci* **19**:2051-2058.

Palczewski K, Kumasaka T, Hori T, Behnke CA, Motoshima H, Fox BA, Le Trong I, Teller DC, Okada T, Stenkamp RE, Yamamoto M and Miyano M (2000) Crystal structure of rhodopsin: A G protein-coupled receptor. *Science* **289**:739-745.

Parker CW, Sullivan TJ and Wedner HJ (1974) Cyclic AMP and the immune response. *Adv Cyclic Nucleotide Res* **4**:1-79.

Parma J, Stengel D, Gannage MH, Poyard M, Barouki R and Hanoune J (1991) Sequence of a human brain adenylyl cyclase partial cDNA: evidence for a consensus cyclase specific domain. *Biochem Biophys Res Commun* **179**:455-462.

Patel TB, Du Z, Pierre S, Cartin L and Scholich K (2001) Molecular biological approaches to unravel adenylyl cyclase signaling and function. *Gene* **269**:13-25.

Paterson JM, Smith SM, Simpson J, Grace OC, Sosunov AA, Bell JE and Antoni FA (2000) Characterisation of human adenylyl cyclase 9 reveals inhibition by Ca^{2+}/calcineurin and differential mRNA polyadenylation. *J Neurochem* **75**:1358-1367.

Ping P, Anzai T, Gao M and Hammond HK (1997) Adenylyl cyclase and G protein receptor kinase expression during development of heart failure. *Am J Physiol* **273**:H707-717.

Pinto C, Hübner M, Gille A, Richter M, Mou TC, Sprang SR and Seifert R (2009) Differential interactions of the catalytic subunits of adenylyl cyclase with forskolin analogs. *Biochem Pharmacol* **78**:62-69.

Pinto C, Papa D, Hübner M, Mou TC, Lushington GH and Seifert R (2008) Activation and inhibition of adenylyl cyclase isoforms by forskolin analogs. *J Pharmacol Exp Ther* **325**:27-36.

Premont RT, Chen J, Ma HW, Ponnapalli M and Iyengar R (1992) Two members of a widely expressed subfamily of hormone-stimulated adenylyl cyclases. *Proc Natl Acad Sci USA* **89**:9809-9813.

Premont RT, Matsuoka I, Mattei MG, Pouille Y, Defer N and Hanoune J (1996) Identification and characterization of a widely expressed form of adenylyl cyclase. *J Biol Chem* **271**:13900-13907.

Robbins JD, Boring DL, Tang WJ, Shank R and Seamon KB (1996) Forskolin carbamates: binding and activation studies with type I adenylyl cyclase. *J Med Chem* **39**:2745-2752.

Robishaw JD, Smigel MD and Gilman AG (1986) Molecular basis for two forms of the G protein that stimulates adenylate cyclase. *J Biol Chem* **261**:9587-9590.

Rodbell M (1980) The role of hormone receptors and GTP-regulatory proteins in membrane transduction. *Nature* **284**:17-22.

Rodbell M (1995) The complex structure and function of G proteins in cellular communication. *Bull Mem Acad R Med Belg* **150**:316-319.

Rosenberg PB and Hillis AE (2009) Biomarkers for Alzheimer's disease: ready for the next step. *Brain* **132**:2002-2004.

Roth DM, Bayat H, Drumm JD, Gao MH, Swaney JS, Ander A and Hammond HK (2002) Adenylyl cyclase increases survival in cardiomyopathy. *Circulation* **105**:1989-1994.

Roth DM, Gao MH, Lai NC, Drumm J, Dalton N, Zhou JY, Zhu J, Entrikin D and Hammond HK (1999) Cardiac-directed adenylyl cyclase expression improves heart function in murine cardiomyopathy. *Circulation* **99**:3099-3102.

Sadana R and Dessauer CW (2009) Physiological roles for G protein-regulated adenylyl cyclase isoforms: insights from knockout and overexpression studies. *Neurosignals* **17**:5-22.

Schäfer ML, Wong ST, Wozniak DF, Muglia LM, Liauw JA, Zhuo M, Nardi A, Hartman RE, Vogt SK, Lüdke CE, Storm DR and Muglia LJ (2000) Altered stress-induced anxiety in adenylyl cyclase type VIII-deficient mice. *J Neurosci* **20**:4809-4820.

Schnecko A, Witte K, Bohl J, Ohm T and Lemmer B (1994) Adenylyl cyclase activity in Alzheimer's disease brain: stimulatory and inhibitory signal transduction pathways are differently affected. *Brain Res* **644**:291-296.

Scholich K, Wittpoth C, Barbier AJ, Müllenix JB and Patel TB (1997) Identification of an intramolecular interaction between small regions in type 5 adenylyl cyclase that influences stimulation of enzyme activity by $G_{S\alpha}$. *Proc Natl Acad Sci USA* **94**:9602-9607.

Seamon KB and Daly JW (1986) Forskolin: its biological and chemical properties. *Adv Cyclic Nucleotide Protein Phosphorylation Res* **20**:1-150.

Seamon KB, Padgett W and Daly JW (1981) Forskolin: unique diterpene activator of adenylate cyclase in membranes and in intact cells. *Proc Natl Acad Sci USA* **78**:3363-3367.

Shen T, Suzuki Y, Poyard M, Miyamoto N, Defer N and Hanoune J (1997) Expression of adenylyl cyclase mRNAs in the adult, in developing, and in the Brattleboro rat kidney. *Am J Physiol* **273**:C323-330.

Smigel MD (1986) Purification of the catalyst of adenylate cyclase. *J Biol Chem* **261**:1976-1982.

Smit MJ, Verzijl D and Iyengar R (1998) Identity of adenylyl cyclase isoform determines the rate of cell cycle progression in NIH 3T3 cells. *Proc Natl Acad Sci USA* **95**:15084-15089.

Somkuti SG, Hildebrandt JD, Herberg JT and Iyengar R (1982) Divalent cation regulation of adenylyl cyclase. An allosteric site on the catalytic component. *J Biol Chem* **257**:6387-6393.

Steer ML and Salzman EW (1980) Cyclic nucleotides in hemostasis and thrombosis. *Adv Cyclic Nucleotide Res* **12**:71-92.

Storm DR, Hänsel C, Hacker B, Parent A and Linden DJ (1998) Impaired cerebellar long-term potentiation in type 1 adenylyl cyclase mutant mice. *Neuron* **20**:1199-1210.

Sullivan LP and Grantham JJ (1996) Mechanisms of fluid secretion by polycystic epithelia. *Kidney Int* **49**:1586-1591.

Sunahara RK, Beuve A, Tesmer JJ, Sprang SR, Garbers DL and Gilman AG (1998) Exchange of substrate and inhibitor specificities between adenylyl and guanylyl cyclases. *J Biol Chem* **273**:16332-16338.

Sunahara RK, Dessauer CW and Gilman AG (1996) Complexity and diversity of mammalian adenylyl cyclases. *Annu Rev Pharmacol Toxicol* **36**:461-480.

Sunahara RK and Taussig R (2002) Isoforms of mammalian adenylyl cyclase: multiplicities of signaling. *Mol Interv* **2**:168-184.

Sunahara RK, Tesmer JJ, Gilman AG and Sprang SR (1997) Crystal structure of the adenylyl cyclase activator $G_{S\alpha}$. *Science* **278**:1943-1947.

Sutherland EW (1972) Studies on the mechanism of hormone action. *Science* **177**:401-408.

Sutkowski EM, Tang WJ, Broome CW, Robbins JD and Seamon KB (1994) Regulation of forskolin interactions with type 1, 2, 5, and 6 adenylyl cyclases by $G_{S\alpha}$. *Biochemistry* **33**:12852-12859.

Suzuki Y, Shen T, Miyamoto N, Defer N, Matsuoka I and Hanoune J (1997) Changes in the expression of adenylyl cyclases in the rat uterus during the course of pregnancy. *Biol Reprod* **57**:778-782.

Takaichi K, Uchida S and Kurokawa K (1986) High Ca^{2+} inhibits AVP-dependent cAMP production in thick ascending limbs of Henle. *Am J Physiol* **250**:F770-776.

Tang WJ and Gilman AG (1991) Type-specific regulation of adenylyl cyclase by G protein $\beta\gamma$ subunits. *Science* **254**:1500-1503.

Tang WJ and Gilman AG (1992) Adenylyl cyclases. *Cell* **70**:869-872.

Tang WJ and Gilman AG (1995) Construction of a soluble adenylyl cyclase activated by $G_{S\alpha}$ and forskolin. *Science* **268**:1769-1772.

Tang WJ and Hurley JH (1998) Catalytic mechanism and regulation of mammalian adenylyl cyclases. *Mol Pharmacol* **54**:231-240.

Tang WJ, Iniguez-Lluhi JA, Mumby S and Gilman AG (1992) Regulation of mammalian adenylyl cyclases by G-protein α and $\beta\gamma$ subunits. *Cold Spring Harb Symp Quant Biol* **57**:135-144.

Tang WJ, Krupinski J and Gilman AG (1991) Expression and characterization of calmodulin-activated (type I) adenylylcyclase. *J Biol Chem* **266**:8595-8603.

Tang WJ, Stanzel M and Gilman AG (1995) Truncation and alanine-scanning mutants of type 1 adenylyl cyclase. *Biochemistry* **34**:14563-14572.

Taussig R and Gilman AG (1995) Mammalian membrane-bound adenylyl cyclases. *J Biol Chem* **270**:1-4.

Taussig R, Iniguez-Lluhi JA and Gilman AG (1993a) Inhibition of adenylyl cyclase by $G_{i\alpha}$. *Science* **261**:218-221.

Taussig R, Quarmby LM and Gilman AG (1993b) Regulation of purified type 1 and type 2 adenylyl cyclases by G protein $\beta\gamma$ subunits. *J Biol Chem* **268**:9-12.

Taussig R, Tang WJ, Hepler JR and Gilman AG (1994) Distinct patterns of bidirectional regulation of mammalian adenylyl cyclases. *J Biol Chem* **269**:6093-6100.

Tepe NM, Lorenz JN, Yatani A, Dash R, Kranias EG, Dorn GW, 2nd and Liggett SB (1999) Altering the receptor-effector ratio by transgenic overexpression of type 5 adenylyl cyclase: enhanced basal catalytic activity and function without increased cardiomyocyte β-adrenergic signalling. *Biochemistry* **38**:16706-16713.

Tesmer JJ, Sunahara RK, Gilman AG and Sprang SR (1997) Crystal structure of the catalytic domains of adenylyl cyclase in a complex with $G_{s\alpha}$·GTPγS. *Science* **278**:1907-1916.

Torres VE and Harris PC (2006) Mechanisms of Disease: autosomal dominant and recessive polycystic kidney diseases. *Nat Clin Pract Nephrol* **2**:40-55; quiz 55.

Torres VE, Harris PC and Pirson Y (2007) Autosomal dominant polycystic kidney disease. *Lancet* **369**:1287-1301.

Vadakkan KI, Jia YH and Zhuo M (2005) A behavioral model of neuropathic pain induced by ligation of the common peroneal nerve in mice. *J Pain* **6**:747-756.

Villacres EC, Wong ST, Chavkin C and Storm DR (1998) Type 1 adenylyl cyclase mutant mice have impaired mossy fiber long-term potentiation. *J Neurosci* **18**:3186-3194.

Villacres EC, Xia Z, Bookbinder LH, Edelhoff S, Disteche CM and Storm DR (1993) Cloning, chromosomal mapping, and expression of human fetal brain type 1 adenylyl cyclase. *Genomics* **16**:473-478.

Vorherr T, Knopfel L, Hofmann F, Mollner S, Pfeuffer T and Carafoli E (1993) The calmodulin binding domain of nitric oxide synthase and adenylyl cyclase. *Biochemistry* **32**:6081-6088.

Wang H, Ferguson GD, Pineda VV, Cundiff PE and Storm DR (2004) Overexpression of type 1 adenylyl cyclase in mouse forebrain enhances recognition memory and LTP. *Nat Neurosci* **7**:635-642.

Wang H, Gong B, Vadakkan KI, Toyoda H, Kaang BK and Zhuo M (2007) Genetic evidence for adenylyl cyclase 1 as a target for preventing neuronal excitotoxicity mediated by *N*-methyl-D-aspartate receptors. *J Biol Chem* **282**:1507-1517.

Watts VJ and Neve KA (2005) Sensitization of adenylate cyclase by $G_{i/o\alpha}$-coupled receptors. *Pharmacol Ther* **106**:405-421.

Wei J, Wayman G and Storm DR (1996) Phosphorylation and inhibition of type 3 adenylyl cyclase by calmodulin-dependent protein kinase II *in vivo*. *J Biol Chem* **271**:24231-24235.

Whisnant RE, Gilman AG and Dessauer CW (1996) Interaction of the two cytosolic domains of mammalian adenylyl cyclase. *Proc Natl Acad Sci USA* **93**:6621-6625.

Wing DR and Robinson DS (1968) Clearing-factor lipase in adipose tissue. A possible role of adenosine 3',5'-(cyclic)-monophosphate in the regulation of its activity. *Biochem J* **109**:841-849.

Wong ST, Athos J, Figueroa XA, Pineda VV, Schäfer ML, Chavkin CC, Muglia LJ and Storm DR (1999) Calcium-stimulated adenylyl cyclase activity is critical for hippocampus-dependent long-term memory and late phase LTP. *Neuron* **23**:787-798.

Wong ST and Storm DR (2002) Generation of adenylyl cyclase knockout mice. *Methods Enzymol* **345**:206-231.

Wong ST, Trinh K, Hacker B, Chan GC, Löwe G, Gaggar A, Xia Z, Gold GH and Storm DR (2000) Disruption of the type 3 adenylyl cyclase gene leads to peripheral and behavioral anosmia in transgenic mice. *Neuron* **27**:487-497.

Wu ZL, Thomas SA, Villacres EC, Xia Z, Simmons ML, Chavkin C, Palmiter RD and Storm DR (1995) Altered behavior and long-term potentiation in type I adenylyl cyclase mutant mice. *Proc Natl Acad Sci USA* **92**:220-224.

Wuthrich RP, Serra AL and Kistler AD (2009) Autosomal dominant polycystic kidney disease: new treatment options and how to test their efficacy. *Kidney Blood Press Res* **32**:380-387.

Xia Z, Choi EJ, Wang F, Blazynski C and Storm DR (1993) Type 1 calmodulin-sensitive adenylyl cyclase is neural specific. *J Neurochem* **60**:305-311.

Xia Z, Choi EJ, Wang F and Storm DR (1992) The type 3 calcium/calmodulin-sensitive adenylyl cyclase is not specific to olfactory sensory neurons. *Neurosci Lett* **144**:169-173.

Xia Z and Storm DR (1997) Calmodulin-regulated adenylyl cyclases and neuromodulation. *Curr Opin Neurobiol* **7**:391-396.

Yamaguchi T, Pelling JC, Ramaswamy NT, Eppler JW, Wallace DP, Nagao S, Rome LA, Sullivan LP and Grantham JJ (2000) cAMP stimulates the *in vitro* proliferation of renal cyst epithelial cells by activating the extracellular signal-regulated kinase pathway. *Kidney Int* **57**:1460-1471.

Yamamoto M, Ozawa H, Saito T, Hatta S, Riederer P and Takahata N (1997) Ca^{2+}/CaM-sensitive adenylyl cyclase activity is decreased in the Alzheimer's brain: possible relation to type 1 adenylyl cyclase. *J Neural Transm* **104**:721-732.

Yan K and Gautam N (1997) Structural determinants for interaction with three different effectors on the G protein β subunit. *J Biol Chem* **272**:2056-2059.

Yan L, Vatner DE, O'Connor JP, Ivessa A, Ge H, Chen W, Hirotani S, Ishikawa Y, Sadoshima J and Vatner SF (2007) Type 5 adenylyl cyclase disruption increases longevity and protects against stress. *Cell* **130**:247-258.

Yan SZ, Beeler JA, Chen Y, Shelton RK and Tang WJ (2001) The regulation of type 7 adenylyl cyclase by its C_{1b} region and *Escherichia coli* peptidylpropyl isomerase, SlyD. *J Biol Chem* **276**:8500-8506.

Yan SZ, Hahn D, Huang ZH and Tang WJ (1996) Two cytoplasmic domains of mammalian adenylyl cyclase form a $G_{S\alpha}$- and forskolin-activated enzyme *in vitro*. *J Biol Chem* **271**:10941-10945.

Yan SZ, Huang ZH, Andrews RK and Tang WJ (1998) Conversion of forskolin-insensitive to forskolin-sensitive (mouse-type IX) adenylyl cyclase. *Mol Pharmacol* **53**:182-187.

Yan SZ, Huang ZH, Rao VD, Hurley JH and Tang WJ (1997a) Three discrete regions of mammalian adenylyl cyclase form a site for $G_{S\alpha}$ activation. *J Biol Chem* **272**:18849-18854.

Yan SZ, Huang ZH, Shaw RS and Tang WJ (1997b) The conserved asparagine and arginine are essential for catalysis of mammalian adenylyl cyclase. *J Biol Chem* **272**:12342-12349.

Yang B, He B, Abdel-Halim SM, Tibell A, Brendel MD, Bretzel RG, Efendic S and Hillert J (1999) Molecular cloning of a full-length cDNA for human type 3 adenylyl cyclase and its expression in human islets. *Biochem Biophys Res Commun* **254**:548-551.

Yoo B, Iyengar R and Chen Y (2004) Functional analysis of the interface regions involved in interactions between the central cytoplasmic loop and the *C*-terminal tail of adenylyl cyclase. *J Biol Chem* **279**:13925-13933.

Yoshimura M and Cooper DM (1992) Cloning and expression of a Ca^{2+}-inhibitable adenylyl cyclase from NCB-20 cells. *Proc Natl Acad Sci USA* **89**:6716-6720.

Yoshimura M, Wu PH, Hoffman PL and Tabakoff B (2000) Overexpression of type 7 adenylyl cyclase in the mouse brain enhances acute and chronic actions of morphine. *Mol Pharmacol* **58**:1011-1016.

Yu HJ, Ma H and Green RD (1993) Calcium entry *via* L-type calcium channels acts as a negative regulator of adenylyl cyclase activity and cyclic AMP levels in cardiac myocytes. *Mol Pharmacol* **44**:689-693.

Yu HJ, Unnerstall JR and Green RD (1995) Determination and cellular localization of adenylyl cyclase isozymes expressed in embryonic chick heart. *FEBS Lett* **374**:89-94.

Zhang G, Liu Y, Qin J, Vo B, Tang WJ, Ruoho AE and Hurley JH (1997a) Characterization and crystallization of a minimal catalytic core domain from mammalian type 2 adenylyl cyclase. *Protein Sci* **6**:903-908.

Zhang G, Liu Y, Ruoho AE and Hurley JH (1997b) Structure of the adenylyl cyclase catalytic core. *Nature* **386**:247-253.

Zimmermann G and Taussig R (1996) Protein kinase C alters the responsiveness of adenylyl cyclases to G protein α and $\beta\gamma$ subunits. *J Biol Chem* **271**:27161-27166.

Chapter 2

Influence of Divalent Metal Ions on the Regulation of Adenylyl Cyclase Isoforms by Forskolin Analogs

B.1 Abstract

Forskolin (FS) is an invaluable research tool, activating mammalian membranous adenylyl cyclase isoforms 1 to 8 (ACs 1-8). ACs play an important role in transmembrane signaling events of many tissues and represent an interesting drug target. AC isoform-selective FS analogs could serve as potential novel therapeutic approach in the treatment of heart failure or Alzheimer's disease.

Therefore, we examined the effects of FS and six FS derivatives on recombinant ACs 1, 2 and 5. Correlations of the pharmacological parameters of these diterpenes between the different AC isoforms showed a distinct isoform-specific profile. The most intensive differences were found by comparisons between the diterpene potencies on AC1 with AC2 and AC5. Correlations illustrated slopes of 23.4 ± 8.3 and 9.04 ± 3.5, respectively. Additionally, we observed a large influence of the divalent metal ions Mg^{2+} or Mn^{2+} on the catalytic activity. Potencies and efficacies of FS derivatives changed for the same AC isoform, depending on the provided metal ion. The most striking effects of Mg^{2+} and Mn^{2+} on the diterpene profile were observed for AC2. The large inverse agonistic effect of BODIPY-FS on AC2 in presence of Mg^{2+} was considerably reduced in presence of Mn^{2+}. Docking experiments and correlations of the efficacies of diterpenes on the purified catalytic subunit C_1/C_2 of AC plus $G_{S\alpha\text{-}GTP\gamma S}$ did not reveal cation-dependent effects. Thus, we suggest an influence of the structural environment of the catalytic core and the transmembrane domains on cation-dependent diterpene effects.

In conclusion, AC isoforms 1, 2 and 5 exhibited a distinct pharmacological diterpene profile. Additionally, these effects are probably modulated by the divalent metal ions serving as cofactors for AC. However, the currently available docking results are not conclusive to solve the impact of the divalent cations on AC regulation.

B.2 Introduction

Magnesium(II)- and manganese(II)-ions are both essential for human life. Mg^{2+} is the fourth-most abundant metal ion in cells (in moles) and the most abundant free divalent cation (Guerrera *et al*., 2009). Over 300 enzymes, e.g. mammalian adenylyl cyclases (mACs) require the presence of magnesium ions for their catalytic action. ACs are integral plasma proteins, which play a central role in transmembrane signaling. Stimulation of G protein-coupled receptors (GPCRs) is translated *via* G protein activation to the AC-mediated conversion of adenosine 5'-triphosphate (ATP) to the second messenger cyclic adenosine 3',5'-monophosphate (cAMP) (Sutherland, 1972). In mammals, nine membrane-bound AC isoforms (ACs 1-9) are expressed with Mg^{2+} being the physiological cation for AC activity *in vivo* (Sunahara *et al*., 1996; Hanoune and Defer, 2001). The various AC subtypes exhibit tissue-specific expression and play a crucial role e.g. in cardiac contractility and the regulation of kidney or brain function (Hanoune *et al*., 1997; Defer *et al*., 2000). The structure of membranous ACs is characterized by an intracellular *N*- and *C*-terminus, two membrane-spanning domains and two cytosolic loops C_1 and C_2 (Tang and Gilman, 1992; Sunahara *et al*., 1996). C_1 and C_2 form the catalytic core (Tang and Gilman, 1995) and are highly conserved among the different AC isoforms (Sunahara *et al*., 1996).

The catalytic unit of AC also exhibits regulatory sites for divalent cation binding, e.g. Mg^{2+}, by which the activation of the enzymes is directly regulated (Londos and Preston, 1977; Limbird, 1981). Additionally, Mg^{2+} interacts with ATP, the substrate of ACs, forming the biologically active chelate Mg-ATP and thus, preparing the molecule for the nucleophilic attack by ACs (Garbers and Johnson, 1975).

In biological systems, manganese ions (Mn^{2+}) are readily capable of replacing Mg^{2+} under certain conditions (Friedberg, 1974; Feig, 2000). Being a trace nutrient, Mn^{2+} functions as cofactor for numerous enzymes like transferases, hydrolases and oxidoreductases (Crowley *et al*., 2000). Since Mn^{2+} is very similar to Mg^{2+} in terms of its chemical properties, manganese is often exerted as divalent cation in *in vitro* studies (Johnson and Sutherland, 1973). Mn^{2+} can also replace Mg^{2+} as the activating ion for a number of Mg^{2+}-dependent enzymes, e.g. mACs (Johnson and Sutherland, 1973; Cech *et al*., 1980). Additionally, ATP combined with Mn^{2+} effectively forms chelate complexes similar to Mg-ATP and serve as substrate of AC reaction (Garbers and Johnson, 1975; Wei *et al*., 1979). However, differences in

catalytic reactivity of AC have been noted depending on whether Mg^{2+} or Mn^{2+} was served as the metal cofactor (Perkins, 1973; Wald and Popovtzer, 1984).

Eight of the nine mammalian membranous AC subtypes (AC1-AC8) are activated by the diterpene forskolin (FS), a lipophilic substance extracted from the roots of the Indian plant *Coleus forskohlii* (Seamon and Daly, 1986). FS directly interacts with AC and robustly stimulates the enzyme activities. Therefore, it is used as a pharmacologic agent promoting cAMP production *via* AC activation (Seamon and Daly, 1981). Although the FS binding site is located at the interface of the catalytic units of ACs, the physiological counterpart to FS is as yet unidentified. However, FS-containing herbal medicines and life-style products are becoming increasingly popular. Moreover, in a recent study, a forskolin-like molecule was identified in the cyst fluid of patients suffering from polycystic kidney disease (Putnam *et al*., 2007). A great advance in understanding the biochemical differences of the AC isoforms is the development of isoform-specific FS analogs (Onda *et al*., 2001). Isoform-specific forskolin analogs would be of great therapeutic interest, e.g. in the treatment of addiction or heart failure and as spasmolytic or antithrombotic agents (Metzger and Lindner, 1981).

In recent studies, we characterized the effects of different diterpenes on ACs and investigated the interactions of AC with FS analogs in the presence of Mn^{2+} (Pinto *et al*., 2008; 2009). However, the precise contribution of Mg^{2+} in comparison to Mn^{2+} to the pharmacological parameters of diterpenes on AC is still unknown. Here, we investigated the influence of Mg^{2+} and Mn^{2+} on the effects of FS and FS analogs on ACs 1, 2 and 5 and C_1/C_2. By measuring diterpene-dependent cAMP production we observed isoform-specific characteristics of potencies and efficacies. Depending on the presence of Mg^{2+} or Mn^{2+}, the diterpene profiles changed for each AC isoform, indicating a profound effect of the metal ion on AC activity. By docking ligands to the isoform-specific mAC model we aimed at explaining preferences of ligands for both metal ions.

B.3 Materials and Methods

B.3.1 Materials

Baculoviruses encoding ACs 1, 2 and 5 were a gift from Drs. A. G. Gilman (UT Southwestern Medical Center, Dallas, TX, USA) and R. K. Sunahara (University of Michigan Medical School, Ann Arbor, MI, USA). *Spodoptera frugiperda* (Sf9) insect cells were from the American Type Cell Culture Collection (Rockville, MD). FS was purchased from LC Laboratories (Woburn, MA). DMB-FS was from Calbiochem (San Diego, CA). BODIPY-FS was from Molecular Probes (Eugene, OR). All other FS analogs were from Sigma-Aldrich (St. Louis, MO). Stock solutions of FS and FS analogs (10 mM each) were prepared in DMSO and stored at -20°C. Dilutions of FS analogs were prepared in such a way that in all AC assays, a final DMSO concentration of 3% (v/v) was achieved. [α–^{32}P]ATP (3,000 Ci/mmol) was purchased from PerkinElmer (Wellesley, MA). Aluminum oxide (N Super 1) was purchased from MP Biomedicals (Eschwege, Germany). Data were analyzed by linear or non-linear regression using the Prism 5.01 program (GraphPad, San Diego, CA).

B.3.2 Membrane Preparation

Sf9 cell membrane preparation was performed as described (Seifert *et al*., 1998). For membrane preparation Sf9 cells (3.0 x 10^6 cells/mL) were infected with correspondent baculovirus encoding different mammalian ACs (1:100 dilutions of high-titer virus stocks) and cultured for 48 hours. Briefly, cells were harvested and cell suspensions were centrifuged for 10 min at 1,000 x rpm at 4°C. Pellets were resuspended in 30 mL PBS buffer containing 137 mM NaCl, 2.6 mM KCl, 0.5 mM $MgCl_2$, 0.9 mM $CaCl_2$, 1.5 mM KH_2PO_4, 0.8 mM Na_2HPO_4, pH 7.4. After a second centrifugation step of 10 min at 1,000 x rpm and 4°C, the pellets were suspended in 15 mL of lysis buffer (10 mM Tris/HCl, 1 mM EDTA, 0.2 mM phenylmethylsulfonyl fluoride, 10 μg/mL leupeptine and 10 μg/mL benzamide, pH 7.4). Thereafter, homogenization was performed with 20-25 strokes using a Dounce homogenizer. The resultant cell fragment suspension was centrifuged for 5 min at 500 x rpm and 4°C to sediment nuclei. The cell membrane-containing supernatant suspension was centrifuged for 20 min at 18,000 x rpm and 4°C. The supernatant fluid was discarded and cell pellets were again suspended in 20 mL lysis buffer. After a second high-

speed centrifugation step, buffer consisting of 75 mM Tris/HCl, 12.5 mM $MgCl_2$, and 1 mM EDTA, pH 7.4 was added to the membrane pellets. Aliquots of 1 mL of membrane suspension were prepared and stored at -80°C. The protein concentration for each membrane preparation was determined by the lowry method using the Bio-Rad DC protein assay kit (Bio-Rad, Hercules, CA) (Lowry *et al*., 1951).

B.3.3 AC Activity Assay

AC activity was determined essentially as described in the literature (Gille *et al*., 2004). Just before experiments, Sf9 membranes with recombinant ACs were washed by adding assay buffer consisting of 50 mM triethanolamine and 1 mM EGTA, pH 7.4 and then centrifuged with 13,000 x g for 10 min at 4°C. Afterwards, membranes were resuspended with syringes in the sequence 21 G and 27 G and diluted in assay buffer to a protein concentration of 1 μg/μL. For the determination of the effects of FS and FS analogs on AC activity, reaction mixtures contained 7 mM Mn^{2+} or Mg^{2+}, 40 μM ATP, 10 μM GTPγS, 100 μM cAMP, 0.4 mg/mL creatine kinase, 9 mM phosphocreatine, 100 μM IBMX and 0.3 μCi [α–^{32}P]ATP. FS or FS analogs at various concentrations (100 nM – 300 μM) in the presence of 3% (v/v) DMSO were added to the assay tubes. After a preincubation time of 2 min at 30°C, reactions were initiated by the addition of 20 μL of membrane suspension. Reactions were conducted for 10 min at 30°C and were terminated by adding 20 mL of 2.2 N HCl. Denatured protein was precipitated by a 2 min centrifugation at room temperature and 13,500 x g. Sixty μL of the supernatant fluid were transferred onto columns filled with 1.4 g neutral alumina. [^{32}P]cAMP was separated from [α–^{32}P]ATP by elution of the product with 4 mL of 0.1 M ammonium acetate, pH 7.0. Samples were filled up with 10 mL double-distilled water, and [^{32}P]cAMP was determined by liquid scintillation counting of Čerenkov radiation.

B.3.4 Docking FS Derivatives to the Isoform-Specific mAC Model

Five forskolin derivatives were built and energy-minimized by SYBYL program. The docking model mAC protein was generated from the crystal structure of membrane-bound adenylyl cyclase VC_1 and IIC_2 in complex with $G_{S\alpha}$ protein subunit and 2',5'-dideoxy-3'-AMP (PDB ID 1CJU), where co-crystallized forskolin was extracted and used as a reference ligand (Tesmer *et al*., 1999). The charge assigned

to the model protein residues and ligands were described previously (Suryanarayana *et al*., 2009). Two magnesium or manganese ions were assigned in the cyclase active sites. The Goldscore and Chemscore scoring functions were used to rank binding poses. The root mean square deviations (RMSD) represent how well the docked ligand conformations were optimally aligned with the reference co-crystallized forskolin molecule in the model protein structure.

B.4 Results

B.4.1 Overview on the Structures of Forskolin Analogs

In order to characterize the activity of different AC subtypes, we examined the effects of FS and six FS analogs (Fig. **B.1**). We studied FS derivatives missing the OH-group at 1- or 9- position of the diterpene ring structure referred to as 1d(eoxy)- or 9d(eoxy)-FS, respectively. The acetyl group at position 7 is also known to be critical for AC activation by direct interaction with Ser942 (Fig. **B.2**) (Tang and Hurley, 1998; Pinto *et al*., 2009). Thus, we examined one derivative without the 7-acetyl-group (7-deacetyl-FS or 7DA-FS) and one where this acetyl-group switched from 7- to the 6-position (6-acetyl-7-deacetyl-FS or 6A7DA-FS). Additionally, we used FS analogs with bulky substituents like the only relatively water-soluble FS analog 7-deacetyl-7-[*O*-(*N*-methylpiperazino)-γ-butyryl]-FS (DMB-FS) (Laurenza *et al*., 1987) and boron-dipyrro-methene-FS (BODIPY-FS), which can also be used for fluorescent studies (Liu *et al*., 1998; Takahashi *et al*., 2002).

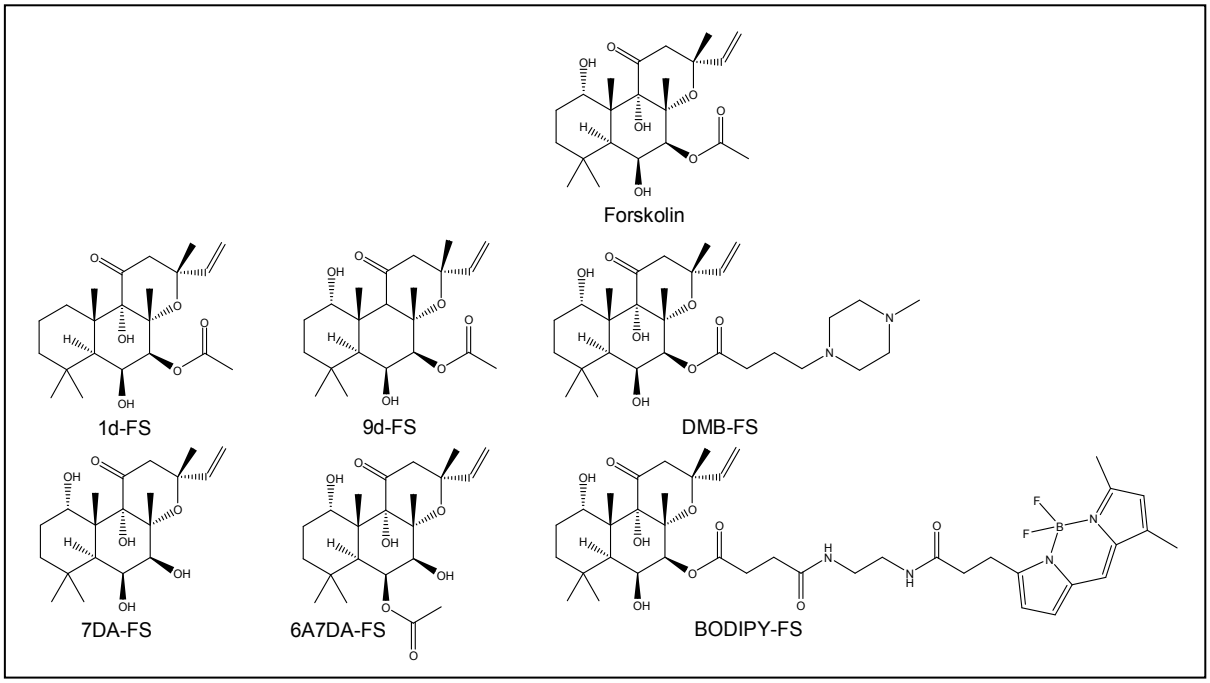

Fig. B.1. Structures of FS and FS analogs analyzed in this study.

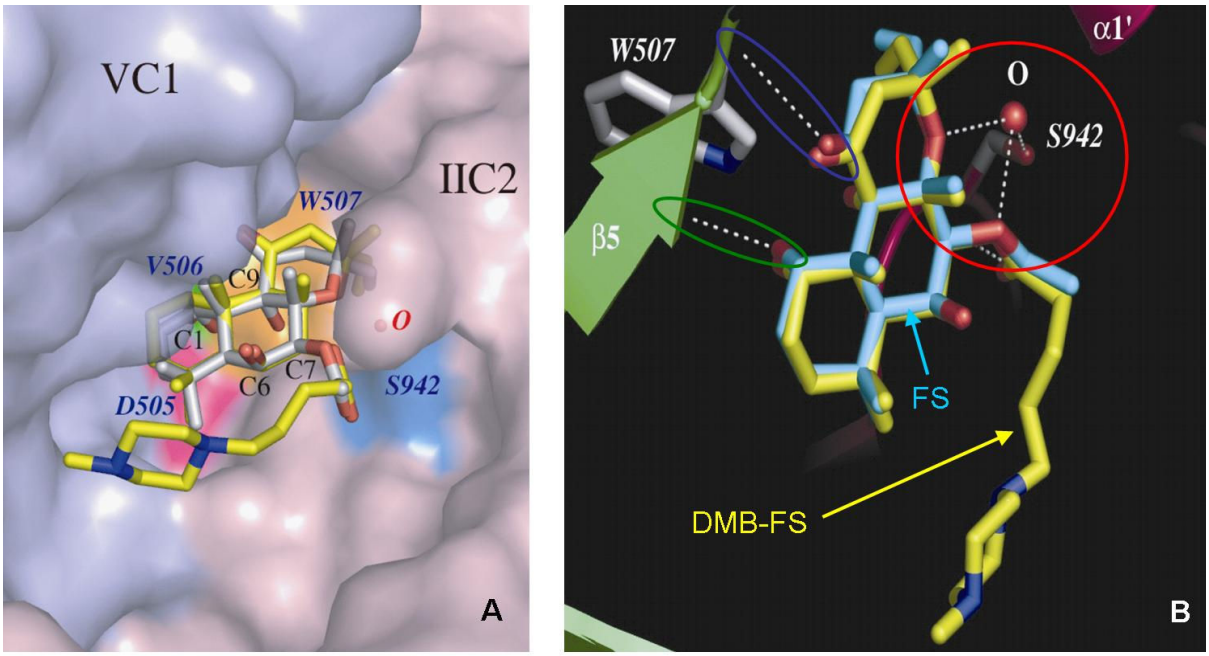

Fig. B.2. Molecular structure of the FS binding site of mAC (Pinto *et al.,* 2009)**.** The AC structure with DMB-FS is superimposed on both C_1 and C_2 domains of the AC structure with FS. **A,** overview of the molecular surface of the diterpene binding pocket coordinated by the purified C_1 protein of AC5 (VC_1/blue) and the C_2 protein of AC2 (IIC_2/pink). FS and DMB-FS are represented in stick models; carbon atoms are gray for FS and yellow for DMB-FS, nitrogens blue, and oxygens red. Amino acids of VC_1 closely related with the 1-OH group of the diterpene are colored magenta for Asp505, green for Val506 and orange for Trp507. A water molecule is coordinated between the Ser942 (cyan) from IIC_2 and two oxygens of the diterpenes. **B,** detailed view of interactions between secondary structure elements of VC_1 (lime), IIC_2 (pink) and the diterpenes FS (cyan) and DMB-FS (yellow), respectively. Side chains of the protein are colored gray, nitrogens blue, and oxygens red. The white dashed lines depict the hydrogen bonds between amino acid residues Val506 of VC_1 and 1-OH of FS (green circle).The hydrogen bonds between Ser942 (IIC_2) and 7-OH of FS *via* a water molecule are highlighted in the red circle, the interaction between Ser508 (VC_1) and 11-OH of FS is shown in the blue circle.

B.4.2 Effects of FS and FS Analogs on Recombinant ACs

Forskolin robustly activates AC isoforms 1, 2 and 5 by the direct interaction of the diterpene with its special binding site at the enzyme (Metzger and Lindner, 1981; Iyengar, 1993). In the AC activity assay, we examined the effects of FS and six FS analogs at increasing concentrations (100 nM to 300 μM) on recombinant ACs 1, 2 and 5. The permanent G protein activator guanosine 5'-[γ-thio]triphosphate as well as the phosphodiesterase inhibitor isobutylmethylxanthine (IBMX) and an ATP regenerating system were always added to the assay system.

Fig. **B.3** shows the characteristic concentration-response curves of the diterpenes on ACs 1, 2 and 5 influenced in the presence of either 7 mM Mg^{2+} or 7 mM Mn^{2+}. The determination of the enzyme activity could be used to characterize each AC isoform by its special rank order of diterpene potencies or efficacies.

Tab. **B.1** summarizes the diterpene effects on the examined ACs under Mg^{2+} conditions. FS and FS analogs activated recombinant AC1 in the presence of Mg^{2+} in the order of potencies BODIPY-FS > DMB-FS ~ FS > 6A7DA-FS > 7DA-FS > 9d-FS. The order of efficacies was 9d-FS ~ DMB-FS ~ 7DA-FS > 6A7DA-FS > BODIPY-FS >> 1d-FS (ineffective).

In contrast, the pharmacological profile of AC2 differed considerably from the other ACs. When Mg^{2+} was the divalent cation, all diterpenes except BODIPY-FS showed lower potencies as compared to ACs 1 and 5 yielding the rank order BODIPY-FS >> FS ~ DMB-FS > 9d-FS > 7DA-FS. A special effect was found with 6A7DA-FS at AC2. In particular, the concentration-dependent effect of 6A7DA-FS revealed an inhibition of AC activity at low concentrations (EC_{50}_1: 1.8 ± 5.5 μM), whereas 6A7DA at high concentrations increased enzyme activity (EC_{50}_2: 61.2 ± 28.6 μM) (Fig. **B.3C**). The maximum inhibition of AC2 was determined at a concentration of 10 μM 6A7DA-FS yielding ~ -20% related to the maximum stimulation of 300 μM FS on AC2. Thereafter, AC activity increased to a level of ~ +20% relative AC activity. BODIPY-FS exhibited a very large inhibitory effect of -115.9 ± 17.5 % relative to the maximum stimulation of 300 μM FS on AC2. The order of efficacy was FS > DMB-FS ~ 7DA-FS > 9d-FS > 6A7DA-FS >> 1d-FS (ineffective) > BODIPY-FS.

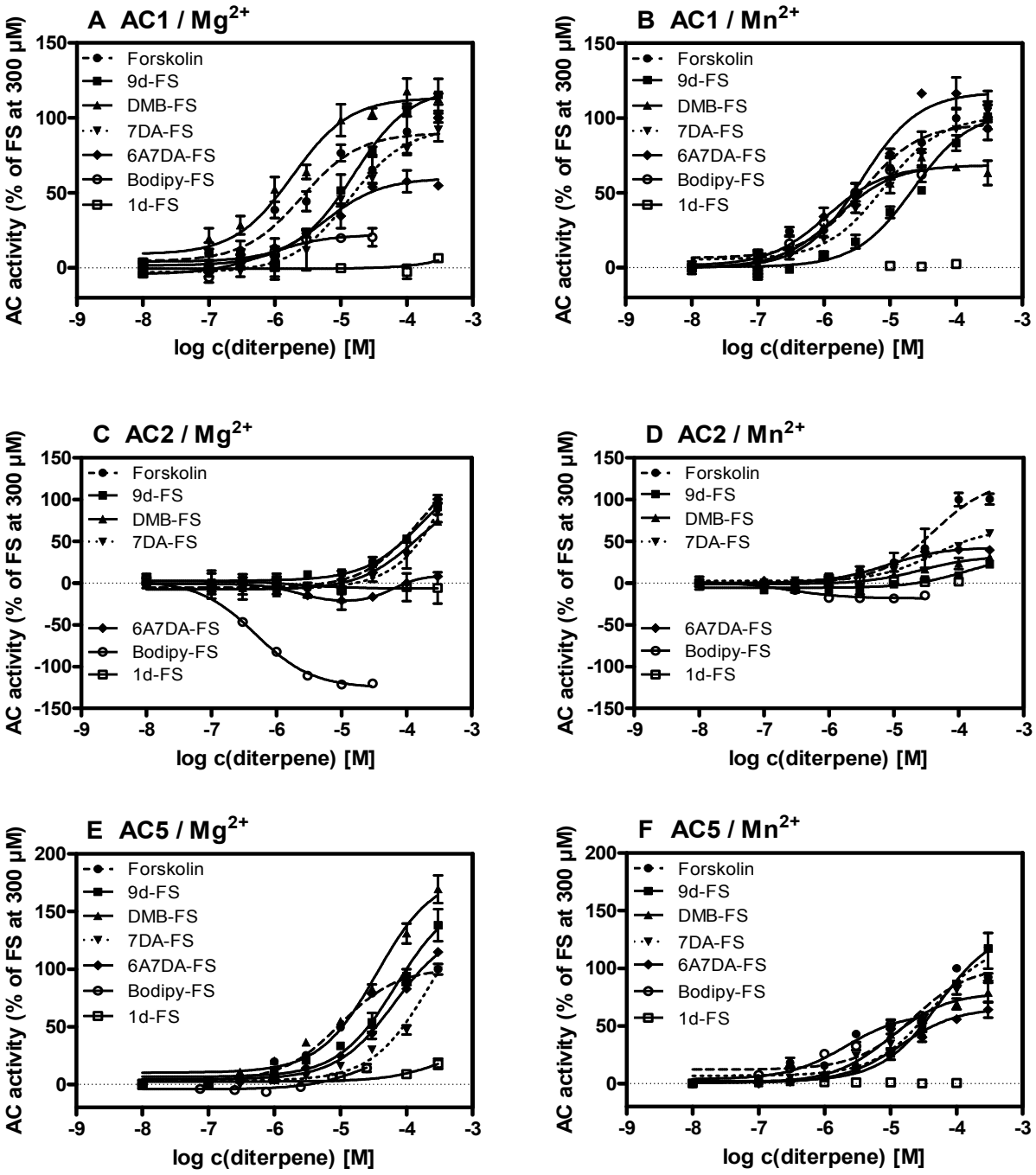

Fig. B.3. Effects of FS and FS analogs on ACs 1, 2 and 5. AC activity was determined as described in "Materials and Methods" for increasing concentrations of different diterpenes (100 nM – 300 µM). Tubes were incubated for 10 min at 30°C. **A**, concentration response curves of various diterpenes on AC1 in presence of Mg^{2+}. **B**, diterpene effects on AC1 in presence of Mn^{2+}. **C**, concentration response curves of different diterpenes on AC2 in presence of Mg^{2+}. **D**, effects of FS and analogs on AC2 under Mn^{2+} conditions. **E**, effects of various diterpenes on AC5 in presence of Mg^{2+}. **F**, diterpene effects on AC5 under Mn^{2+} conditions. Data shown are representative results (mean ± SD) of one of 2-5 experiments performed in duplicates or triplicates. The efficacy for each analog was determined by dividing the maximal stimulation obtained for the analog by the maximum stimulation obtained by treatment with 300 µM FS expressed in percent.

Tab. B.1. Potencies and efficacies of FS and FS analogs on recombinant ACs 1, 2 and 5 in the presence of 7 mM Mg^{2+}.

Mg^{2+}	AC1		AC2		AC5	
Diterpene	**EC_{50} [μM]**	**Efficacy [%]**	**EC_{50} [μM]**	**Efficacy [%]**	**EC_{50} [μM]**	**Efficacy [%]**
Forskolin	3.3 ± 1.9	100	47.2 ± 8.1	100	4.6 ± 1.5	100
DMB-FS	2.5 ± 0.8	101.5 ± 11.0	50.5 ± 22.8	93.5 ± 1.7	26.2 ± 11.0	190.4 ± 42.6
6A7DA-FS	6.2 ± 1.7	69.9 ± 9.2	EC_{50}_1: 1.8 ± 5.5 EC_{50}_2: 61.2 ± 28.6	22.9 ± 1	52.1 ± 16.7	99.6 ± 11.3
7DA-FS	14.1 ± 3.9	99.2 ± 8.7	507 ± 196	93.6 ± 21.6	215 ± 91.4	103.3 ± 11.1
9d-FS	16.8 ± 3.0	103.2 ± 13.9	242 ± 113	79.5 ± 10.9	84.2 ± 41.5	138.1 ± 27.0
1d-FS	ineffective	11.1 ± 4.7	ineffective	1.7 ± 3.4	ineffective	11.6 ± 6.3
BODIPY-FS	0.7 ± 0.3	20.0 ± 2.9	0.5 ± 0.04	-115.9 ± 17.5	18.3 ± 9.7	13.2 ± 1.7

AC activities were determined as described in “Materials and Methods”. Reaction mixtures contained 7 mM Mg^{2+}, [α–^{32}P]ATP (0.3 μCi/tube), 10 μM GTPγS, 100 μM cAMP, 0.4 mg/mL creatine kinase, 9 mM phosphocreatine, 100 μM IBMX and diterpenes at concentrations from 100 nM – 300 μM. Data were analyzed by non-linear regression to determine the EC_{50}-values. The efficacy for each analog was determined by dividing the maximal stimulation obtained for the analog by the maximum stimulation obtained by treatment with 300 μM FS expressed in percent.

The Mg^{2+}-dependent rank order of potencies on AC5 was FS > BODIPY-FS > DMB-FS > 6A7DA-FS > 9d-FS > 7DA-FS. DMB-FS generated a remarkably high enzyme activity of 190.4 ± 42.6 % related to the stimulation of 300 μM FS. The order of efficacies on AC5 was DMB-FS >> 9d-FS > 7DA-FS ~ FS ~ 6A7DA-FS > BODIPY-FS ~ 1d-FS.

Tab. B.2. Effects of FS and FS analogs for recombinant ACs 1, 2 and 5 in the presence of 7 mM Mn^{2+}.

Mn^{2+}	AC1		AC2		AC5	
Diterpene	**EC_{50} [μM]**	**Efficacy [%]**	**EC_{50} [μM]**	**Efficacy [%]**	**EC_{50} [μM]**	**Efficacy [%]**
Forskolin	3.3 ± 1.3	100	38.4 ± 14.9	100	17.8 ± 6.5	100
DMB-FS	2.8 ± 1.6	65.4 ± 8.9	50.8 ± 31.2	46.0 ± 14.5	10.9 ± 1.0	81.4 ± 14.3
6A7DA-FS	3.0 ± 1.0	110 ± 2.2	16.7 ± 7.4	69.6 ± 3.5	13.4 ± 3.4	69.8 ± 7.1
7DA-FS	9.3 ± 1.7	108.8 ± 4.6	65.1 ± 43.0	57.4 ± 3.1	38.2 ± 6.3	124.2 ± 12.9
9d-FS	17.0 ± 3.3	98.3 ± 3.7	127 ± 31.8	29.5 ± 6.2	51.3 ± 2.8	108.1 ± 12.9
1d-FS	ineffective	5.5 ± 4.3	ineffective	0 ± 0	ineffective	0.5 ± 0.4
BODIPY-FS	1.1 ± 0.2	73.1 ± 10.3	0.17 ± 0.07	-22.7 ± 11.7	2.7 ± 1.1	68.5 ± 9.3

AC activities were determined as described in “Materials and Methods”. Reaction mixtures contained 7 mM Mn^{2+}, [α–^{32}P]ATP (0.3 μCi/tube), 10 μM GTPγS, 100 μM cAMP, 0.4 mg/mL creatine kinase, 9 mM phosphocreatine, 100 μM IBMX and diterpenes at concentrations from 100 nM – 300 μM. Data were analyzed by non-linear regression to determine the EC_{50}-values. The efficacy for each analog was determined by dividing the maximal stimulation obtained for the analog by the maximum stimulation obtained by treatment with 300 μM FS expressed in percent.

The replacement of Mg^{2+} by Mn^{2+} had a profound influence on the action of FS and FS analogs on ACs.

Tab. **B.2** documents the Mn^{2+} effects on AC activation, revealing changes in the pharmacological profiles of the AC isoforms. Although the rank order of potencies on AC1 did not change, the order of efficacies changed to 6A7DA-FS ~ 7DA-FS > FS ~ 9d-FS > BODIPY-FS > DMB-FS >> 1d-FS (ineffective).

The influence of the cation species is most clearly seen with the effect of 6A7DA-FS on AC2 (Fig. **B.3D**). In the presence of Mn^{2+}, only stimulation on AC2 by 6A7DA-FS without inhibition at low concentrations was determined. Additionally, the inhibitory effect of BODIPY-FS was much smaller under Mn^{2+} conditions as compared to the presence of Mg^{2+} and reached only -22.7 ± 11.7 % related to FS

stimulation at 300 μM. AC2 utilizing Mn-ATP as substrate yielded the rank order of potencies BODIPY-FS >> 6A7DA-FS > FS > DMB-FS > 7DA-FS > 9d-FS. The order of efficacies on AC2 in presence of Mn^{2+} was FS > 6A7DA-FS > 7DA-FS > DMB-FS > 9d-FS > 1d-FS (ineffective) > BODIPY-FS.

When the effects of FS analogs on AC5 were assayed using Mn^{2+}, the order of potencies showed moderate variations compared to Mg^{2+} conditions: BODIPY-FS > DMB-FS ~ 6A7DA-FS > FS > 7DA-FS > 9d-FS. The rank order of efficacies was 7DA-FS > 9d-FS > FS > DMB-FS > 6A7DA-FS ~ BODIPY-FS >> 1d-FS. Interestingly, maximal relative AC stimulation on AC5 is lower for all diterpenes except BODIPY-FS in presence of Mn^{2+} than in presence of Mg^{2+}. However, absolute values of AC activity were higher with Mn^{2+} compared to Mg^{2+} (data not shown).

B.4.3 Comparison of the Biochemical Profiles of Recombinant AC Isoforms

For each AC isoform we determined a characteristic diterpene profile, distinguishing the different AC subtypes. Linear regression analysis assists to illustrate differences in enzyme activities. In the presence of Mg^{2+}, correlations of the EC_{50}-values on ACs 1, 2 and 5 with each other identified differences in their pharmacological profiles. As shown in Fig. **B.4A** and **B**, stimulatory potencies on AC1 compared to AC2 and AC5 resulted in very steep slopes of 23.4 ± 8.3 and 9.04 ± 3.5, respectively. If the pharmacological profiles of two different AC isoforms under comparison are identical, a slope of 1.0 should be obtained. Thus, remarkable differences in the diterpene profile were obtained presenting lower affinities of FS analogs to AC5 as compared to AC1 and very low potencies on AC2 (Fig. **B.4A** and **B**). The corresponding correlation coefficients (r^2) of 0.73 and 0.62 differ considerably from unity and various diterpenes show very different deviations from the ideal correlation line with a slope of 1.0. Therefore, the profound divergence of the obtained correlation lines from the ideal correlation line is a result of both, the unique biochemical properties of the different AC isoforms and the specific nature of the individual diterpenes.

The correlation of AC2 and AC5 shown in Fig. **B.4C**, revealed a slope of 0.41 ± 0.04 with an r^2 of 0.97 indicating that FS and the six FS analogs bind only with less than half of the affinity to AC2 than to AC5 in presence of Mg^{2+}.

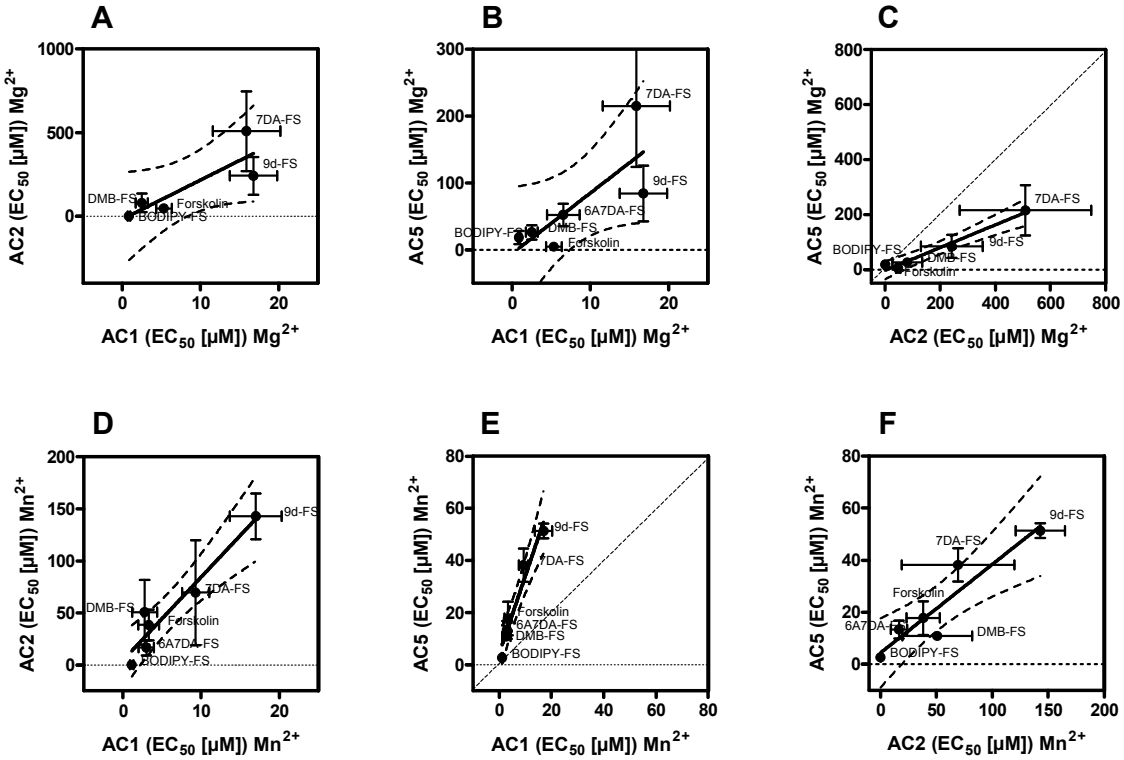

Fig. B.4. Correlation of the potencies of FS analogs on the different AC isoforms. A, correlation of AC1 *vs.* AC2 in presence of Mg^{2+} (r^2 = 0.73; slope = 23.4 ± 8.3; p = 0.07). **B**, correlation of AC1 *vs.* AC5 under Mg^{2+} conditions (r^2 = 0.62; slope = 9.04 ± 3.5; p = 0.06). **C**, correlation of AC2 with AC5 in presence of Mg^{2+} (r^2 = 0.97; slope = 0.41 ± 0.04; p = 0.002). **D**, correlation of AC1 *vs.* AC2 under Mn^{2+} conditions (r^2 = 0.92; slope = 8.00 ± 1.2; p = 0.003). **E**, correlation of AC1 with AC5 in the presence of Mn^{2+} (r^2 = 0.94; slope = 3.0 ± 0.36; p = 0.001). **F**, correlation of AC2 and AC5 under Mn^{2+} conditions (r^2 = 0.86; slope = 0.34 ± 0.07; p = 0.008). Note the different scales of the x- and y-axes in **A**, **B**, **D** and **F**. Comparisons were analyzed by linear regression; the dashed lines indicate 95% confidence intervals. The diagonal dotted line has a slope of 1.0 and represents a theoretical curve for identical values.

The influence of Mn^{2+} revealed isoform-specific patterns of EC_{50}-values determined for FS and FS analogs. Consistently for all diterpenes (r^2 ~ 1), the stimulatory potencies on AC1 compared to AC2 and AC5 were considerably higher, expressed by slopes of 8.0 ± 1.2 for AC1 *vs*. AC2 and 3.0 ± 0.36 for AC1 *vs.* AC5 (Fig. **B.4D**-**F**).

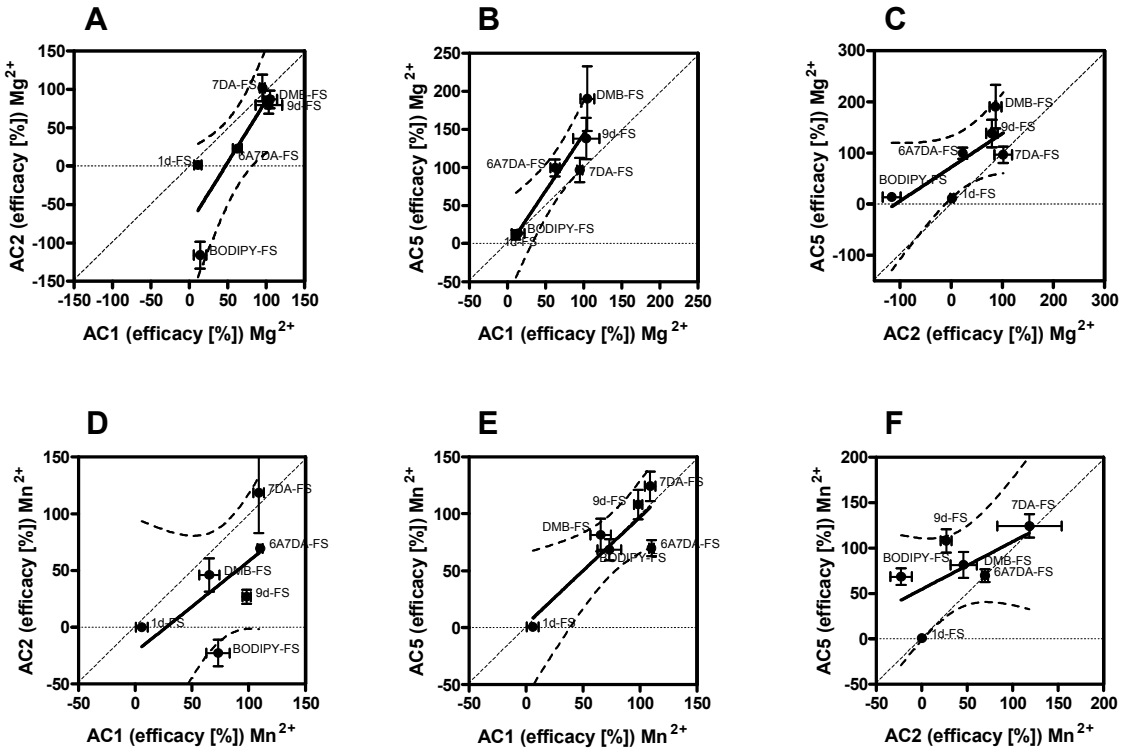

Fig. B.5. Correlation of the efficacies of the diterpenes on each recombinant AC isoform compared to each other. A, correlation of AC1 *vs.* AC2 in presence of Mg^{2+} (r^2 = 0.75; slope = 1.61 ± 0.5; p = 0.026). **B**, correlation of AC1 *vs.* AC5 under Mg^{2+} conditions (r^2 = 0.86; slope = 1.49 ± 0.3; p = 0.008). **C**, correlation of AC2 with AC5 in presence of Mg^{2+} (r^2 = 0.59; slope = 0.66 ± 0.28; p = 0.074). **D**, correlation of AC1 *vs.* AC2 under Mn^{2+} conditions (r^2 = 0.39; slope = 0.80 ± 0.50; p = 0.19). **E**, correlation of AC1 with AC5 in the presence of Mn^{2+} (r^2 = 0.76; slope = 0.94 ± 0.27; p = 0.02). **F**, correlation of AC2 and AC5 under Mn^{2+} conditions (r^2 = 0.38; slope = 0.52 ± 0.33; p = 0.19). Comparisons were analyzed by linear regression; the dashed lines indicate 95% confidence intervals. The diagonal dotted line has a slope of 1.0 and represents a theoretical curve for identical values.

Focusing on the comparison of the efficacies determined for the diterpenes on ACs 1, 2 and 5, no similarity was found under Mg^{2+} conditions (Fig. **B.5A**-**C**). Independently from the divalent metal ion, the maximum stimulation of the different ACs by FS analogs does not yield a uniform picture (Fig. **B.5**). Some substances like 7DA-FS or DMB-FS stimulate ACs 1, 2 or 5 more effectively, whereas other compounds, e.g. 6A7DA-FS or BODIPY-FS, yield lower AC activity in some cases, reflected by data points outside the 95% confidence interval. Under Mn^{2+} conditions correlations of efficacies of FS analogs on AC1 with AC2 or AC5, respectively, are characterized by slopes close to 1.0, but the correlation coefficients are very low (r^2 = 0.39, r^2 = 0.76) (Fig. **B.5D** and **E**). Thus, no correlation could be detected for the

efficacies of the different AC subtypes among each other with Mn^{2+} used as the divalent cation ($p > 0.01$) (Fig. **B.5D**-**F**).

The correlations shown in Fig. **B.4** and **B.5** do not only illustrate differences in the diterpene profiles of the different AC isoforms, they also point to the high impact of the divalent cations on AC reaction. In the presence of either Mg^{2+} or Mn^{2+}, biochemical parameters were clearly modulated yielding considerable variations of the regression profiles. In Fig. **B.4**, a clear influence of the divalent metal ion on the potencies of the diterpenes is documented. However, the impact of Mg^{2+} or Mn^{2+} on the efficacies is smaller than the effects on the potencies of FS analogs (Fig. **B.5**).

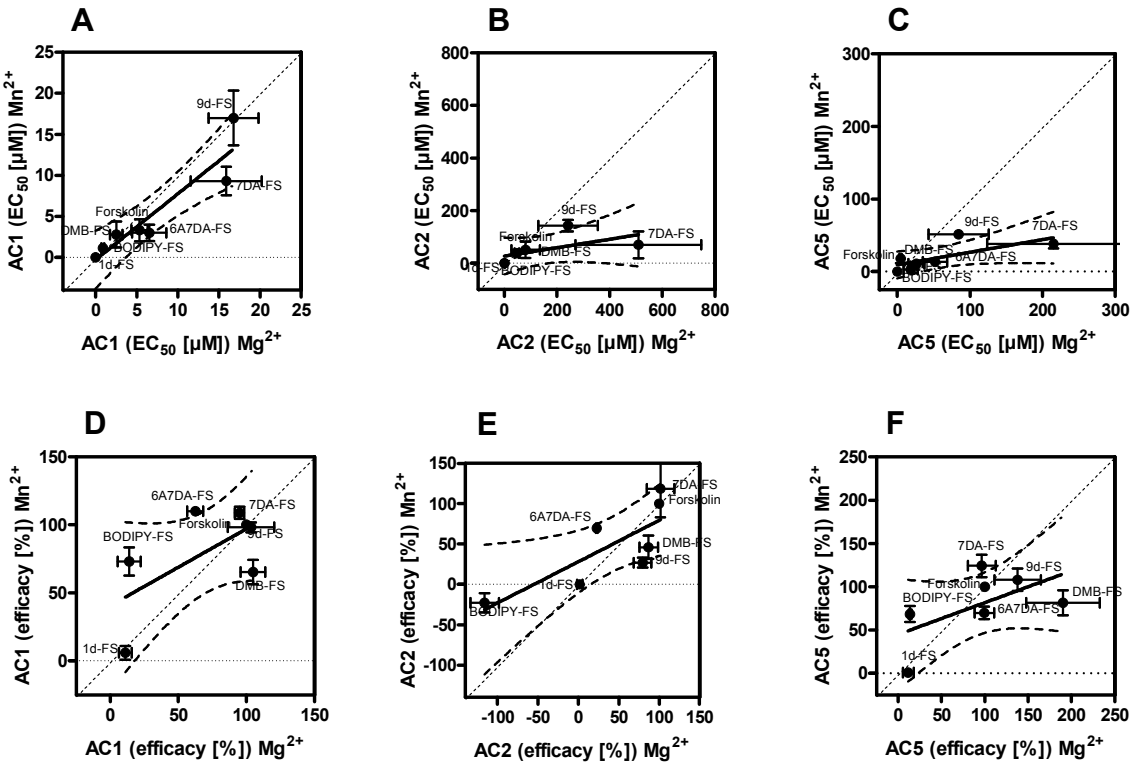

Fig. B.6. Correlation of potencies and efficacies of FS and FS analogs under Mg^{2+} conditions *vs.* under Mn^{2+} conditions. A-**C**, correlation of isoform-specific EC_{50}-values determined in presence of Mg^{2+} *vs.* in presence of Mn^{2+}. **D**-**F**, correlation of the efficacies on ACs 1, 2 and 5, respectively, Mg^{2+} conditions *vs.* Mn^{2+} conditions. **A**, $r^2 = 0.86$; slope = 0.80 ± 0.2; $p = 0.0028$. **B**, $r^2 = 0.36$; slope = 0.16 ± 0.11; $p = 0.21$. **C**, $r^2 = 0.49$; slope = 0.17 ± 0.08; $p = 0.08$. **D**, $r^2 = 0.41$; slope = 0.56 ± 0.18; $p = 0.12$. **E**, $r^2 = 0.61$; slope = 0.51 ± 0.18; $p = 0.04$. **F**, $r^2 = 0.34$; slope = 0.37 ± 0.23; $p = 0.17$. Data were analyzed by linear regression; the dashed lines indicate 95% confidence intervals. The diagonal dotted line has a slope of 1.0 and represents a theoretical curve for identical values.

To highlight the AC-sensitivity to divalent cations, we compared the corresponding pharmacological parameters of each AC isoform determined in use of Mg^{2+} with those in presence of Mn^{2+} (Fig. **B.6**). Striking effects on the diterpene profile depending on whether Mg^{2+} or Mn^{2+} serves the role of cation cofactor are confirmed for AC2 and AC5 (Fig. **B.6B**, **C**, **E** and **F**). The lowest impact of the cations was determined for the potencies of AC1 (r^2 = 0.86; slope = 0.80 ± 0.2) (Fig. **B.6A**). All other correlations showed clear deviations from theoretical identity with slopes and r^2 of 1.0.

In our previous work (Pinto *et al*., 2009), we determined efficacies of FS and analogs on C_1/C_2 catalytic activity plus $G_{S\alpha\text{-}GTP\gamma S}$ either in presence of Mg^{2+} or Mn^{2+} (Tab. **B.3**). Correlating these data, we found that the cation effect is less prominent in case of the purified catalytic subunit C_1/C_2 of AC plus $G_{S\alpha\text{-}GTP\gamma S}$ (Fig. **B.7**). Only 6A7DA-FS and 9d-FS differ from the theoretical curve for identical values shown as the dotted line in Fig. **B.7**.

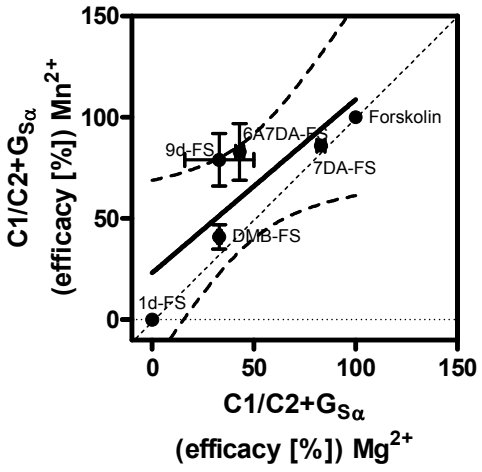

Fig. B.7. Correlation of efficacies of FS and analogs on C_1/C_2 catalytic activity plus $G_{S\alpha\text{-}GTP\gamma S}$. The data of Tab. **B.3** were analyzed by linear regression; the dashed lines indicate 95% confidence intervals. The diagonal dotted line has a slope of 1.0 and represents a theoretical curve for identical values.

	C_1/C_2 + $G_{S\alpha}$	
Diterpene	**Efficacy [%] Mg^{2+}**	**Efficacy [%] Mn^{2+}**
Forskolin	100	100
DMB-FS	33 ± 1	41 ± 6
6A7DA-FS	43 ± 2	83 ± 14
7DA-FS	83 ± 2	86 ± 3
9d-FS	33 ± 17	79 ± 13
1d-FS	ineffective (0)	0.5 ± 0.4

Tab. B.3. Efficacies of diterpenes for activation of C_1/C_2 catalytic activity. Data were taken from (Pinto *et al*., 2009). Experiments were conducted in the presence of Mg^{2+} or Mn^{2+} (10 mM each), and in presence of C_1 (3 nM), C_2 (15 nM) plus $G_{S\alpha\text{-}GTP\gamma S}$ (50 nM).

B.4.4 Docking Results for mAC to Forskolin Derivatives

By docking FS and analogs to the mAC protein, we aimed to predict preferences of diterpenes for binding to AC in the presence of Mg^{2+} or Mn^{2+}. However, the docking preferences of the ligands were about the same for both metal ions. For Mg^{2+} ions as well as for Mn^{2+} ions, the resulting order was DMB-FS > 9d-FS > FS > 1d-FS > 7DA-FS > 6A7DA-FS (Tab. **B.4**). Thus, the docking method appeared to be insufficiently to reproduce the effects of the divalent cations.

Tab. B.4. Results of docking studies for mAC to FS and FS analogs.

Ligands	Mg^{2+}		Mn^{2+}	
	Fitness	RMSD	Fitness	RMSD
FS	40.32	0.603	39.4	0.574
DMB-FS	48.50	1.030	50.73	0.997
1d-FS	30.22	2.649	29.10	2.622
9d-FS	44.38	2.345	43.80	2.341
7DA-FS	27.41	2.310	26.62	2.259
6A7DA-FS	24.69	2.422	25.94	2.540

Five forskolin derivatives were built and energy-minimized by SYBYL program. The docking was generated on a model mAC protein, i.e. the crystal structure of membrane-bound AC VC_1 and IIC_2 in complex with $G_{S\alpha}$ protein subunit and 2',5'-dideoxy-3'-AMP (PDB ID 1CJU). Co-crystallized forskolin was used as a reference ligand. The root mean square deviations (RMSD) represent the goodness of alignment compared to the reference ligand in the model protein structure.

B.5 Discussion

B.5.1 Interaction of Diterpenes with mAC Isoforms

Forskolin is an essential tool for the investigation of AC activity. FS and the different FS analogs interact with the catalytic subunit of all mAC isoforms except type 9 (Seamon and Daly, 1981; Tang and Gilman, 1995). Yan *et al*. identified a mutation in one single amino acid in the C_2 domain of AC9 being responsible for the loss of activation by FS (Yan *et al*., 1997). The change of this amino acid Tyr1082 to the highly conserved leucine of FS-sensitive ACs 1 to 8 can confer both binding of FS to, and activation of AC9 (Zhang *et al*., 1997; Yan *et al*., 1998).

Due to its diterpene structure, interactions between FS and AC are predominantly hydrophobic involving ten aliphatic and aromatic side chains within the FS binding pocket (Zhang *et al*., 1997). The interactions of mACs and FS are highly conserved among the FS-sensitive ACs 1 to 8. Crystallographic studies showed a crucial role of the hydrogen bonds between the 1-OH group of FS and the backbone oxygen of Val506 at the C_1 catalytical domain of AC (Fig. **B.2**) (Sutkowski *et al*., 1994; Tesmer *et al*., 1997). Thus, the missing 1-OH group at 1d-FS yielded an antagonizing effect at all AC isoforms due to the loss of the interaction with Val506. The 9-OH group of FS resides in a binding region at AC without any hydrogen bonds, just set in a close distance to the hydrogen bond of 1-OH (Zhang *et al*., 1997). This only indirect interaction of 9d-FS with AC was reflected by effective stimulation of ACs 1 and 5. This indicates that the interactions between the 9-OH group of the diterpene and the C_1 domain of AC1 or AC5 are of less importance for catalysis. However, on AC2 the missing 9-OH group reduces efficacy, particularly in presence of Mn^{2+}. This may be due to a further, as yet unidentified hydrogen bond between the 9-OH group and this AC isoform. The absence of the acetyl-group at position 7 was tolerated well by all ACs, as is evident from effective AC stimulation. However, it resulted in a decrease in potency compared to FS. These results are consistent with the evidence of Zhang *et al.* that the interaction of the 7-acetyl-group with Ser942 is important but not essential for FS activity (Fig. **B.2**) (Zhang *et al*., 1997). Additionally, the switch of the acetyl-group from position 7 to 6 resulted in effective stimulation of ACs 1 and 5. Since the efficacy of 6A7DA-FS on AC2 was smaller, the 6-acetyl-substitution seems to partially prevent this isoform from catalysis. Surprisingly, the bulky FS analog BODIPY-FS, originally introduced as fluorescent probe for

localization of ACs in intact cells (Liu *et al*., 1998; Takahashi *et al*., 2002), showed considerable inverse agonistic effects on AC2 in presence of Mn^{2+} and to a larger extent in the presence of Mg^{2+}. Previously, we described the position of the BODIPY-group outside the FS binding pocket during interaction with AC (Pinto *et al*., 2008). Probably, there is a distinct environment of the catalytic core at AC2 with several amino acids surrounding the BODIPY-substituent differently compared to the other ACs. The exceedingly effective AC5 activation by DMB-FS suggests that the DMB-group exhibits favorable interactions with this isoform.

Studying the diterpene effects on the purified catalytic subunits C_1/C_2, most of the FS analogs yield similar efficacies, particularly in the presence of Mn^{2+}. Compared to the corresponding efficacies on recombinant ACs 1, 2 and 5, the efficacies on C_1/C_2 are lower in all cases, except compared to AC2 with Mn^{2+}. Although the functional groups of the crucial amino acids are similar in all examined AC isoforms (Tang and Hurley, 1998), the non-homologous regions of AC seem to modify diterpene binding. Mou *et al.* demonstrated by mutational analysis of two non-conserved amino acids, that residues outside the catalytic site also influence isoform selectivity (Mou *et al*., 2005). Additionally, an involvement of some sidechains of the transmembrane domains in AC catalysis is postulated by binding the nucleotide substrate, stabilizing the transition state and neutralizing the negative charge of the PP_i leaving group (Tesmer and Sprang, 1998). Thus, the structural environment of the catalytic core influences the confomational change of the catalytic core undergoing from the inactive “open” to the active “closed” domain arrangement.

In agreement with our previous study, all seven diterpenes affect the examined AC isoforms in a characteristic manner (Pinto *et al*., 2008). Correlations of the biochemical parameters illustrate characteristic properties of the different AC isoforms, suggesting that not only the highly conserved amino acids essential for FS binding have an influence on diterpene affinity (Iyengar, 1993; Tang and Hurley, 1998). Moreover, the significant differences in the structural environment of the catalytic core and the transmembrane domains between the distinct AC isoforms modify diterpene binding indirectly (Sunahara *et al*., 1996; Tang and Hurley, 1998).

This hypothesis will be further examined in molecular modeling studies based on the mAC crystal structure adopted in the inactive open conformation or the catalytically active closed structure (Tesmer *et al*., 1997). FS analogs can be modeled in both conformations to illustrate differences in the residues responsible for

the arrangement of the diterpenes in the binding pocket. Additionally, crystallographic studies should detect conformational changes after binding of diterpenes to the catalytic core. Unfortunately, at first issues concerning the solubility of the diterpenes and the stability of the protein complex have to be handled successfully.

B.5.2 Comparison of Mg^{2+} *vs.* Mn^{2+} as Divalent Metal Ions

ACs require the binding of metal ions for catalytic activity (Seamon and Daly, 1981; Johnson *et al*., 1989; Dessauer *et al*., 1997). Tesmer *et al.* demonstrated the binding of two metal ions in a crystal structure of the C_1/C_2-substrate complex (Tesmer *et al*., 1999). The first metal ion (metal A) is coordinated to the aspartic acid residues Asp396 and Asp440 and a water molecule (Tesmer *et al*., 1999). This ion serves as Lewis acid and enhances the intracellular nucleophilic attac on the 3'-OH of ATP by the α-phosphate (Zimmermann *et al*., 1998; Tesmer *et al*., 2000). The second metal ion (metal B) is chelated by Asp396, Asp440 and the carbonyl oxygen of Ile397 (Tesmer and Sprang, 1998). In closed conformation of the enzyme, it is coordinated to the β- and γ-phosphates of the substrate and stabilizes the transition state (Mou *et al*., 2005).

Mg^{2+} or Mn^{2+} can satisfy this cation requirement and influence the binding of activators such as FS and FS analogs (Cech *et al*., 1980). In this study, we focused on the role of metal-enzyme interactions with Mg^{2+} and Mn^{2+} ions as divalent cations. Comparisons of potencies and efficacies determined with FS and its analogs in relation to the divalent metal ion showed significant influence of the metal cofactor on enzyme activity. In previous studies with mACs, we already obtained differential impacts of Mg^{2+} and Mn^{2+} on inhibitors like MANT-nucleotides (Gille and Seifert, 2003; Gille *et al*., 2004) or activators like FS and analogs (Göttle *et al*., 2009; Pinto *et al*., 2009). In most cases, the exchange of Mn^{2+} against Mg^{2+} increased potencies and efficacies of inhibitors as well as of activators. Additionally, the determination of kinetic parameters showed a preference of Mn^{2+} at AC isoforms, supporting the view that the metal ions interact differentially with ACs (Gille *et al*., 2004; Göttle *et al*., 2009). These data indicate that Mn^{2+} is a much more effective activator than the physiological ligand Mg^{2+} (Mou *et al*., 2005). Additionally, different AC subtypes yield distinct signal recognition using Mg^{2+} or Mn^{2+} with effects shown on basal activity as well as on FS activated ACs (Pieroni *et al*., 1995).

Analysis of crystal structures and docking experiments obtained only small global and local differences between the arrangements of Mg^{2+} and Mn^{2+} complexes (Gille *et al*., 2004). Electron density for the B-site metal ion is well defined with Mg^{2+} and Mn^{2+}, but density for A-site is weaker than that for the B-site in the Mg^{2+}-bound complex (Mou *et al*., 2005). Additionally, weak electrostatic interactions are possible between the substrate and Mn^{2+}, whereas the smaller Mg^{2+} is less accessible (Gille *et al*., 2004). Thus, the occupancy of Mg^{2+} at the A-site appears to be lower than that of Mn^{2+} and the active site of the enzyme adopts a slightly more open conformation with Mg^{2+} than in presence of Mn^{2+} (Mou *et al*., 2005; Mou *et al*., 2009).

However, the metal cofactors showed no impact on the efficacies of FS and analogs of the isolated C_1/C_2 catalytic subunit plus $G_{S\alpha\text{-}GTP\gamma S}$ (Pinto *et al*., 2009). Moreover, in this study, we focused on the structural basis by docking FS and analogs to the C_1/C_2 mAC protein, but no metal ion-dependent change in the docking preferences was observed. Since all amino acids involved in FS binding are present at all FS-sensitive AC isoforms (Tang and Hurley, 1998), the currently available docking methods are not sensitive enough to identify the long-distance conformational changes between the catalytic and the regulatory site of cation binding. Moreover, the resolution of the data by molecular modeling is insufficient to allow accurate measurement of metal coordination bond lengths.

Although there are substantial differences in the activity of AC isoforms, due to differential regulation by metal ions, the biological significance of Mn^{2+} in the regulation of substrate binding and catalyzing cAMP production remains unclear (Mitterauer *et al*., 1998; Zimmermann *et al*., 1998; Tesmer *et al*., 1999). mACs acquire two metal ion binding sites coordinated to the catalytic core, where Mn^{2+} preferentially binds to the binding site B (Mitterauer *et al*., 1998; Tesmer and Sprang, 1998). Although it cannot be excluded that Mn^{2+} serves as cofactor for catalysis *in vivo*, it is more likely that Mg^{2+} is the relevant divalent cation under physiological conditions (Sunahara and Taussig, 2002).

B.6 References

Cech SY, Broaddus WC and Maguire ME (1980) Adenylate cyclase: the role of magnesium and other divalent cations. *Mol Cell Biochem* **33**:67-92.

Crowley JD, Traynor DA and Weatherburn DC (2000) Enzymes and proteins containing manganese: an overview. *Met Ions Biol Syst* **37**:209-278.

Defer N, Best-Belpomme M and Hanoune J (2000) Tissue specificity and physiological relevance of various isoforms of adenylyl cyclase. *Am J Physiol Renal Physiol* **279**:F400-416.

Dessauer CW, Scully TT and Gilman AG (1997) Interactions of forskolin and ATP with the cytosolic domains of mammalian adenylyl cyclase. *J Biol Chem* **272**:22272-22277.

Drummond GI (1981) Mg^{2+} and Mn^{2+} effects on membrane-bound and detergent-solubilized adenylate cyclase. *Can J Biochem* **59**:748-756.

Drummond GI, Severson DL and Duncan L (1971) Adenyl cyclase. Kinetic properties and nature of fluoride and hormone stimulation. *J Biol Chem* **246**:4166-4173.

Feig AL (2000) The use of manganese as a probe for elucidating the role of magnesium ions in ribozymes. *Met Ions Biol Syst* **37**:157-182.

Friedberg F (1974) Effects of metal binding on protein structure. *Q Rev Biophys* **7**:1-33.

Garbers DL and Johnson RA (1975) Metal and metal-ATP interactions with brain and cardiac adenylate cyclases. *J Biol Chem* **250**:8449-8456.

Gille A, Lushington GH, Mou TC, Doughty MB, Johnson RA and Seifert R (2004) Differential inhibition of adenylyl cyclase isoforms and soluble guanylyl cyclase by purine and pyrimidine nucleotides. *J Biol Chem* **279**:19955-19969.

Guerrera MP, Volpe SL and Mao JJ (2009) Therapeutic uses of magnesium. *Am Fam Physician* **80**:157-162.

Hanoune J and Defer N (2001) Regulation and role of adenylyl cyclase isoforms. *Annu Rev Pharmacol Toxicol* **41**:145-174.

Hanoune J, Pouille Y, Tzavara E, Shen T, Lipskaya L, Miyamoto N, Suzuki Y and Defer N (1997) Adenylyl cyclases: structure, regulation and function in an enzyme superfamily. *Mol Cell Endocrinol* **128**:179-194.

Iyengar R (1993) Molecular and functional diversity of mammalian G_S-stimulated adenylyl cyclases. *FASEB J* **7**:768-775.

Iyengar R and Birnbaumer L (1982) Hormone receptor modulates the regulatory component of adenylyl cyclase by reducing its requirement for Mg^{2+} and enhancing its extent of activation by guanine nucleotides. *Proc Natl Acad Sci USA* **79**:5179-5183.

Johnson RA and Sutherland EW (1973) Detergent-dispersed adenylate cyclase from rat brain. Effects of fluoride, cations, and chelators. *J Biol Chem* **248**:5114-5121.

Laurenza A, Khandelwal Y, De Souza NJ, Rupp RH, Metzger H and Seamon KB (1987) Stimulation of adenylate cyclase by water-soluble analogues of forskolin. *Mol Pharmacol* **32**:133-139.

Limbird LE (1981) Activation and attenuation of adenylate cyclase. The role of GTP-binding proteins as macromolecular messengers in receptor--cyclase coupling. *Biochem J* **195**:1-13.

Liu CY, Zhang H and Christofi FL (1998) Adenylyl cyclase co-distribution with the CaBPs, calbindin-D28 and calretinin, varies with cell type: assessment with the fluorescent dye, BODIPY forskolin, in enteric ganglia. *Cell Tissue Res* **293**:57-73.

Londos C and Preston MS (1977) Activation of the hepatic adenylate cyclase system by divalent cations. *J Biol Chem* **252**:5957-5961.

Lowry OH, Rosebrough NJ, Farr AL and Randall RJ (1951) Protein measurement with the Folin phenol reagent. *J Biol Chem* **193**:265-275.

Metzger H and Lindner E (1981) The positive inotropic-acting forskolin, a potent adenylate cyclase activator. *Arzneimittelforschung* **31**:1248-1250.

Mittag TW, Tormay A and Podos SM (1988) Manganous chloride stimulation of adenylate cyclase responsiveness in ocular ciliary process membranes. *Exp Eye Res* **46**:841-851.

Mitterauer T, Hohenegger M, Tang WJ, Nanoff C and Freissmuth M (1998) The C_2 catalytic domain of adenylyl cyclase contains the second metal ion (Mn^{2+}) binding site. *Biochemistry* **37**:16183-16191.

Onda T, Hashimoto Y, Nagai M, Kuramochi H, Saito S, Yamazaki H, Toya Y, Sakai I, Homcy CJ, Nishikawa K and Ishikawa Y (2001) Type-specific regulation of adenylyl cyclase. Selective pharmacological stimulation and inhibition of adenylyl cyclase isoforms. *J Biol Chem* **276**:47785-47793.

Perkins JP (1973) Adenyl cyclase. *Adv Cyclic Nucleotide Res* **3**:1-64.

Pinto C, Hübner M, Gille A, Richter M, Mou TC, Sprang SR and Seifert R (2009) Differential interactions of the catalytic subunits of adenylyl cyclase with forskolin analogs. *Biochem Pharmacol* **78**:62-69.

Pinto C, Papa D, Hübner M, Mou TC, Lushington GH and Seifert R (2008) Activation and inhibition of adenylyl cyclase isoforms by forskolin analogs. *J Pharmacol Exp Ther* **325**:27-36.

Putnam WC, Swenson SM, Reif GA, Wallace DP, Helmkamp GM, Jr. and Grantham JJ (2007) Identification of a forskolin-like molecule in human renal cysts. *J Am Soc Nephrol* **18**:934-943.

Rodbell M and Londos C (1976) Regulation of hepatic adenylate cyclase by glucagon, GTP, divalent cations, and adenosine. *Metabolism* **25**:1347-1349.

Seamon KB and Daly JW (1981) Forskolin: a unique diterpene activator of cyclic AMP-generating systems. *J Cyclic Nucleotide Res* **7**:201-224.

Seamon KB and Daly JW (1986) Forskolin: its biological and chemical properties. *Adv Cyclic Nucleotide Protein Phosphorylation Res* **20**:1-150.

Seifert R, Lee TW, Lam VT and Kobilka BK (1998) Reconstitution of β_2-adrenoceptor-GTP-binding-protein interaction in Sf9 cells--high coupling efficiency in a β_2-adrenoceptor-G($_{S\alpha}$) fusion protein. *Eur J Biochem* **255**:369-382.

Somkuti SG, Hildebrandt JD, Herberg JT and Iyengar R (1982) Divalent cation regulation of adenylyl cyclase. An allosteric site on the catalytic component. *J Biol Chem* **257**:6387-6393.

Steinberg SF, Chow YK and Bilezikian JP (1986) Regulation of rat heart membrane adenylate cyclase by magnesium and manganese. *J Pharmacol Exp Ther* **237**:764-772.

Sunahara RK, Dessauer CW and Gilman AG (1996) Complexity and diversity of mammalian adenylyl cyclases. *Annu Rev Pharmacol Toxicol* **36**:461-480.

Suryanarayana S, Göttle M, Hübner M, Gille A, Mou TC, Sprang SR, Richter M and Seifert R (2009) Differential inhibition of various adenylyl cyclase isoforms and soluble guanylyl cyclase by 2',3'-*O*-(2,4,6-trinitrophenyl)-substituted nucleoside 5'-triphosphates. *J Pharmacol Exp Ther* **330**:687-695.

Sutherland EW (1972) Studies on the mechanism of hormone action. *Science* **177**:401-408.

Sutkowski EM, Tang WJ, Broome CW, Robbins JD and Seamon KB (1994) Regulation of forskolin interactions with type I, II, V, and VI adenylyl cyclases by $G_{S\alpha}$. *Biochemistry* **33**:12852-12859.

Takahashi N, Nemoto T, Kimura R, Tachikawa A, Miwa A, Okado H, Miyashita Y, Iino M, Kadowaki T and Kasai H (2002) Two-photon excitation imaging of pancreatic islets with various fluorescent probes. *Diabetes* **51**:S25-28.

Tang WJ and Gilman AG (1992) Adenylyl cyclases. *Cell* **70**:869-872.

Tang WJ and Gilman AG (1995) Construction of a soluble adenylyl cyclase activated by $G_{S\alpha}$ and forskolin. *Science* **268**:1769-1772.

Tang WJ and Hurley JH (1998) Catalytic mechanism and regulation of mammalian adenylyl cyclases. *Mol Pharmacol* **54**:231-240.

Tesmer JJ, Sunahara RK, Gilman AG and Sprang SR (1997) Crystal structure of the catalytic domains of adenylyl cyclase in a complex with $G_{S\alpha}$–GTPγS. *Science* **278**:1907-1916.

Tesmer JJ, Sunahara RK, Johnson RA, Gösselin G, Gilman AG and Sprang SR (1999) Two-metal-Ion catalysis in adenylyl cyclase. *Science* **285**:756-760.

Torres HN, Flawia MM, Medrano JA and Cuatrecásas P (1978) Kinetic studies of adenylyl cyclase of fat cell membranes. I. Comparisons of activities measured in the presence of Mg^{2+}-ATP and Mn^{2+}-ATP. Effects of insulin, GMP-P(NH)P, isoproterenol, and fluoride. *J Membr Biol* **43**:19-44.

Wald H and Popovtzer MM (1984) Effect of divalent ions on basal and hormone-activated renal adenylate cyclase/cyclic AMP system. *Miner Electrolyte Metab* **10**:133-140.

Wei JW, Narayanan N and Sulakhe PV (1979) Adenylate cyclase of guinea pig skeletal muscle sarcolemma: comparison of the properties of the enzyme with Mg^{2+} and Mn^{2+} as divalent cation cofactors. *Int J Biochem* **10**:109-116.

Yan SZ, Huang ZH, Andrews RK and Tang WJ (1998) Conversion of forskolin-insensitive to forskolin-sensitive (mouse-type IX) adenylyl cyclase. *Mol Pharmacol* **53**:182-187.

Yan SZ, Huang ZH, Rao VD, Hurley JH and Tang WJ (1997) Three discrete regions of mammalian adenylyl cyclase form a site for $G_{S\alpha}$ activation. *J Biol Chem* **272**:18849-18854.

Zhang G, Liu Y, Ruoho AE and Hurley JH (1997) Structure of the adenylyl cyclase catalytic core. *Nature* **386**:247-253.

Chapter 3

Pharmacological Characterization of Adenylyl Cyclase Isoforms in Rabbit Kidney Membranes

C.1 Abstract

Polycycstic kidney disease (PKD) is the most common life-threatening genetic disorder without an adequate therapy against disease progression. PKD is characterized by numerous bilateral renal cysts caused by an increased level of cyclic adenosine 3',5'-monophosphate (cAMP). With adenylyl cyclases (ACs) catalyzing the synthesis of cAMP, the pharmacological characterization of the renal AC isoforms is essential.

Therefore, we analyzed differences in activation, inhibition and regulation of the AC isoforms in rabbit cortex and medulla membranes. Glucagon, [8-arginine]vasopressin and catecholamines significantly activated cortical AC, however, GPCR agonist-dependent cAMP accumulation in medulla was only observed by glucagon and AVP. Under Mg^{2+} conditions the profile of cortical membrane AC regarding enzyme kinetics and the inhibitory profile of eight 2'(3')-*O*-(*N*-methylanthraniloyl) (MANT)-nucleoside 5'-([γ-thio])triphosphates resembled recombinant AC5. In contrast, the K_i-values of MANT-nucleotides for medullary membrane AC in the presence of the physiological cation Mg^{2+} and its kinetic properties were similar to those determined for recombinant AC1. PCR confirmed these correlations detecting mRNA of AC1 and AC5 in medulla and cortex, respectively. Cortical AC was sensitive to inhibition by Ca^{2+}, confirming the importance of AC5. However, Ca^{2+}/CaM-dependency specific for AC1 was not found in medulla.

In conclusion, according to expression, kinetics and inhibition by MANT-nucleotides both parts of the kidney differ in their AC isoform activation. Whereas Ca^{2+}-inhibitable AC5 was confirmed in renal cortex, the assumed AC1 activation in medulla was rejected, pointing to the involvement of another AC isoform with some similarity to AC1. Since PKD is characterized by predominant involvement of the collecting duct and the distal nephrons located in renal cortex, AC5 might be the major AC isoform in this part where cAMP increases cyst growth. Thus, potent and selective AC5 inhibitors could constitute a novel approach to treat PKD.

C.2 Introduction

Polycystic kidney disease (PKD) is a genetic renal cystic disorder, inherited in an autosomal dominant or recessive form (Sweeney and Avner, 2006; Torres *et al*., 2007). PKD pathogenesis is associated with numerous fluid-filled cysts in the kidneys, malfunction of primary cilia and hematuria (Harris and Torres, 2006). Frequent urinary tract infections and nephrolithiasis weaken the kidney function to the end-stage of renal insufficiency (Grantham, 1997). Unfortunately, only palliative therapies help to ease the symptoms. However, up to now, no effective treatments are known to slow cyst formation in PKD. In the last years, cyclic adenosine 3',5'-monophosphate (cAMP) has been unmasked to play a major role in renal cyst growth (Grantham, 2003; Yamaguchi *et al*., 2003). cAMP mediates the increased fluid production and secretion as well as the proliferation of epithelial cells in cyst walls (Hanaoka and Guggino, 2000). An overproduction of cAMP was detected in polycystic tissues, caused by an enhanced activity of renal adenylyl cyclases (ACs) (Torres, 2004a; Wang *et al*., 2010). A changed regulation of AC activity in the kidney leads to alterations in the second messenger pathway and thus, causes an imbalance of signal transduction of diverse growth factors and physiological stimuli (Cheng and Grande, 2007).

All nine membrane-bound AC isoforms (AC1-AC9) have unique tissue distribution patterns. Gene expression studies showed the presence of ACs 4, 5 and 6 mRNA along the nephron (Defer *et al*., 2000). More precisely, AC6 has been shown to be expressed along the entire nephron (Chabardés *et al*., 1996) but ACs 4 and 5 were differently distributed in specific segments of the kidney (Bek *et al*., 2001). However, little is known about the renal distribution of individual AC isoforms on the protein level. A crucial problem in the field is the lack of availability of AC isoform-specific and sensitive antibodies (Defer *et al*., 2000; Ortíz-Capisano *et al*., 2007; Göttle *et al*., 2009). Moreover, it is still an open question whether a correlation exists between the existence of a specific AC protein and regulatory properties.

Mammalian ACs can be classified into three groups demonstrating significant diversity in their regulation in presence of free Ca^{2+} (Patel *et al*., 2001). Group one is characterized as Ca^{2+}/calmodulin-sensitive and consists of AC types 1, 3 and 8 (Sunahara *et al*., 1996; Patel *et al*., 2001). Binding of calmodulin (CaM), a Ca^{2+}-dependent protein, enhances their enzyme activity in the presence or absence of the

direct AC activator forskolin (FS) (Cooper, 2003). In contrast, enzyme activities of types 5 and 6 ACs are effectively inhibited by low concentrations of free Ca^{2+}. The last group of AC isoforms contains the types 2, 4, 7 and 9. These isoforms are stimulated by $G_{\beta\gamma}$ subunits and are insensitive to Ca^{2+}-modulation in physiological concentrations. The various AC isoforms also differ from each other with respect to their activation (and inhibition) pattern by diterpenes (Pinto *et al*., 2008). Moreover, AC isoforms exhibit differential sensitivity to competitive inhibition by MANT-nucleotides (Gille *et al*., 2004; Göttle *et al*., 2009). Furthermore, various AC isoforms differ from each other in their kinetic properties.

The identification of the prevalent AC isoform on protein level in renal cortex and medulla would be a further step to a better understanding of kidney function. The modulation of one specific AC isoform in cortex or medulla could lead towards a new therapy for PKD. cAMP-mediated cell proliferation and fluid secretion in PKD (Wang *et al*., 2010) could be reduced by isoform-dependent inhibition of AC.

In a recent study, we have characterized mouse heart AC by studying expression pattern at the mRNA level and biochemical characterization with respect to kinetics, regulation by diterpenes and inhibition by MANT-nucleotides (Göttle *et al*., 2009). We compared the properties of heart AC with those of recombinant AC isoforms expressed in Sf9 cells and found that the major AC isoform in heart is AC5. Using a similar approach, in the present study, we characterized AC in rabbit kindney cortex and medulla. Here, we report their identification by biochemical and pharmacological analysis. It is far from clear, whether one prevalent AC isoform can be identified to be predominantly activated by the variety of modulators. By analysis of GPCR agonist-mediated, Ca^{2+}-dependent or calmodulin-sensitive cAMP formation we differentiated between the AC types in the two parts of the kidney.

C.3 Materials and Methods

C.3.1 Materials

Baculoviruses encoding ACs 1, 2 and 5 were kindly provided by Drs. A. G. Gilman (UT Southwestern Medical Center, Dallas, TX, USA) and R. K. Sunahara (University of Michigan Medical School, Ann Arbor, MI, USA). Sf9 insect cells were from the American Type Cell Culture Collection (Rockville, MD, USA). MANT-ITP, MANT-CTP and MANT-UTP were synthesized as previously described (Taha *et al*., 2009). MANT-ATP, MANT-GTP, MANT-ATPγS, MANT-GTPγS and MANT-ITPγS were from Jena Bioscience (Jena, Germany). [α–^{32}P]ATP (3,000 Ci/mmol) was purchased from PerkinElmer (Wellesley, MA). Aluminum oxide (N Super 1) was purchased from MP Biomedicals (Eschwege, Germany). Glucagon and AVP were purchased from American Peptide Company (Sunnyvale, CA). Histamine, serotonin, dopamine, (-)-epinephrine, (-)-norepinephrine, (-)-isoproterenol, cAMP, phosphocreatine, IBMX and triethanolamine were from Sigma-Aldrich (St. Louis, MO). FS was from LC Laboratories (Woburn, MA). GTP, GTPγS, ATP and creatine kinase were purchased from Roche (Mannheim, Germany). $CaCl_2$ dihydrate, $MnCl_2$ tetrahydrate and $MgCl_2$ hexahydrate (highest quality) were from Merck (Darmstadt, Germany). Lyophilized calmodulin from bovine brain was purchased from EMD Biosciences (Calbiochem, Darmstadt, Germany).

C.3.2 Semi-Quantitative PCR

Total RNA was extracted from renal cortex and medulla using 1 mL TRIzol reagent (Peqlab, Erlangen, Germany) per 100 mg tissue. Total RNA was reverse-transcribed into cDNA according to standard protocols by Invitrogen (Gibco BRL). In brief, cDNA was synthesized in a 22 μL reaction per sample with 2 μg total RNA, 0.5 μg/μL oligo$(dT)_{12\text{-}18}$, 0.5 μL 20 U RNAsin (Promega, Madison, WI), 4 μL of 5 x RT-buffer, 5 μL of 2.5 mM dNTPs, and 20 U Moloney murine leukemia virus RT enzyme (GIBCO Life Technologies). Semi-quantitative PCR was performed with the TPersonal Thermocycler System from Biometra (Göttingen, Germany), all primer sequences were adopted from (Younes *et al*., 2008) and shown in Tab. **C.1**. Each reaction contained 1 μL cDNA, $MgCl_2$ of 3 mM final concentration in case of AC1, otherwise 2.5 mM, 2.5 mM dNTP, 5 μL 10 x RT-buffer, 1 pmol of each primer and

0.25 μL 5 U A-Taq polymerase (Promega, Madison, WI). The PCR reaction was initiated with a 2-min hot start at 95°C followed by denaturation at 95°C for 30 sec. Annealing was perfomed at 66°C for AC1 and 56°C for detection of ACs 4, 5 and 6 for 30 sec, and extension took place at 72°C for 30 sec. The last 3 steps were repeated in 35 cycles for all three AC isoforms and the PCR reaction was terminated with a final 5-min extension period at 72°C followed by cooling at 4°C. In parallel experiments, each PCR reaction was performed without renal RNA for negative control to test for DNA contamination. Finally, the PCR products were separated on a 2% (m/v) agarose gel and stained with ethidium bromide.

Tab. C.1. Primer sequences for reverse-transcription PCR of AC isoforms in rabbit cortex and medulla.

AC isoform	Primer sequence
AC1	Forward: 5´-TGGCAGCTGCTGCTGGTCAC-3´
	Reverse: 5´-CCACCGCGAGCCCGAAGC-3´
AC4	Forward: 5´-ATCAGGAAACTTCGGGTAGC-3´
	Reverse: 5´-ATATGGTTGGCCAATGTGAC-3´
AC5	Forward: 5´-CATGTTCATGTGCAACTCCA-3´
	Reverse: 5´-ATGGATCACGCTGATGTTGT-3´
AC6	Forward: 5´-GCTGCGGAGAATCACTGTC-3´
	Reverse: 5´-TACCCCCATCTCCACACAG-3´

C.3.3 Sf9 Cell Culture and Expression of Recombinant ACs

Sf9 cells were cultured and infected with 1:100 dilutions of high-titer virus stocks as described previously (Houston *et al*., 2002). Sf9 membranes were prepared according to standard protocols (Seifert *et al*., 1998) and stored at -80°C until use. Protein concentrations were determined using the Lowry method (Lowry *et al*., 1951). For the AC activity assay, Sf9 membranes were thawed, washed and sedimented by a 10-min centrifugation at 4°C and 13,000 x g to remove residual endogenous nucleotides as much as possible. After that they were resuspended in assay buffer as described below.

C.3.4 Preparation of Renal Cortical and Medullary Membranes

Whole kidneys were removed from 8 months old male chinchilla bastard rabbits, which were housed in cages in a temperature- and light-controlled environment according to the German animal protection law. The animals were sacrificed by Narcoren i.v. 2 mL/kg body weight. After removal of both kidneys, the tissues were immediately separated into cortical and medullary parts, shock-frozen in liquid nitrogen as soon as possible and stored at -80°C until use. The next day, rabbit kidneys were prepared to membranes according to a previously described protocol (Göttle *et al*., 2009). All membrane preparation and centrifugation steps were performed at 4°C. In brief, still frozen parts of cortex or medulla were cut into small pieces and transferred into ice-cold homogenization buffer containing 5 mM Tris·HCl, pH 7.4, and 5 mM EDTA. Homogenization was performed in a buffer volume amounting to 20-fold the tissue weight using a glass-glass homogenizer (Braun, Melsungen, Germany) at 1,500 rpm, applying 5 series of 5 strokes each with a 1-min cooling period between each series. Organ debris was removed by an 8-min centrifugation at 500 x g. The supernatant suspension was sedimented by a 30-min centrifugation at 40,000 x g. Membranes were washed in a buffer volume amounting to 60-fold of renal tissue weight and sedimented by a 30-min centrifugation at 40,000 x g. In order to remove residual endogenous ligands and nucleotides, this washing procedure was performed three times before the membranes were resuspended in assay buffer consisting of 50 mM triethanolamine and 1 mM EGTA, pH 7.4. After resuspension with syringes in the sequence 21 G and 27 G, membranes were shock-frozen in liquid nitrogen and stored at -80°C. Protein concentration was determined using Bradford method (Bradford, 1976) with the DC protein assay kit (Bio-Rad, Hercules, CA).

C.3.5 AC Activity Assay

AC activity was determined essentially as described in literature (Göttle *et al*., 2009). Just before use, renal membranes were resuspended with syringes and diluted with assay buffer to a concentration of 1 μg/μL. AC inhibition was measured using 20 μL of reaction mixture consisting of (final) 7 mM Mn^{2+} or Mg^{2+}, 40 μM ATP, 10 μM GTP, 10 μM GTPγS, 100 μM cAMP, 0.4 mg/mL creatine kinase, 9 mM phosphocreatine, 100 μM IBMX, 100 μM FS and 0.3 μCi [α-^{32}P]ATP. This mixture

was added to 10 μL of MANT-nucleotide and preincubated for 2 min at 30°C. Reactions were initiated by the addition of 20 μL of membrane suspension. To avoid nucleotide degradation, incubation time was reduced to 1-2 min. For activation experiments described subsequently, Sf9 membranes expressing recombinant ACs were washed and centrifuged with 13,000 x g for 10 min at 4°C before use. Afterwards, the protein pellet was resuspended in assay buffer resulting in a concentration of 1 μg/μL. In case of cortical or medullary membranes, the protein was resuspended to a concentration of 1 μg/μL without previous centrifugation. In order to confirm comparability, the AC activity assay was performed under same conditions and with same reaction mixtures for recombinant and renal membranes. We ensured linear reaction progress for AC activation by incubating tubes for 10 min at 30°C. For identification of K_m- and V_{max}-values, the reaction mixture was added to 10 μL ATP/Mn^{2+} or ATP/Mg^{2+} in increasing concentrations (1 μM to 1 mM). Experiments aiming to detect an influence of CaM on AC activity contained FS dilution (300 nM to 300 μM) combined with CaM (2 μM) or double-distilled water and 20 μL reaction mixture without GTP and FS. For the examination of Ca^{2+}-influence, all AC membranes were maximally activated with 300 μM FS. In these experiments, reaction mixtures contained varying $CaCl_2$ concentrations from 100 nM to 1 mM. Free Ca^{2+}-concentrations were calculated with the WebMax C standard (*http://www.stanford.edu/~cpatton/maxc.html*). For stimulation of ACs *via* GPCR activation GTPγS and FS were omitted from reaction mixtures. All reactions were terminated by the addition of 20 μL of 2.2 N HCl, and denatured protein was sedimented by a 2-min centrifugation at 13,500 x g. [^{32}P]cAMP was separated from [α–^{32}P]ATP by transferring the samples onto columns containing 1.4 g of neutral alumina. [^{32}P]cAMP was eluted by adding 4 mL of 0.1 M ammonium acetate, pH 7.0. Blank values were ~0.02% of the total amount of [α–^{32}P]ATP added; substrate turnover was < 3% of the total added [α–^{32}P]ATP. Samples were filled up with 10 mL ddH_2O and Čerenkov radiation was determined.

C.3.6 Data Analysis

Data shown in Tabs. **C.1** and **C.2** and in Figs. **C.2**, **C.3** and **C.8** were obtained by non-linear regression analysis, correlations were obtained by linear regression analysis performed with the Prism 5.01 software (Graphpad, San Diego, CA). Statistical comparisons were performed using the Student's *t*-test. Differences were considered as statistically significant with $p < 0.05$ (*), $p < 0.01$ (**) and $p < 0.001$ (***).

C.4 Results

C.4.1 Detection of AC Isoforms in Rabbit Renal Membranes of Cortex and Medulla by Semi-Quantitative PCR

In order to assess the expression of AC isoforms at the mRNA levels in rabbit kidney, reverse-transcription polymerase chain reaction (RT-PCR) analysis was performed. After mRNA extraction, cDNA synthesis and PCR, cortical and medullary samples of same amounts were transferred to 2% (m/v) agarose gels. The AC4 fragment showed the expected length of 143 base paires (bp), the fragment for AC5 of 70 bp and the fragment for AC6 of 114 bp in renal cortex and medulla, respectively (Fig. **C.1**). In direct comparison the darker band of AC4 indicated a higher AC4 mRNA content in the medullary part of the kidney than in the cortex. In contrast, the concentration of AC5 mRNA seemed to be higher in renal cortex. AC6 mRNA was detected in both cortex and medulla at the same intensity, indicating that this AC isoform is expressed along the entire nephron. Additionally, AC1 (84 bp) was detected at a low level in both parts of the kidney.

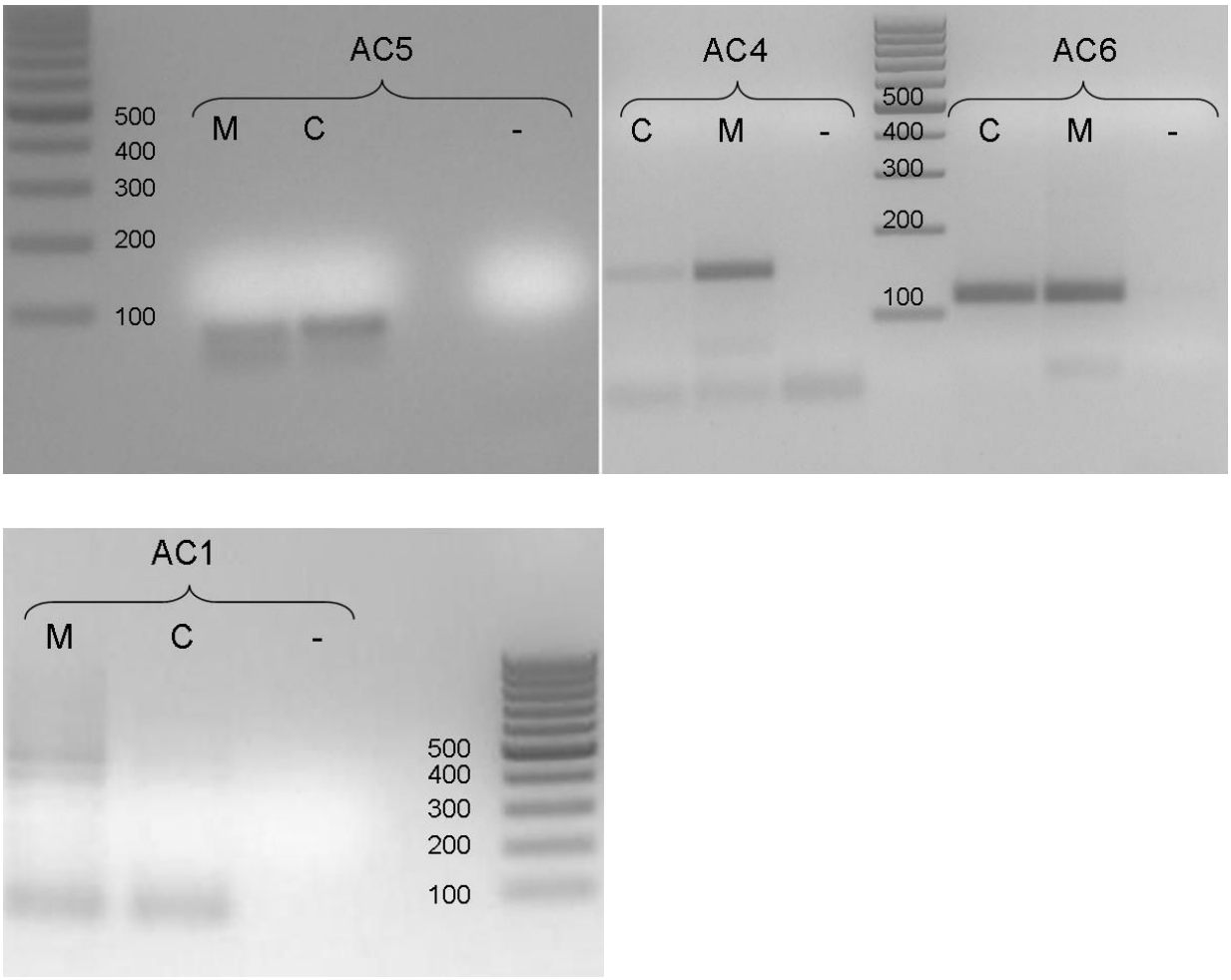

Fig. C.1. Detection of AC isoforms in different kidney segments by reverse-transcription PCR. mRNA was prepared from isolated cortex and medulla, and analyzed with primers specific for ACs 1, 4, 5 and 6. Potential contamination was checked by excluding the RNA (-). Expected sizes of the PCR products were 84 bp for AC1, 143 bp for AC4, 70 bp for AC5 and 114 bp for AC6.

C.4.2 Stimulation of Rabbit Renal ACs with GPCR Agonists

Membranous ACs are activated *via* the GPCR – G protein cascade (Chabardés *et al*., 1975; Sunahara and Taussig, 2002). In the AC activity assay we examined the effects of various neurotransmitters and hormones on cortical and medullary membranes. In the presence of 7 mM Mg^{2+}, glucagon was the most efficient GPCR agonist with an over 3-fold increase of AC activity in both cortex and medulla. Among all other tested GPCR agonists, significant activation of medullary AC was only obtained with AVP (10 μM) (Fig. **C.2B**). In contrast, in the cortical part, more GPCRs mediating AC stimulation were detected. The order of efficacy of the tested GPCR agonists was glucagon (40 μM) > vasopressin (10 μM) > epinephrine (100 μM) > isoproterenol (100 μM) ~ norepinephrine (100 μM) (Fig. **C.2A**). The most

potent receptor ligands for AC stimulation in cortical membranes were AVP (EC_{50}: 14 ± 7 nM) and isoproterenol (EC_{50}: 22 ± 0.8 nM) followed by glucagon (EC_{50}: 162 ± 64 nM), epinephrine (EC_{50}: 383 ± 171 nM) and norepinephrine (EC_{50}: 1,250 ± 67 nM).

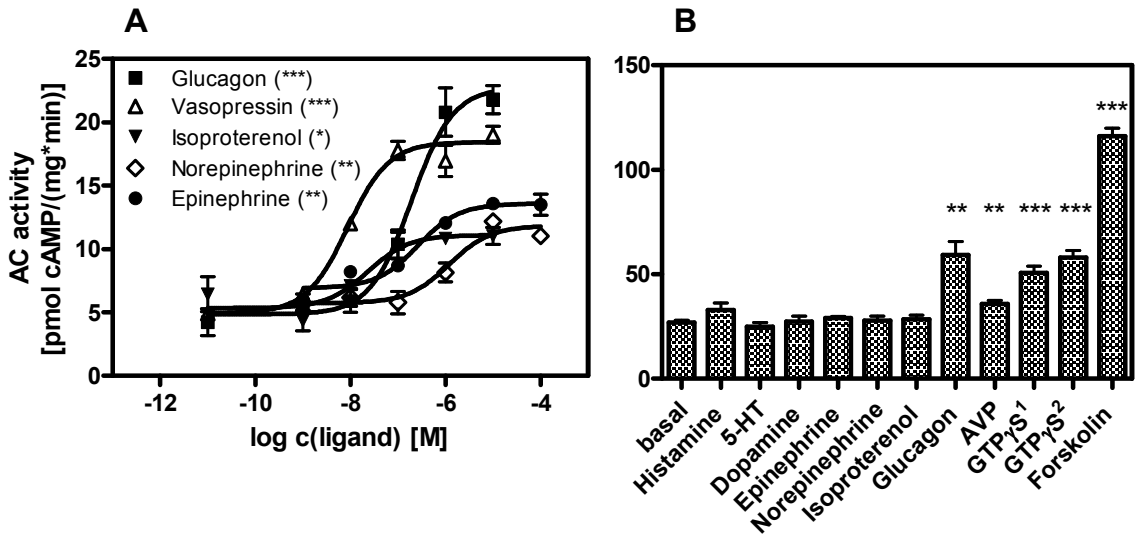

Fig. C.2. Effects of various GPCR agonists on rabbit renal membranes. AC activity was determined as described in "Materials and Methods". Reaction mixtures contained 7 mM Mg^{2+} and were carried out for 10 min at 30°C. **A**, Concentration response curves were determined for renal cortex. **B**, AC activity in renal medulla was measured for histamine, 5-HT, dopamine, (-)-epinephrine, (-)-norepinephrine and (-)-isoproterenol (100 μM each), glucagon (40 μM), AVP (10 μM) and GTPγS (^{1}10 μM) and (^{2}100 μM). Data shown are representative results (mean ± SD) of one of at least 3 experiments performed in triplicates. (* $p < 0.05$; ** $p < 0.01$; *** $p < 0.001$).

C.4.3 Enzyme Kinetics of Cortical and Medullary ACs

Substrate saturation experiments were performed using membranes of both parts of the rabbit kidney to determine the K_m- and V_{max}-values. Under Mn^{2+} conditions, saturation was already reached at much lower substrate concentrations than with Mg^{2+}. In the presence of 7 mM Mg^{2+}, the K_m-value of cortical AC was 86 ± 7.6 μM, consistent with the K_m-value determined for recombinant AC5 and closely related to cardiac AC (Fig. **C.3A**, Tab. **C.2**). The investigation of medullary membranes exhibited a K_m-value similar to AC1 (Fig. **C.3C**). Moreover, experiments with 7 mM Mn^{2+} yielded K_m-values for cortical and medullary AC in the lower μM range, similar to heart AC and recombinant AC5 (Fig. **C.3B** and **D**, Tab. **C.2**).

Tab. C.2. Kinetic properties of renal cortical and medullary ACs in comparison with heart AC and recombinant ACs 1, 2 and 5 in presence of Mg^{2+} and Mn^{2+}.

Parameter Mg^{2+}	Cortical AC	Medullary AC	Cardiac AC	AC1	AC2	AC5
K_m [μM]	86 ± 7.6	130 ± 1.8	68 ± 5$^{\#\#}$	160 ± 20$^{\#}$	110 ± 30$^{\#}$	87 ± 31$^{\#\#}$
V_{max} [pmol·mg^{-1}·min^{-1}]	727 ± 116	616 ± 81	1,600 ± 160$^{\#\#}$	660 ± 90$^{\#}$	300 ± 70$^{\#}$	2,400 ± 760$^{\#\#}$
Mn^{2+}						
K_m [μM]	13 ± 2.6	27 ± 3.5	11 ± 2$^{\#\#}$	110 ± 29$^{\#}$	99 ± 22$^{\#}$	40 ± 5$^{\#\#}$
V_{max} [pmol·mg^{-1}·min^{-1}]	994 ± 286	616 ± 121	1,010 ± 370$^{\#\#}$	1,500 ± 230$^{\#}$	1,200 ± 140$^{\#}$	1,300 ± 400$^{\#\#}$

Saturation experiments were performed as described in “Materials and Methods” with increasing ATP/cation concentrations (1-1000 μM under Mg^{2+} conditions / 1-150 μM under Mn^{2+} conditions). K_m- and V_{max}-values were obtained by non-linear regression analysis and represent the means ± SD of 2-3 independent experiments performed in duplicates or triplicates. Values labeled with ($^{\#}$) were taken from (Gille *et al*., 2004), those labeled with ($^{\#\#}$) were taken from (Göttle *et al*., 2009).

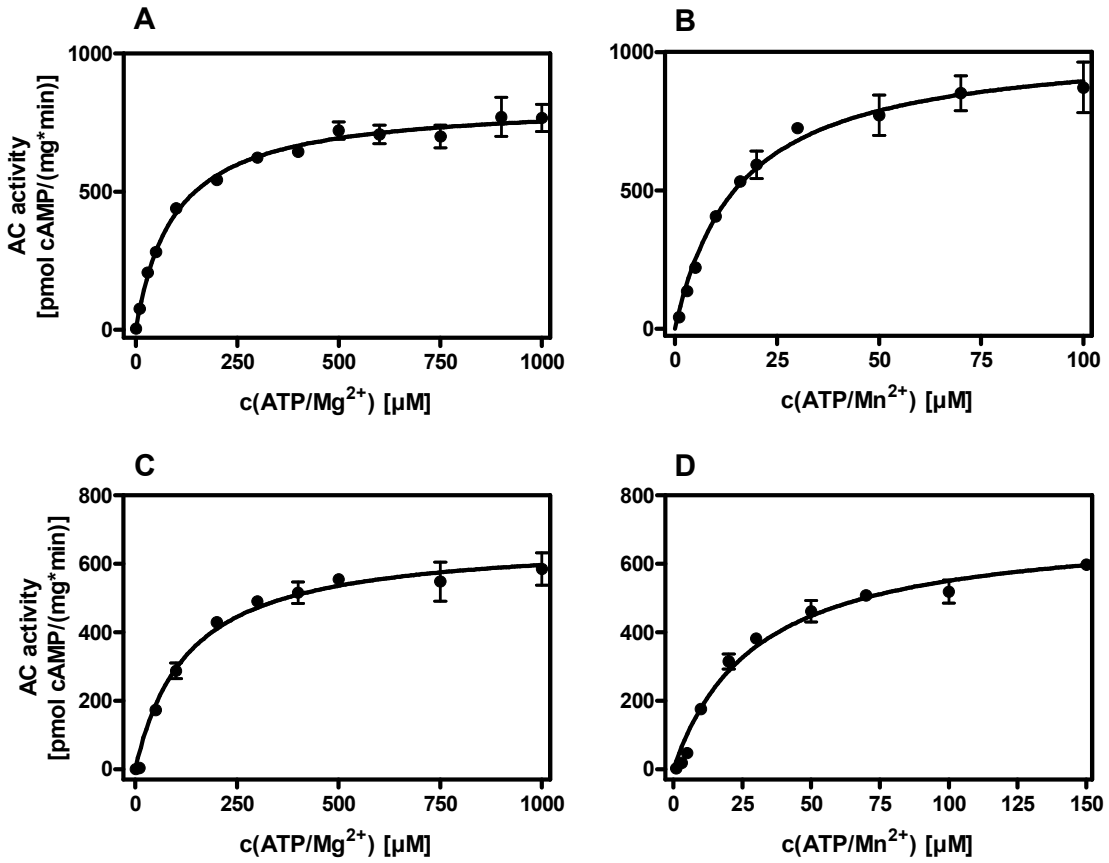

Fig. C.3. Saturation experiments for determination of K_m and V_{max} on rabbit renal cortex and medulla. Reaction mixtures contained 7 mM Mn^{2+} or Mg^{2+}, [α–^{32}P]ATP (0.3 µCi/tube), 10 µM GTP, 10 µM GTPγS, 100 µM cAMP, 0.4 mg/mL creatine kinase, 9 mM phosphocreatine, 100 µM IBMX and 100 µM FS. ATP/Mn^{2+} or ATP/Mg^{2+} (1 µM to 150 µM and 1 µM to 1 mM, respectively) plus 7 mM of free Mn^{2+} or Mg^{2+} were added to reaction mixtures. In order to ensure linear reaction progress, tubes were incubated for 10 min at 30°C. **A**, substrate saturation curve for renal cortex in the presence of Mg^{2+}. **B**, substrate saturation curve for cortical membrane AC in the presence of Mn^{2+}. **C**, substrate saturation curve for renal medulla in the presence of Mg^{2+}. **D**, substrate saturation curve for medullary membrane AC in the presence of Mn^{2+}. Data shown are representative results (mean ± SD) of one of 2-3 experiments performed in triplicates. Substrate saturation curves were plotted by non-linear regression curve fit of Michaelis-Menten enzyme saturation.

C.4.4 Inhibition of Renal ACs by MANT-Nucleotides in Comparison with ACs 1, 2 and 5

Inhibition data were obtained in the AC activity assay following maximum stimulation of renal ACs with forskolin and the G protein activator guanosine 5'-[γ-thio]triphosphate. 2'(3')-*O*-(*N*-Methylanthraniloyl) (MANT)-ITP displayed the highest potency on both cortical and medullary AC in presence of Mn^{2+} as well as in presence of Mg^{2+} with K_i-values in the lower nM range.

Tab. C.3. Inhibitory potencies of MANT-nucleotides on rabbit kidney ACs in presence of Mg^{2+} and Mn^{2+}.

	Cortex K_i [nM]		Medulla K_i [nM]	
Nucleotide	**Mg^{2+}**	**Mn^{2+}**	**Mg^{2+}**	**Mn^{2+}**
MANT-ATP	1,628 ± 381	61 ± 7	3,558 ± 1930	125 ± 48
MANT-ATPγS	706 ± 114	60 ± 10	872 ± 53	75 ± 6
MANT-CTP	4,141 ± 47	51 ± 9	3,115 ± 290	72 ± 6
MANT-GTP	1,087 ± 364	13 ± 4	1,285 ± 3	32 ± 2
MANT-GTPγS	666 ± 120	27 ± 0.3	450 ± 86	42 ± 15
MANT-ITP	30 ± 6	6 ± 2	29 ± 1	9 ± 4
MANT-ITPγS	47 ± 9	10 ± 3	48 ± 12	14 ±7
MANT-UTP	1,500 ± 148	22 ± 3	1,468 ± 192	31 ± 4

Inhibition constants (K_i) on renal ACs were determined as described in "Materials and Methods". To avoid nucleotide degradation, incubation time was reduced to 1-2 min. Inhibition curves were analyzed by non-linear regression. K_i-values were calculated by Cheng-Prusoff equation and represent the means ± SD of 2-4 independent experiments performed in duplicates.

In the presence of Mg^{2+}, the rank order of potency of inhibitors for cortical AC was MANT-ITP > MANT-ITPγS >> MANT-GTPγS > MANT-ATPγS > MANT-GTP > MANT-UTP > MANT-ATP >> MANT-CTP (Tab. **C.3**). Under the same conditions, the order of inhibitory potency at mouse heart AC was MANT-ITP ~ MANT-ITPγS > MANT-GTPγS > MANT-ATPγS ~ MANT-GTP > MANT-UTP > MANT-ATP > MANT-CTP (Göttle *et al*., 2009). Recombinant AC5 yielded the following order of potencies: MANT-ITP > MANT-ITPγS > MANT-GTPγS > MANT-GTP > MANT-UTP ~ MANT-ATPγS > MANT-ATP > MANT-CTP (Göttle *et al*., 2009). The characteristic sequence of the inhibitory affinities on AC1 looked quite similar with MANT-ITP > MANT-ITPγS > MANT-GTPγS > MANT-ATPγS ~ MANT-GTP > MANT-UTP > MANT-ATP > MANT-CTP and was closely related to the sequence of inhibitors' potency on AC2: MANT-ITP > MANT-ITPγS > MANT-GTPγS > MANT-ATPγS > MANT-GTP > MANT-ATP > MANT-UTP > MANT-CTP (Göttle *et al*., 2009). Comparing all these sequences by linear regression, a significant correlation between cortical AC and AC5 as well as between cortical AC and cardiac AC was found, $p \leq 0.0001$, respectively (Fig. **C.4**). However, linear regression analysis of inhibitor affinities on AC1 revealed a less significant correlation with renal cortical AC (r^2 = 0.8; slope = 0.86 ± 0.2; p = 0.003).

The correlation of the order of K_i-values on AC2 with cortical AC was even less significant with a slope of 3.7 ± 0.5.

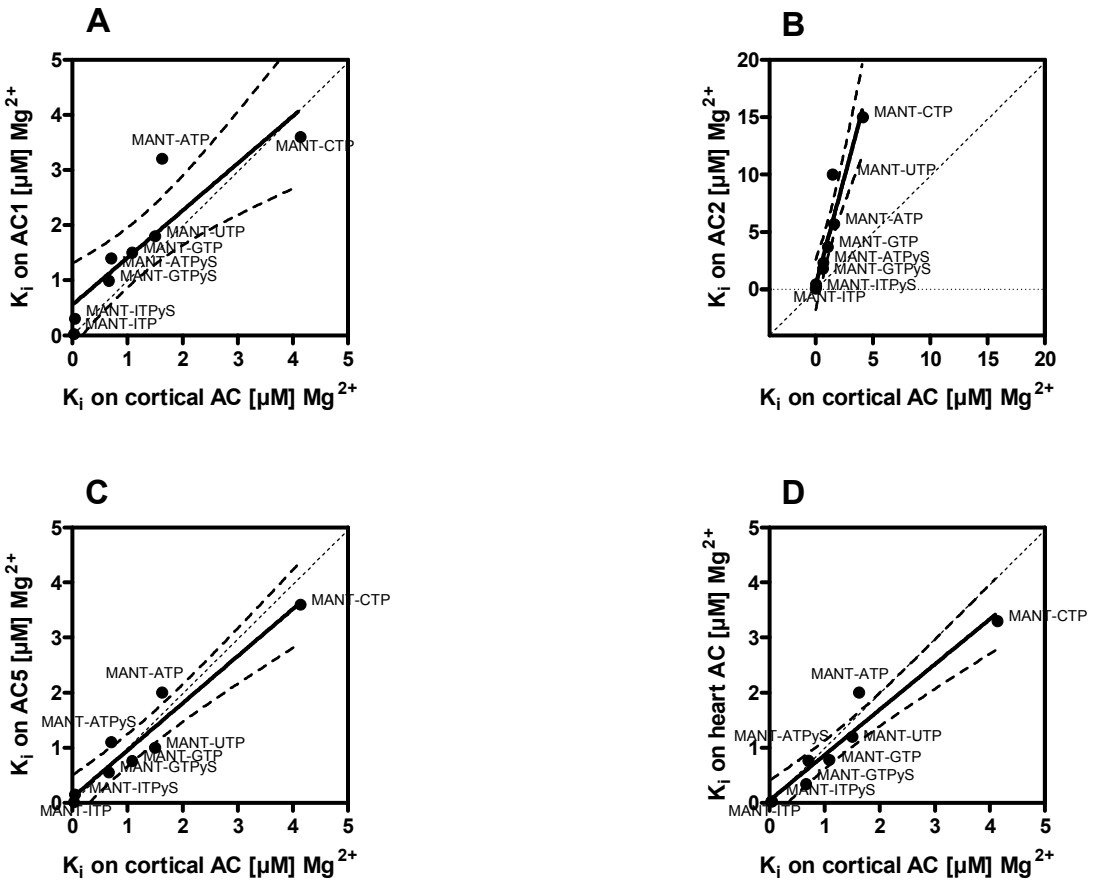

Fig. C.4. Correlations of cortical K_i-values with the profiles of recombinant and cortical ACs under Mg^{2+} conditions. Data shown in Tab. **C.3** were correlated with the inhibition constants of MANT-nucleotides on recombinant AC1, AC2 and AC5, respectively, and on mouse heart membranes. These values were taken from (Göttle *et al.*, 2009). **A**, correlation of cortical AC *vs.* AC1 (r^2 = 0.80; slope = 0.86 ± 0.2; p = 0.003). **B**, correlation of cortical AC *vs.* AC2 (r^2 = 0.90; slope = 3.7 ± 0.5; p = 0.0004). **C**, correlation of cortical AC *vs.* AC5 (r^2 = 0.93; slope = 0.86 ± 0.1; p = 0.0001). **D**, correlation of cortical AC *vs.* cardiac AC (r^2 = 0.94; slope = 0.8 ± 0.08; p < 0.0001). Data were analysed by linear regression; the dashed lines indicate the 95% confidence intervals of the regression lines. The diagonal dotted line has a slope of 1.0 and represents a theoretical curve for identical values.

Inhibition constants obtained under Mn^{2+} conditions were generally lower, from 3- to 5-fold for MANT-ITP and MANT-ITPγS up to almost 45- to 70-fold for MANT-UTP. The rank order of inhibition potency on cortical AC was MANT-ITP > MANT-ITPγS > MANT-GTP > MANT-UTP > MANT-GTPγS > MANT-CTP > MANT-ATPγS ~ MANT-ATP (Tab. **C.3**). Compared to the rank order of recombinant AC1 only MANT-

GTP changed its position: MANT-ITP > MANT-ITPγS > MANT-UTP > MANT-GTPγS > MANT-GTP > MANT-CTP > MANT-ATPγS > MANT-ATP. Cardiac AC revealed a more considerably altered inhibition sequence of MANT-ITP > MANT-ITPγS > MANT-UTP > MANT-GTP ~ MANT-GTPγS > MANT-CTP > MANT-ATP > MANT-ATPγS. However, the rank orders of inhibition on AC2 (MANT-ITP > MANT-ITPγS > MANT-GTPγS ~ MANT-ATPγS > MANT-UTP > MANT-GTP > MANT-CTP > MANT-ATP) and AC5 (MANT-ITP > MANT-ITPγS > MANT-UTP > MANT-GTPγS > MANT-GTP > MANT-ATPγS > MANT-CTP > MANT-ATP) showed only little similarity compared to cortical AC. Additionally, no significant correlation with AC1, 2 and 5, was found, and the slope was >> 2. However, the comparison of the inhibition profile obtained for cortical membranes and cardiac AC yielded the best fit (r^2 = 0.83; slope = 0.98 ± 0.18; p = 0.0014) (Fig. **C.5**), suggesting similar AC isoform composition in cortex and heart.

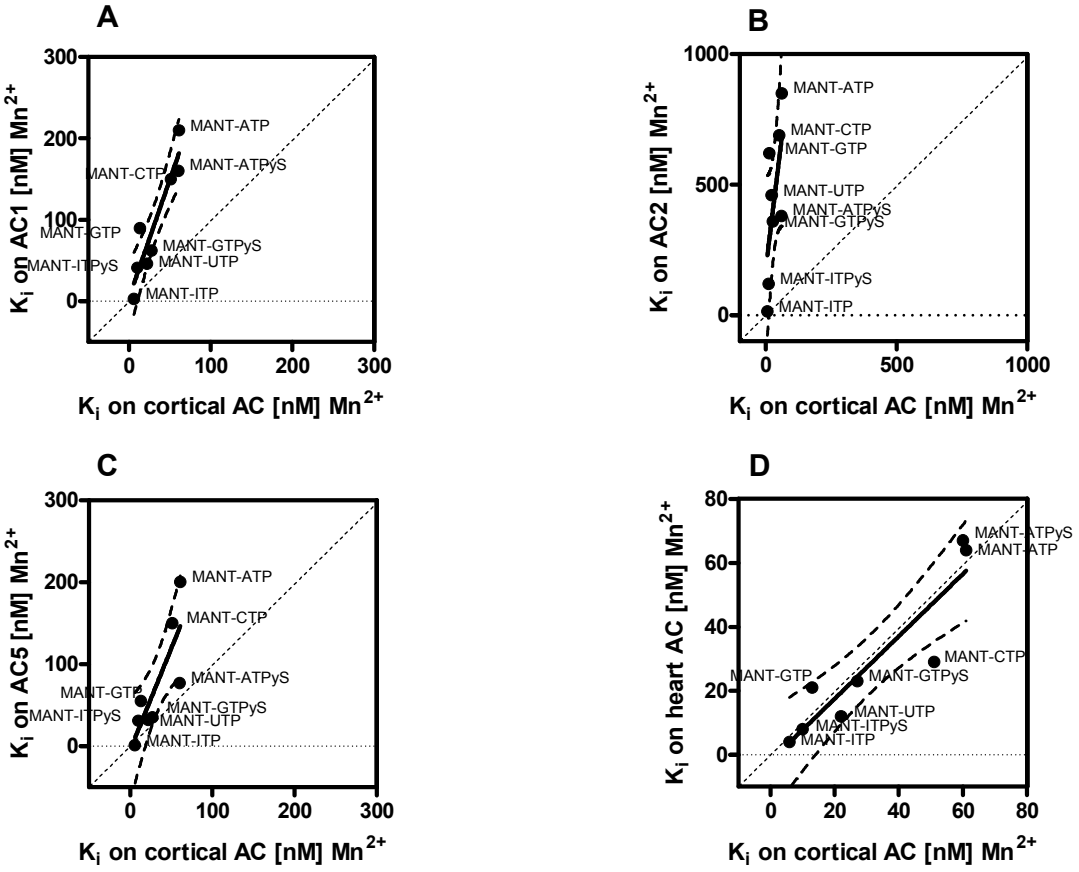

Fig. C.5. Correlations of cortical K_i-values with the profiles of recombinant ACs and cortical AC in the presence of Mn^{2+}. Data shown in Tab. **C.3** were correlated with the inhibition constants of MANT-nucleotides on Sf9 membranes expressing AC1, AC2 and AC5, respectively, and on mouse heart membranes adopted from (Göttle *et al*., 2009). **A**, correlation of cortical AC *vs.* AC1 (r^2 = 0.86; slope = 2.9 ± 0.5; p = 0.0008). **B**, correlation of cortical AC *vs.* AC2 (r^2 = 0.44; slope = 8.2 ± 3.8; p = 0.0725). **C**, correlation of cortical AC *vs.* AC5 (r^2 = 0.70; slope = 2.5 ± 0.7; p = 0.0110). **D**, correlation of cortical AC *vs.* cardiac AC (r^2 = 0.83; slope = 0.98 ± 0.18; p = 0.0014). Comparisons were analyzed by linear regression; the dashed lines indicate 95% confidence intervals. The diagonal dotted line has a slope of 1.0 and represents a theoretical curve for identical values.

The rank order of K_i-values for medullary AC in presence of Mg^{2+} was MANT-ITP > MANT-ITPγS >> MANT-GTPγS > MANT-ATPγS > MANT-GTP ~ MANT-UTP > MANT-CTP ~ MANT-ATP (Tab. **C.3**). The K_i-values for medullary AC correlated well with those for AC1 (r^2 = 0.95; slope = 0.92 ± 0.1; p < 0.0001) (Fig. **C.6**) while correlations with AC5 as well as with mouse heart AC showed moderate differences, r^2 < 0.85, respectively. The inhibitor profile of AC2 was again completely different, r^2 = 0.56; slope = 2.9 ± 1.1; p = 0.0332.

The medullary inhibition profile in presence of Mn^{2+} resulted in the potency rank order MANT-ITP > MANT-ITPγS > MANT-UTP ~ MANT-GTP > MANT-GTPγS > MANT-CTP > MANT-ATPγS > MANT-ATP (Tab. **C.3**). Compared to ACs 1, 2, 5 and mouse heart AC (Fig. **C.7**), no significant correlation was observed with medullary AC, indicating that under these conditions another AC isoform than AC1, 2, 5 or cardiac AC was unmasked.

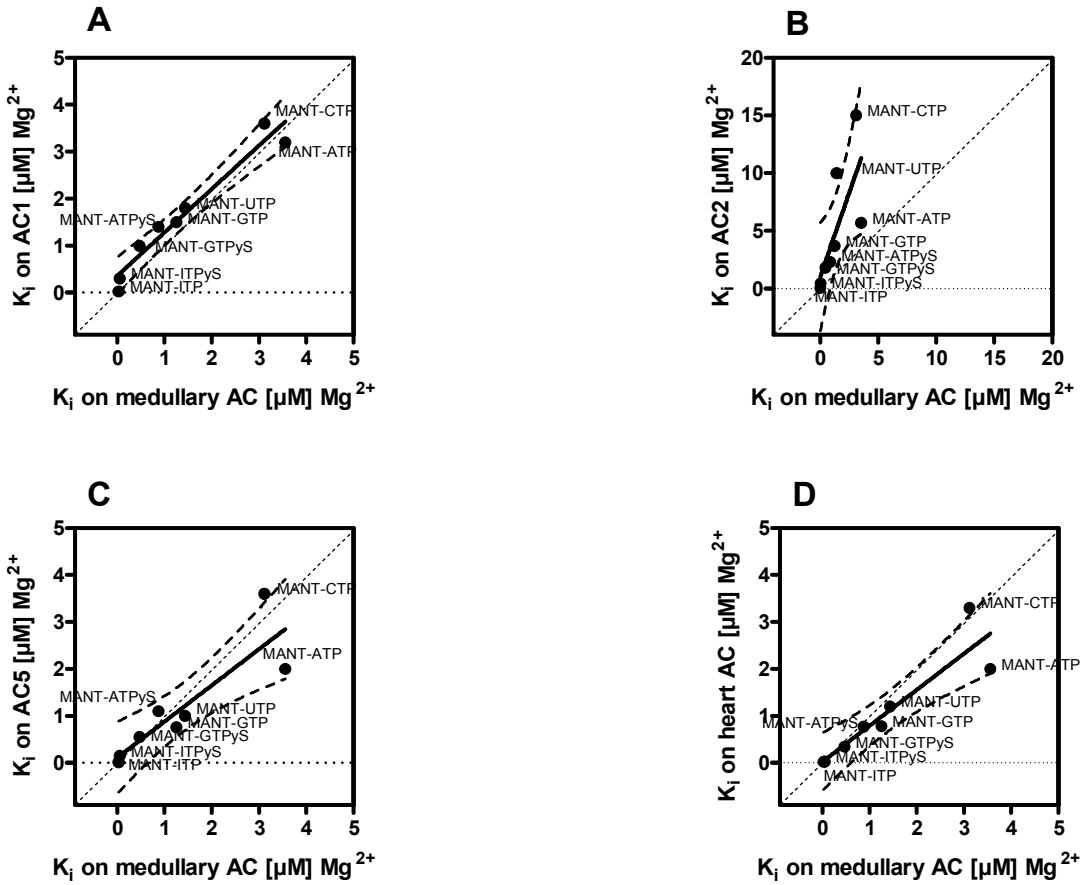

Fig. C.6. Correlations of medullary K_i-values with the order of inhibition constants of MANT-nucleotides on AC1, AC2, AC5 and cortical AC under Mg^{2+} conditions. Results shown in Tab. **C.3** were compared with the K_i-values of recombinant AC1, AC2 and AC5, respectively, and on mouse heart membranes. These data were taken from (Göttle *et al*., 2009). **A**, correlation of cortical AC *vs.* AC1 (r^2 = 0.95; slope = 0.92 ± 0.1; p < 0.0001). **B**, correlation of cortical AC *vs.* AC2 (r^2 = 0.56; slope = 2.9 ± 1.1; p = 0.0332). **C**, correlation of cortical AC *vs.* AC5 (r^2 = 0.77; slope = 0.78 ± 0.17; p = 0.0041). **D**, correlation of cortical AC *vs.* cardiac AC (r^2 = 0.84; slope = 0.77 ± 0.14; p = 0.0014). Comparisons were analyzed by linear regression; the dashed lines indicate the 95% confidence intervals of the regression lines. The diagonal dotted line has a slope of 1.0 and represents a theoretical curve for identical values.

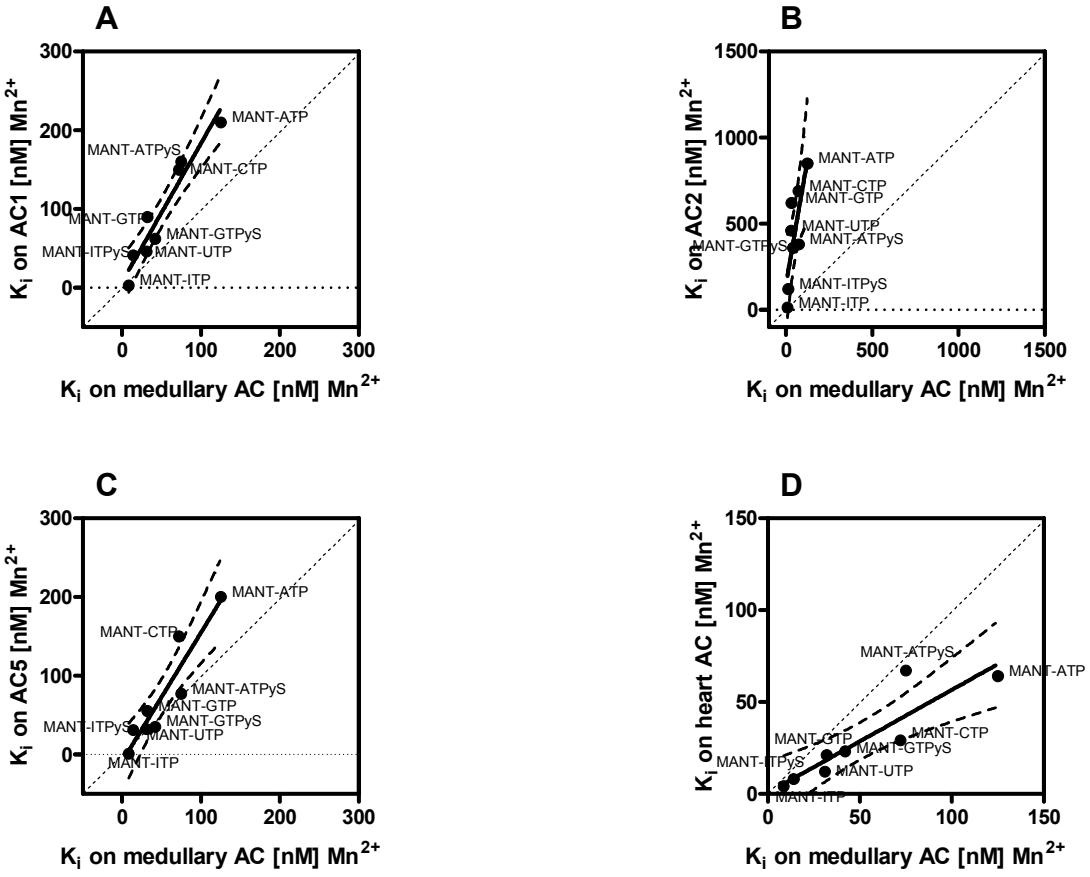

Fig. C.7. Correlations of medullary K_i-values with the order of inhibition constants of MANT-nucleotides on recombinbant and cortical AC in presence of Mn^{2+}. Results shown in Tab. **C.3** were compared with the K_i-values of recombinant AC1, AC2 and AC5, respectively, and on mouse heart membranes (Göttle *et al.*, 2009). **A**, r^2 = 0.92; slope = 1.76 ± 0.2; p = 0.0002. **B**, r^2 = 0.63; slope = 5.8 ± 1.8; p = 0.0179. **C**, r^2 = 0.87; slope = 1.64 ± 0.26; p = 0.0007. **D**, r^2 = 0.80; slope = 0.56 ± 0.1; p = 0.0027. Data were analyzed by linear regression; the dashed lines indicate the 95% confidence intervals of the regression lines. The diagonal dotted line has a slope of 1.0 and represents a theoretical curve for identical values.

Correlation of the cortical inhibiton profile *vs.* medullary K_i-values (Fig. **C.8**) identified moderate differences in presence of Mg^{2+} (r^2 = 0.65; slope = 0.82 ± 0.24; p = 0.0008) whereas in presence of Mn^{2+} the differences between the two parts of the kidney were more considerable with a slope of 1.6 ± 0.26 pointing to different AC isoform expression patterns.

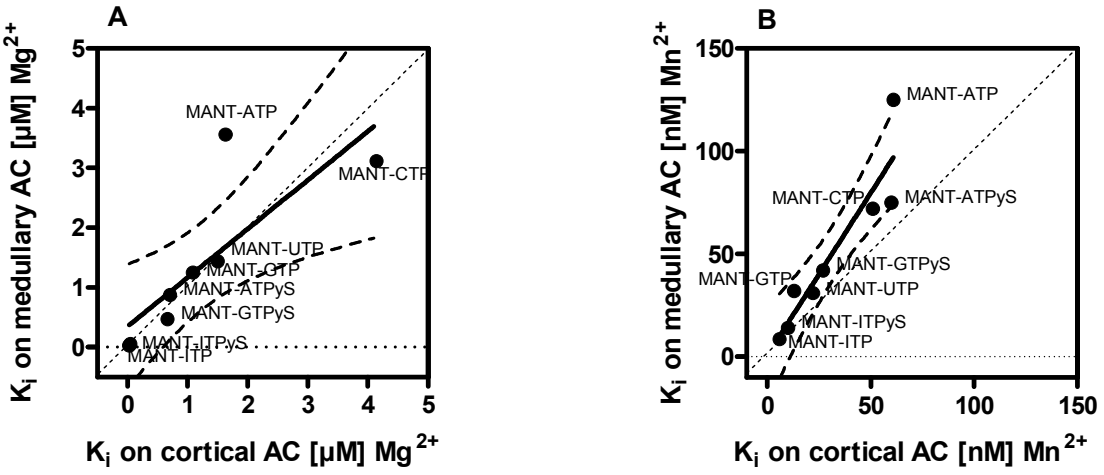

Fig. C.8. Correlation of cortical inhibition profile *vs.* medullary K_i-values. Data shown in Tab. **C.3** were analyzed by linear regression. **A**, correlation of cortical AC with medullary AC in presence of Mg^{2+} (r^2 = 0.65; slope = 0.82 ± 0.24; p = 0.0008). **B**, correlation of cortical AC with medullary AC in presence of Mn^{2+} (r^2 = 0.86; slope = 1.6 ± 0.26; p = 0.0155). Comparisons were analyzed by linear regression; the dashed lines indicate the 95% confidence intervals of the regression lines. The diagonal dotted line has a slope of 1.0 and represents a theoretical curve for identical values.

C.4.5 Analysis of Ca^{2+}/CaM-Dependency of AC 1 and Medullary AC

Detection of AC1 mRNA by PCR, the lack of curve fit of the inhibition profiles between medullary AC and cortical AC and cardiac AC, respectively (Fig. **C.8**) and the good correlation with AC1 under Mg^{2+} conditions (Fig. **C.6**) suggested that AC isoform 1 could play an important role in renal medulla. To further assess the potential involvement of AC1 in renal medulla, we studied the effect of calmodulin to discriminate Ca^{2+}/CaM-dependent AC1 from other AC isoforms. CaM increased basal activity of recombinant AC1 by ~ 4-fold (Fig. **C.9A**). In contrast, medullary AC showed identical responses to FS activation in presence and absence of CaM (Fig. **C.9B**) indicating the presence of another AC isoform than AC1 but characterized by similar inhibition properties.

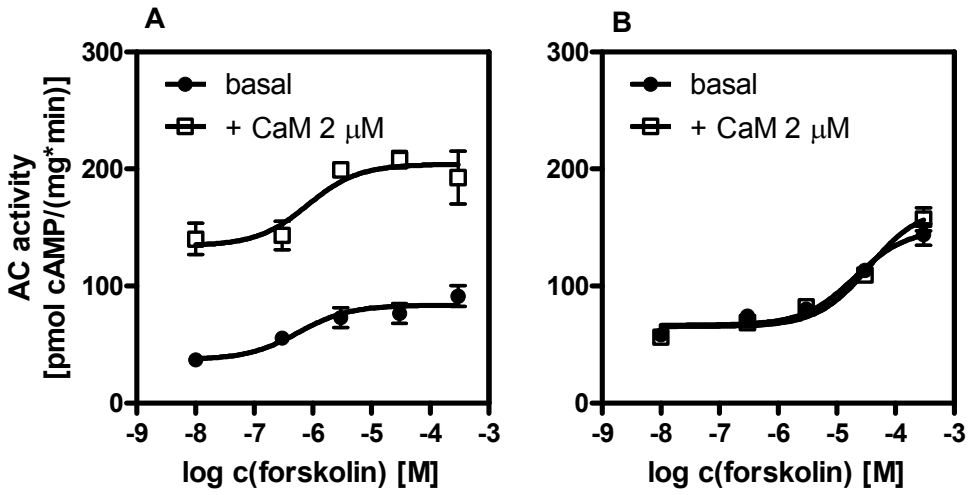

Fig. C.9. Activation of recombinant AC1 and renal medullary AC by FS in presence and absence of calmodulin (CaM). Both experiments were performed in presence of 7 mM Mg^{2+} and enzyme activity was determined as described in "Materials and Methods". **A**, Concentration response curves of recombinant AC1. **B**, Determination of AC activation on medullary AC. The data points are presented as the mean activities ± SD of duplicate determinations from representative experiments performed three times on two separate membrane preparations.

C.4.6 Ca^{2+}-Dependent Regulation of Recombinant and Renal AC Isoforms

Ca^{2+} added to the reaction mixture differentially influenced enzyme activity (Fig. **C.10**). AC2 showed a linear inhibition pattern. The inhibition profiles of AC5 and cortical AC were biphasic illustrating physiologically relevant AC inhibition with Ca^{2+}-concentrations in the submicromolar range (EC_{50}_1: 300 nM) and by non-physiological submillimolar Ca^{2+}-concentrations (EC_{50}_2: 200 μM). Both ACs showed a similar sensitivity to increasing Ca^{2+}-concentrations. In contrast, ACs 1 and medullary AC were rather insensitive to inhibition by Ca^{2+}. Only high concentrations of free Ca^{2+} decreased cAMP synthesis.

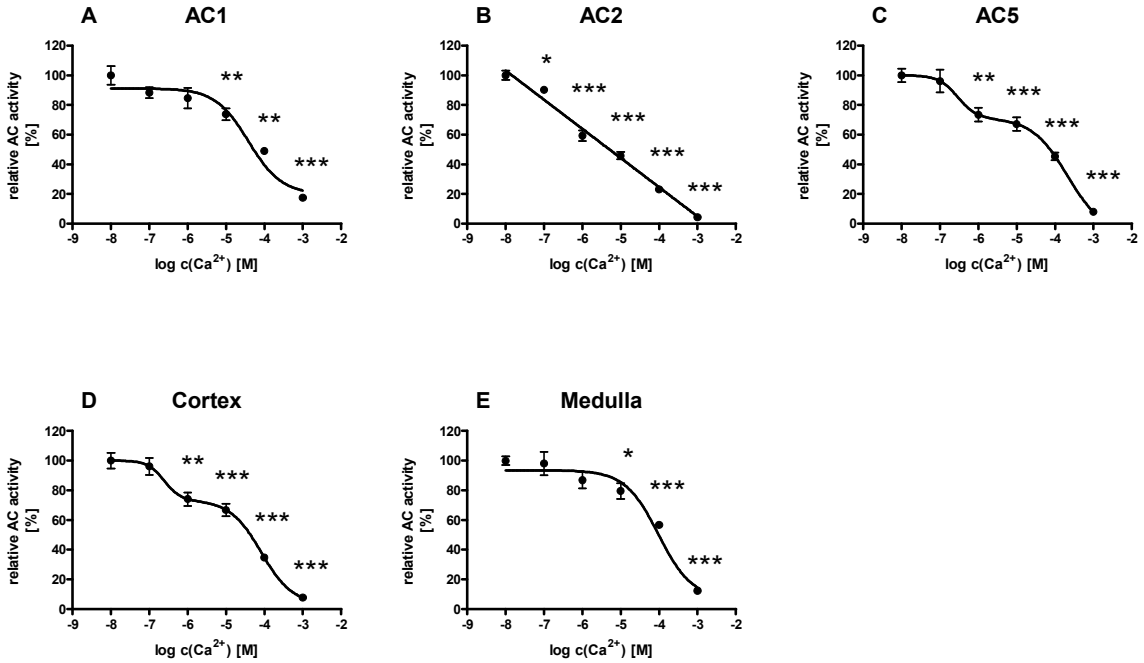

Fig. C.10. Differential inhibition of various ACs by Ca^{2+}. Reaction mixtures contained 7 mM Mg^{2+}, [α–^{32}P]ATP (0.3 μCi/tube), 10 μM GTP, 10 μM GTPγS, 100 μM cAMP, 0.4 mg/mL creatine kinase, 9 mM phosphocreatine, 100 μM IBMX, 300 μM FS and Ca^{2+} in increasing concentrations from 100 nM to 1 mM. To ensure linear reaction progress, tubes were incubated for 10 min at 30°C. **A,** inhibition of AC activity by Ca^{2+} on recombinant AC1. **B,** Ca^{2+}-dependent inhibition of AC2. **C,** effects of increasing Ca^{2+}-concentrations on AC5. **D,** inhibition of AC activity by Ca^{2+} on cortical membranes. **E,** Ca^{2+}-dependent inhibition of medullary AC. Data shown are the combinations of 3 independent experiments, presented as the mean activities ± SD. Statistical significance was tested using the Student's *t*-test (* $p < 0.05$; ** $p < 0.01$; *** $p < 0.001$).

C.5 Discussion

There is much evidence that overproduction of cAMP plays an essential role in cyst growth and the pathogenesis of polycystic kidney disease (Schwiebert *et al*., 2002; Wallace *et al*., 2002). With ACs catalyzing cAMP synthesis, we focused on the identification of the predominant AC isoforms in the kidney cortex and medulla.

C.5.1 Semi-Quantitative PCR

First, we analyzed the expression of ACs in the kidney on mRNA levels. RT-PCR studies demonstrated the presence of ACs 4, 5 and 6 in rabbit cortex and medulla. Ca^{2+}-inhibitable isoform 6 was determined at similar concentrations in both parts of the tissue, according to literature, where AC6 expression has been demonstrated along the entire nephron (Chabardés *et al*., 1996). Compared to medulla, we found AC5 occurring in higher amounts in the cortex corresponding to the data of Heliés-Toussaint *et al.* (Heliés-Toussaint *et al*., 2000). Type 4 mRNA seemed to be more abundant in the medullary part. Bek *et. al.* initially discussed a more widely distribution of AC4 in the kidney than previously thought (Bek *et al*., 2001). This assumption confirms our results that AC4 mRNA is not only restricted to the glomerulus (Chabardés *et al*., 1996; Ludwig and Seuwen, 2002). Additionally, we demonstrated mRNA presence of AC1 in rabbit kidney. In literature, this isoform is discussed to be neurospecific (Xia *et al*., 1993) and expressed in special areas of the brain (Xia and Storm, 1997). However, since kidney is densely innervated (Barajas *et al*., 1992), the detection of AC1 may reflect the presence of this isoform in neurons. It is also possible that AC1 is present in cortical or medullary parenchymal tissue (Tiniakos *et al*., 2004).

For further investigation, AC expression should have been analyzed at the protein level. Unfortunately, there is a paucity of selective and sensitive AC isoform antibodies (Defer *et al*., 2000; Ortíz-Capisano *et al*., 2007). To this end, all of our substantial efforts in this area have been without success both with respect to detection of recombinant ACs and ACs in native tissues (data not shown) (Göttle *et al*., 2009). Considering these substantial limitations, we took a biochemical approach to characterize AC in cortical and medullary membranes in comparison to selected recombinant AC isoforms.

C.5.2 Effects of GPCR Agonists on Renal ACs

Various hormones and neurotransmitters such as glucagon, AVP, epinephrine and norepinephrine regulate tubular functions by activation of G protein-coupled receptors (Störk and Schmitt, 2002). AVP effectively activates AC in renal cortex and medulla. Gattone *et al.* demonstrated the up-regulation of AVP in PKD and its function as modulator of cystogenesis (Gattone *et al*., 2003; Belibi and Edelstein, 2010). Consequently, the development of V_2-receptor antagonists may reduce renal cAMP and inhibit disease progression (Torres, 2004; Wang *et al*., 2005).

Moreover, the renin-angiotensin system is involved in functional and structural changes during PKD (Belibi and Edelstein, 2010). With glucagon influencing the regulation of renin release (Schweda *et al*., 2007), it appears to be a second peptide modulating cyst formation. Glucagon increased AC ~3-fold in cortex and medulla. Appropriately, it excites the most effective responsiveness of all activators. Glucagon is also known to modulate water and salt homeostasis, glomerular filtration rate and renal blood flow (Ahloulay *et al*., 1995; Marks *et al*., 2003).

In contrast, we observed biological responses to catecholamines with restriction to the cortical part. α- and β-Adrenergic receptors are expressed along the renal tubule (Cohen and Katz, 1991; Meister *et al*., 1994; Mandon *et al*., 1995) and mediate the physiological effects like stimulation of renin synthesis and antidiuresis (Beck *et al*., 1972). Up to now, there is no evidence for an involvement of catecholamines to the pathogenesis of PKD.

C.5.3 Comparison of Renal AC to Recombinant and Cardiac AC

The determination of the kinetic properties for cortex and medulla showed modest differences compared to recombinant ACs. However, the K_m-values are necessary to calculate the associated inhibition constants of the MANT-nucleotides. The inhibition of cortical and medullary ACs by eight different MANT-nucleotides yielded a characteristic rank order of potencies for each part of the kidney. In presence of Mg^{2+}, the physiological cation involved in AC enzyme activity, there was a poor correlation of cortical AC with AC2. Consequently, it is rather unlikely that AC2 is of major importance in renal cortical tissue. A closer correlation was obtained for cortical AC and AC1, however, recombinant AC5 showed the best correlation. Another hint for AC5 being the prevalent isoenzyme in renal cortex is the high

similarity of cortical AC with cardiac AC. Recently, we confirmed the consistency of cardiac AC with AC5 (Göttle *et al*., 2009). The correlation of the inhibitor profile in cortex and heart points to the predominance of AC5 in both systems.

Under Mn^{2+} conditions, no correlation of inhibitor profiles was found for cortical AC and recombinant ACs. Only cardiac AC showed high similarity. Previously, we noticed the varying influences of the different divalent cations on the inhibitor profile (Göttle *et al*., 2009). Under physiological conditions, cortical as well as cardiac AC activity resembled AC5 activation. Under non-physiological Mn^{2+} conditions, another AC isoform seemed to be unmasked.

To verify AC5 as major cortical AC, the different sensitivity of specific ACs to Ca^{2+} was studied. AC subtypes are classified into three distinct families, (i) Ca^{2+}-stimulated ACs 1, 3 and 8, (ii) Ca^{2+}-inhibited AC5 and AC6 and (iii) unresponsive to Ca^{2+} (ACs 2, 4 and 7) (Cooper *et al*., 1994a; Cooper *et al*., 1995; Sunahara *et al*., 1996). Independently of this classification, Ca^{2+} at supramicromolar concentrations reduces cAMP formation by all AC isoforms (Cooper *et al*., 1994a; Guillou *et al*., 1999). This inhibition by non-physiological Ca^{2+}-concentrations is not isoform-specific and a competition between Ca^{2+} and Mg^{2+}, the physiological cation needed for AC activation (Hu *et al*., 2002). Physiologically relevant AC inhibition with Ca^{2+}-concentrations in the submicromolar range has only been described for ACs 5 and 6 (Guillou *et al*., 1999). Their Ca^{2+}-dependent inhibition yields biphasic curves based on the combination of the physiological and the non-physiological inhibitory effects (Hu *et al*., 2002; Mou *et al*., 2009).

In the present study, we compared the inhibition patterns of Ca^{2+} on recombinant ACs 1, 2 and 5 and both renal parts to differentiate between the AC subclasses. Although AC2 is known to be insensitive for physiological Ca^{2+}-inhibition (Cooper *et al*., 1995), we showed a linear reduction of cAMP accumulation due to increasing Ca^{2+}-concentrations. However, no renal AC resembled the AC2 characteristic. In contrast, the Ca^{2+}-influence on AC5 membrane was biphasic (Hu *et al*., 2002). With rabbit cortical membranes we detected an analogous biphasic inhibition, compatible with AC5.

Contrary to cortical AC, the examination of medullary AC inhibition by MANT-nucleotides revealed low similarity with AC5 under both Mg^{2+} and Mn^{2+} conditions. The obtained rank orders showed clear variations from a theoretical identitiy with a slope of 1.0. Direct comparison of cortical and medullary AC inhibition also revealed

moderate differences in presence of Mg^{2+}, whereas Mn^{2+} emphasized the discrepancies between the two renal parts. Additionally, the inhibitor profiles of renal medulla and mouse heart showed divergent correlations indicating the predominance of another AC isoform in medulla than AC5.

Surprisingly, in presence of Mg^{2+}, inhibition data of renal medulla resembled the one of Ca^{2+}/CaM sensitive AC1. This unexpected similarity and the detection of AC1 mRNA in medulla suggested the presence of AC1 also on protein level. Moreover, focusing on the Ca^{2+}-dependence, medullary AC revealed a Ca^{2+}-sensitive profile similar to AC1. Membranes expressing recombinant AC1 only exhibited the inhibition effect with high concentrations of Ca^{2+} and in the absence of CaM (Cooper *et al*., 1994). At low Ca^{2+}-concentrations, stimulation of AC1 only appears in presence of calmodulin (Guillou *et al*., 1999).

To confirm the AC1 hypothesis, we performed studies with CaM on medullary and recombinant Sf9 cell membranes. Ca^{2+} and CaM activate AC1 by interacting with the first cytoplasmatic loop (Cooper *et al*., 1995; Ferguson and Storm, 2004; Masada *et al*., 2009). CaM also increased sensitivity of AC1 to FS and yielded an additive effect (Tang *et al*., 1991). This effect was confirmed for the recombinant Sf9 membrane. In contrast, this additive activation was missing at medulla. Although, under Mg^{2+} conditions the prevalent isoform in medulla represented characteristics similar to AC1, with respect to the lack of Ca^{2+}/CaM sensitivity, this isoform could be excluded. Therefore, another AC different from type 1 was stimulated.

The intention of our study was the biochemical characterization of renal ACs in rabbit kidney. Our data suggest that AC5 is the prevalent isoform in cortex. Although, in case of medulla, we could not identify a major AC isoform, we excluded the predominance of ACs 1, 2 and 5. Therefore another isoform, different from type 1, but with similar pharmacological characteristics seemed to play a crucial role in the medulla. Our findings and the confirmation of AC5 in renal cortex are an important step to the development of isoform-selective AC inhibitors and a prospective therapeutic strategy for PKD. In future studies, further AC isoforms should be tested to get detailed information about isoform-specific AC regulation. Unfortunately, the stable and active expression of the remaining AC isoforms has to be solved first.

C.6 References

Ahloulay M, Dechaux M, Laborde K and Bankir L (1995) Influence of glucagon on GFR and on urea and electrolyte excretion: direct and indirect effects. *Am J Physiol* **269**:F225-235.

Barajas L, Liu L and Powers K (1992) Anatomy of the renal innervation: intrarenal aspects and ganglia of origin. *Can J Physiol Pharmacol* **70**:735-749.

Bek MJ, Zheng S, Xu J, Yamaguchi I, Asico LD, Sun XG and Jose PA (2001) Differential expression of adenylyl cyclases in the rat nephron. *Kidney Int* **60**:890-899.

Belibi FA and Edelstein CL (2010) Novel targets for the treatment of autosomal dominant polycystic kidney disease. *Expert Opin Investig Drugs* **19**:315-328.

Bradford MM (1976) A rapid and sensitive method for the quantitation of microgram quantities of protein utilizing the principle of protein-dye binding. *Anal Biochem* **72**:248-254.

Chabardés D, Firsov D, Aarab L, Clabecq A, Bellanger AC, Siaume-Perez S and Elalouf JM (1996) Localization of mRNAs encoding Ca^{2+}-inhibitable adenylyl cyclases along the renal tubule. Functional consequences for regulation of the cAMP content. *J Biol Chem* **271**:19264-19271.

Chabardés D, Imbert-Teboul M, Montegut M, Clique A and Morel F (1975) Catecholamine sensitive adenylate cyclase activity in different segments of the rabbit nephron. *Pflugers Arch* **361**:9-15.

Cheng J and Grande JP (2007) Cyclic nucleotide phosphodiesterase (PDE) inhibitors: novel therapeutic agents for progressive renal disease. *Exp Biol Med (Maywood)* **232**:38-51.

Cooper DM (1994) Regulation of Ca^{2+}-sensitive adenylyl cyclases by calcium ion *in vitro* and *in vivo*. *Methods Enzymol* **238**:71-81.

Cooper DM (2003) Regulation and organization of adenylyl cyclases and cAMP. *Biochem J* **375**:517-529.

Cooper DM, Mons N and Fagan K (1994) Ca^{2+}-sensitive adenylyl cyclases. *Cell Signal* **6**:823-840.

Gattone VH, 2nd, Wang X, Harris PC and Torres VE (2003) Inhibition of renal cystic disease development and progression by a vasopressin V_2-receptor antagonist. *Nat Med* **9**:1323-1326.

Gille A, Lushington GH, Mou TC, Doughty MB, Johnson RA and Seifert R (2004) Differential inhibition of adenylyl cyclase isoforms and soluble guanylyl cyclase by purine and pyrimidine nucleotides. *J Biol Chem* **279**:19955-19969.

Göttle M, Geduhn J, König B, Gille A, Höcherl K and Seifert R (2009) Characterization of mouse heart adenylyl cyclase. *J Pharmacol Exp Ther* **329**:1156-1165.

Grantham JJ (1997) Polycystic kidney disease: huge kidneys, huge problems, huge progress. *Trans Am Clin Climatol Assoc* **108**:165-170; discussion 170-162.

Guillou JL, Nakata H and Cooper DM (1999) Inhibition by calcium of mammalian adenylyl cyclases. *J Biol Chem* **274**:35539-35545.

Hanaoka K and Guggino WB (2000) cAMP regulates cell proliferation and cyst formation in autosomal polycystic kidney disease cells. *J Am Soc Nephrol* **11**:1179-1187.

Harris PC and Torres VE (2006) Understanding pathogenic mechanisms in polycystic kidney disease provides clues for therapy. *Curr Opin Nephrol Hypertens* **15**:456-463.

Heliés-Toussaint C, Aarab L, Gasc JM, Verbavatz JM and Chabardés D (2000) Cellular localization of type 5 and type 6 ACs in collecting duct and regulation of cAMP synthesis. *Am J Physiol Renal Physiol* **279**:F185-194.

Houston C, Wenzel-Seifert K, Burckstummer T and Seifert R (2002) The human histamine H_2-receptor couples more efficiently to Sf9 insect cell G_S-proteins than to insect cell G_q-proteins: limitations of Sf9 cells for the analysis of receptor/G_q-protein coupling. *J Neurochem* **80**:678-696.

Hu B, Nakata H, Gu C, De Beer T and Cooper DM (2002) A critical interplay between Ca^{2+} inhibition and activation by Mg^{2+} of AC5 revealed by mutants and chimeric constructs. *J Biol Chem* **277**:33139-33147.

Lowry OH, Rosebrough NJ, Farr AL and Randall RJ (1951) Protein measurement with the Folin phenol reagent. *J Biol Chem* **193**:265-275.

Mandon B, Siga E, Champigneulle A, Imbert-Teboul M and Elalouf JM (1995) Molecular analysis of β-adrenergic receptor subtypes in rat collecting duct: effects on cell cAMP and Ca^{2+} levels. *Am J Physiol* **268**:F1070-1080.

Masada N, Ciruela A, Macdougall DA and Cooper DM (2009) Distinct mechanisms of regulation by Ca^{2+}/calmodulin of type 1 and 8 adenylyl cyclases support their different physiological roles. *J Biol Chem* **284**:4451-4463.

Meister B, Dagerlind A, Nicholas AP and Hokfelt T (1994) Patterns of messenger RNA expression for adrenergic receptor subtypes in the rat kidney. *J Pharmacol Exp Ther* **268**:1605-1611.

Ortíz-Capisano MC, Ortíz PA, Harding P, Garvin JL and Beierwaltes WH (2007) Decreased intracellular calcium stimulates renin release *via* calcium-inhibitable adenylyl cyclase. *Hypertension* **49**:162-169.

Patel TB, Du Z, Pierre S, Cartin L and Scholich K (2001) Molecular biological approaches to unravel adenylyl cyclase signaling and function. *Gene* **269**:13-25.

Pinto C, Papa D, Hübner M, Mou TC, Lushington GH and Seifert R (2008) Activation and inhibition of adenylyl cyclase isoforms by forskolin analogs. *J Pharmacol Exp Ther* **325**:27-36.

Schweda F, Friis U, Wagner C, Skott O and Kurtz A (2007) Renin release. *Physiology (Bethesda)* **22**:310-319.

Seifert R, Lee TW, Lam VT and Kobilka BK (1998) Reconstitution of β_2-adrenoceptor-GTP-binding-protein interaction in Sf9 cells--high coupling efficiency in a β_2-adrenoceptor-$G_{S\alpha}$ fusion protein. *Eur J Biochem* **255**:369-382.

Störk PJ and Schmitt JM (2002) Crosstalk between cAMP and MAP kinase signaling in the regulation of cell proliferation. *Trends Cell Biol* **12**:258-266.

Sunahara RK, Dessauer CW and Gilman AG (1996) Complexity and diversity of mammalian adenylyl cyclases. *Annu Rev Pharmacol Toxicol* **36**:461-480.

Sunahara RK and Taussig R (2002) Isoforms of mammalian adenylyl cyclase: multiplicities of signaling. *Mol Interv* **2**:168-184.

Sweeney WE, Jr. and Avner ED (2006) Molecular and cellular pathophysiology of autosomal recessive polycystic kidney disease (ARPKD). *Cell Tissue Res* **326**:671-685.

Taha HM, Schmidt J, Göttle M, Suryanarayana S, Shen Y, Tang WJ, Gille A, Geduhn J, König B, Dove S and Seifert R (2009) Molecular analysis of the interaction of anthrax adenylyl cyclase toxin, edema factor, with 2'(3')-*O*-(*N*-(methyl)anthraniloyl)-substituted purine and pyrimidine nucleotides. *Mol Pharmacol* **75**:693-703.

Tang WJ, Krupinski J and Gilman AG (1991) Expression and characterization of calmodulin-activated (type I) adenylylcyclase. *J Biol Chem* **266**:8595-8603.

Tiniakos D, Anagnostou V, Stavrakis S, Karandrea D, Agapitos E and Kittas C (2004) Ontogeny of intrinsic innervation in the human kidney. *Anat Embryol (Berl)* **209**:41-47.

Torres VE (2004) Cyclic AMP, at the hub of the cystic cycle. *Kidney Int* **66**:1283-1285.

Torres VE, Harris PC and Pirson Y (2007) Autosomal dominant polycystic kidney disease. *Lancet* **369**:1287-1301.

Wallace DP, Christensen M, Reif G, Belibi F, Thrasher B, Herrell D and Grantham JJ (2002) Electrolyte and fluid secretion by cultured human inner medullary collecting duct cells. *Am J Physiol Renal Physiol* **283**:F1337-1350.

Wang X, Gattone V, 2nd, Harris PC and Torres VE (2005) Effectiveness of vasopressin V2 receptor antagonists OPC-31260 and OPC-41061 on polycystic kidney disease development in the PCK rat. *J Am Soc Nephrol* **16**:846-851.

Wang X, Ward CJ, Harris PC and Torres VE (2010) Cyclic nucleotide signaling in polycystic kidney disease. *Kidney Int* **77**:129-140.

Xia Z, Choi EJ, Wang F, Blazynski C and Storm DR (1993) Type 1 calmodulin-sensitive adenylyl cyclase is neural specific. *J Neurochem* **60**:305-311.

Younes A, Lyashkov AE, Graham D, Sheydina A, Volkova MV, Mitsak M, Vinogradova TM, Lukyanenko YO, Li Y, Ruknudin AM, Böheler KR, van Eyk J and Lakatta EG (2008) Ca^{2+}-stimulated basal adenylyl cyclase activity localization in membrane lipid microdomains of cardiac sinoatrial nodal pacemaker cells. *J Biol Chem* **283**:14461-14468.

Chapter 4

Summary / Zusammenfassung

D.1 Summary

Mammalian adenylyl cyclases (mACs) are integral membrane proteins involved in various physiological processes. For instance, they regulate cardiac contractility and kidney function. Malfunctions or the abnormal regulation of AC isoforms cause numerous disease states such like heart failure, polycystic kidney disease (PKD), neurodegenerative diseases, or pain and drug dependency. During the past decades, nine distinct mammalian membranous AC isoforms have been identified. These exhibit isoform-specific expression patterns and different regulatory mechanisms. ACs play an important role in transmembrane signaling events of the G protein-coupled receptor (GPCR) cascade and catalyze the conversion from ATP to the second messenger cAMP. Activation of these effector proteins transfers signals from receptors on the cell surface to target molecules inside the cell and contributes to cross-talks in different cell systems and signaling structures.

The first part of this thesis characterizes the detailed interactions of forskolin and six forskolin analogs with recombinant ACs 1, 2 and 5 and determines their effects on isoform-specific AC activity. All seven diterpenes affected the examined AC isoforms in a characteristic manner, strongly rendering the pharmacological profile. Correlations of the pharmacological parameters of these diterpenes between the different AC isoforms showed a distinct isoform-specific profile. Since the amino acids exhibiting direct interactions with the diterpenes are highly conserved among the AC isoforms, the results of this study indicated a contribution of the structural environment around the catalytic core to substrate binding and catalysis. Moreover, differential impacts of Mg^{2+} and Mn^{2+} were obtained on mAC activation by diterpenes. However, the metal cofactors showed only low impact on the efficacies of forskolin and its analogs of the purified C_1/C_2 catalytic subunit plus $G_{S\alpha\text{-}GTP\gamma S}$. Additionally, docking of diterpenes to the C_1/C_2 mAC protein did not offer metal ion-dependent changes in the docking preferences. Since only small global and local differences between the arrangements of Mg^{2+} and Mn^{2+} complexes are obtained, the currently available docking results are not conclusive to solve the impact of the cofactors on AC regulation. Although there are substantial differences in the activity of mAC isoforms, due to differential regulation by metal ions, the biological significance of Mn^{2+} in the regulation of substrate binding and catalyzing cAMP production remains unclear.

The second part describes a biochemical approach to characterize AC in renal cortical and medullary membranes in comparison to selected recombinant AC isoforms. Considering the paucity of selective and sensitive AC isoform antibodies, the characterization of the renal AC isoforms was performed using a biochemical approach. Analysis of GPCR agonist-mediated, Ca^{2+}-dependent or calmodulin-sensitive cAMP formation were used to differentiate between the AC types in the two main parts of the kidney. The effects of various hormones and neurotransmitters on cortical and medullary ACs detected a tissue-specific distribution of GPCRs and subsequently a distinct regulation of tubular functions. The inhibition of cortical and medullary ACs by eight 2'(3')-*O*-(*N*-methylanthraniloyl) (MANT)-nucleoside 5'-([γ-thio])triphosphates yielded characteristic rank orders of pharmacological parameters for each part of the kidney. In combination with the inhibition patterns of Ca^{2+} on recombinant ACs 1, 2 and 5 and both renal parts, the classification of the predominant cortical AC isoform as AC type 5 was possible. In the case of medulla, the pharmacological profiles resembled AC isoform 1. The identification of a major AC isoform with biochemical approaches failed, because medullary AC missed the characteristic calmodulin-dependency of AC1. However, the predominance of ACs 1, 2 and 5 could be excluded. Therefore, another isoform – different from type 1, but with similar pharmacological characteristics – seemed to play a crucial role in the medulla. This identification of the prevalent AC isoform provides the basis for exploring ACs as target for the treatment of PKD.

D.2 Zusammenfassung

Adenylylcyclasen (mACs) von Säugetieren sind integrale Membranproteine, die an diversen physiologischen Prozessen beteiligt sind. Beispielsweise regulieren sie die Kontraktilität des Herzens und die Nierenfunktion. Enzymdefekte oder abnormale Regulationen der mAC Isoformen verursachen zahlreiche Krankheitszustände wie Herzinsuffizienz, polycystische Nierenerkrankung (PKD), neurodegenerative Erkrankungen oder Schmerzzustände und Sucht. Während der letzten Jahrzehnte wurden neun verschiedene membrangebundene AC Isoformen in Säugetieren entdeckt. Diese werden charakterisiert durch isoform-spezifische Gewebeexpression und unterschiedliche Regulationsmechanismen. ACs spielen eine wichtige Rolle in transmembranären Signaltransduktionswegen vermittelt durch G Protein-gekoppelte Rezeptoren (GPCRs) und katalysieren die Umwandlung von ATP in den sekundären Botenstoff cAMP. Die Aktivierung dieser Effektorproteine leiten Signale von Rezeptoren auf der Zelloberfläche weiter zu Zielstrukturen im Inneren der Zelle. Dadurch tragen sie zur Verständigung zwischen verschiedenen Zellsystemen und Signalstrukturen bei.

Der erste Teil dieser Doktorarbeit charakterisiert die Interaktionen von Forskolin und sechs Forskolin-Analoga mit den rekombinanten AC Isoformen 1, 2 und 5 und untersucht deren Effekte auf die AC Aktivität der einzelnen Subtypen. Alle sieben Diterpene beeinflussten die Enzymaktivität der untersuchten mAC Isoformen auf charakteristische Weise und gaben dadurch das pharmakologische Profil wieder. Korrelationen der pharmakologischen Parameter der Diterpene mit den unterschiedlichen mACs zeigten ein individuelles Profil für jede AC Isoform. Da die Aminosäuren, die an der Forskolin-Bindung direkt beteiligt sind, unter den AC Isoformen stark konserviert sind, deuteten die Ergebnisse dieser Untersuchung auf eine Beteiligung der strukturellen Umgebung der katalytischen Tasche an der Substratbindung und dem Katalysemechanismus hin. Zusätzlich wurden unterschiedliche Auswirkungen von Mg^{2+} und Mn^{2+} auf die Diterpen-abhängige Aktivität der mACs beobachtet. Die Kofaktoren zeigten jedoch nur unerheblichen Einfluss auf den Maximaleffekt von Forskolin und den Analoga auf die gereinigte katalytische Einheit C_1/C_2 plus $G_{S\alpha\text{-}GTP\gamma S}$. Auch das Docking der Diterpene in die C_1/C_2 mAC-Bindetasche bot keine Kofaktor-abhängigen Unterschiede bei den Docking-Präferenzen. Da nur geringe allgemeine und lokale Unterschiede zwischen

der Anordnung von Mg^{2+} oder Mn^{2+} in der Kristallstruktur aufgedeckt wurden, stellt das momentan mögliche, molekulare Docking keine beweiskräftige Methode dar, um den Einfluss der Kofaktoren auf die AC Regulation zu ergründen. Trotz grundlegender Unterschiede in der Aktivität der mAC Isoformen bedingt durch die Wahl der Metallionen, ist die biologische Bedeutung von Mn^{2+} bei der Regulation der Substratbindung und der Katalyse unklar.

Der zweite Teil beschreibt einen biochemischen Ansatz, um die AC Isoformen in Cortex- und Medulla-Membranen der Niere im Vergleich mit ausgewählten rekombinanten AC Isoformen zu charakterisieren. Aufgrund des Mangels an selektiven und sensitiven Antikörpern erfolgte die Charakterisierung der AC Isoformen der Niere mit biochemischen Methoden. Durch GPCR-Agonisten vermittelte cAMP-Bildung, Ca^{2+}-abhängige AC Aktivierung und die Sensitivität gegenüber Calmodulin wurde zwischen den AC Isoformen in den beiden Nierenbereichen unterschieden. Die Effekte einiger Hormone und Neurotransmitter auf die ACs von Cortex und Medulla zeigten eine gewebsspezifische Verteilung der GPCRs und somit eine unterschiedliche Regulation der Tubulusfunktionen. Die Hemmung der Nieren-ACs durch acht 2'(3')-*O*-(*N*-methylanthraniloyl) (MANT)-Nucleosid 5'-([γ-thio])triphosphate erzielten charakteristische Reihenfolgen der pharmakologischen Kenngrößen für jeden Teil der Niere. Zusammen mit dem Inhibitionsschema mittels Ca^{2+} an rekombinanten ACs 1, 2 und 5 und beiden Nierenbereichen konnte die Identifizierung der vorrangigen AC Isoform des Nierencortex als AC5 vorgenommen werden. Bei der Medulla ähnelten die pharmakologischen Profile jenen von AC1. Die Identifizierung der Haupt-AC mit biochemischen Methoden schlug jedoch fehl, da die medulläre AC Isoform nicht die Calmodulin-Abhängigkeit entsprechend der AC1 aufwies. Es konnten allerdings die ACs 1, 2 und 5 als vorherrschende Isoformen ausgeschlossen werden. Es scheint eine andere Isoform als AC1, aber mit ähnlichem pharmakologischen Profil, die Hauptrolle in der Regulation der Medulla zu spielen. Die Identifizierung der vorrangigen AC Isoform in der Niere schafft die Grundlage für die Erforschung von ACs als Zielstrukturen zur Behandlung der PKD.

Appendix

E.1 Publications

Parts of this thesis will be published as publications:

Erdorf, M and Seifert, R (2010) Pharmacological Characterization of Adenylyl Cyclase Isoforms in Rabbit Kidney Membranes. *JPET*; (*submitted*)

E.2 Poster Presentations

Parts of this thesis were presented as posters:

2010

Pharmacological Characterization of Adenylyl Cyclase Isoforms in Rabbit Kidney Membranes
Erdorf, M. and Seifert, R.
51. Jahrestagung der Deutschen Gesellschaft für Experimentelle und Klinische Pharmakologie und Toxikologie (DGPT), Mainz (Germany), März 2010

Differences in Intracellular Ca^{2+}-Mobilization in a Lesch-Nyhan Disease Cell Model
Erdorf, M. and Seifert, R.
Rare disease day – Symposium 2010, Hannover (Germany), Februar 2010

2009

Differences of ATP-Induced Increases in Intracellular Ca^{2+} in a Lesch-Nyhan Disease Model
Erdorf, M. and Seifert, R.
50. Jahrestagung der Deutschen Gesellschaft für Experimentelle und Klinische Pharmakologie und Toxikologie (DGPT), Mainz (Germany), März 2009

2008

Differences of Intracellular Ca^{2+}-Mobilization in a Lesch-Nyhan Cell Model
Erdorf, M. and Seifert, R.
Symposium aus Anlass der Verabschiedung von Prof. Dr. med. K. Resch und des Dienstantritts von Prof. Dr. med. R. Seifert als Direktor des Instituts für Pharmakologie an der Medizinischen Hochschule Hannover, Hannover (Germany), November 2008

Analysis of Adenyly Cyclase Activity in Rabbit Kidney Membranes
Erdorf, M. and Seifert, R.
49. Jahrestagung der Deutschen Gesellschaft für Experimentelle und Klinische Pharmakologie und Toxikologie (DGPT), Mainz (Germany), März 2008

E.3 Lebenslauf

Persönliche Daten

Name:	Miriam Elena Theresa Erdorf
Geburtsdatum:	20.07.1982
Geburtsort:	Burghausen

Beruflicher Werdegang

Seit 07/2007	Promotion in Pharmakologie und Toxikologie Doktorvater Prof. Dr. R. Seifert (MHH-Hannover) Institut für Chemie und Pharmazie Universität Regensburg
07/2007	Approbation als Apothekerin
06/2007	Abschluss der Pharmazeutischen Prüfung (3. Abschnitt)
11/2006 – 04/2007	2. Hälfte des Praktischen Jahres: Fakultät für Pharmakologie und Toxikologie Betreuer Prof. Dr. R. Seifert Institut für Chemie und Pharmazie Universität Regensburg
05/2006 – 10/2006	1. Hälfte des Praktischen Jahres: Apollo-Apotheke Burghausen
08/2004 – 09/2004	Praktikum in der Business Unit Transplantation Abteilung Klinische Forschung Novartis Pharma GmbH Nürnberg
07/2002 – 08/2002	Werkstudent im GC-Labor Abteilung Qualitätskontrolle Organica Wacker-Chemie GmbH Burghausen
08/2002 – 09/2002	Famulatur in der Apollo-Apotheke Burghausen
02/2002 – 03/2002	Famulatur in der Stadt-Apotheke Burghausen
07/2001 – 09/2001	Freiwilliges Praktikum im Altenheim Heilig Geist Burghausen

Universitärer Werdegang

04/2006	Abschluss des 2. Abschnitts der Pharmazeutischen Prüfung
10/2001 – 04/2006	Studium der Pharmazie an der Universität Regensburg

Schulbildung

06/2001	Abitur
09/1992 – 06/2001	Aventinus-Gymnasium Burghausen
09/1988 – 07/1992	Johannes-Hess-Grundschule Burghausen

E.4 Ausgewählte Zusatzqualifikationen / Fortbildung

03/2010	Advanced Courses in Pharmacology Teil 1: Methoden zur Analyse G Protein-gekoppelter Rezeptoren Teil 2: Moderne Massenspektrometrie in Pharmakologie und Toxikologie
03/2009	Advanced Courses in Pharmacology Teil 1: Tiermodelle in der Pharmakologischen Forschung Teil 2: Arzneimittelinteraktion, -metabolismus und -transport
02/2009 – 09/2009	Weiterbildung „Versuchstierkunde und Tierschutz“ Bestandteil des Nachweises der Sachkunde für den Umgang mit Versuchstieren (FELASA Kategorie B) innerhalb der EU
04/2008	Fortbildungsveranstaltung für Projektleiter und Beauftragte für Biologische Sicherheit (BBS) Nach §15 und 17 der Gentechniksicherheitsverordnung

E.5 Teilnahme an Austauschprogrammen

06/2008 – 08/2008	RISE – Research Internships in Science and Engineering Deutscher Akademischer Austauschdienst (DAAD)

E.6 Eidesstattliche Erklärung

Hiermit erkläre ich an Eides statt, dass ich die vorliegende Arbeit ohne unzulässige Hilfe Dritter und ohne Benutzung anderer als der angegebenen Hilfsmittel angefertigt habe. Die aus anderen Quellen direkt oder indirekt übernommenen Daten und Konzepte sind unter Angabe des Literaturzitats gekennzeichnet. Weitere Personen waren an der inhaltlich-materiellen Herstellung der vorliegenden Arbeit nicht beteiligt. Insbesondere habe ich hierfür nicht die entgeltliche Hilfe eines Promotionsberaters oder anderer Personen in Anspruch genommen. Niemand hat von mir weder unmittelbar noch mittelbar geldwerte Leistungen für Arbeiten erhalten, die im Zusammenhang mit dem Inhalt der vorgelegten Dissertation stehen. Die Arbeit wurde bisher weder im In- noch im Ausland in gleicher oder ähnlicher Form einer anderen Prüfungsbehörde vorgelegt.

Regensburg, den _____ _____

Miriam Erdorf